THE EVOLUTION OF PLATELET RESPONSES TO COLLAGEN UNDER CONDITIONS OF HEMODYNAMIC FLOW

Alec A. Schmaier

A Dissertation in Pharmacological Sciences

Presented to the Faculties of the University of Pennsylvania in Partial Fulfillment of the Requirements for the Degree of Doctor in Philosophy

2010

Mark L. Kahn, MD	Vladimir Muzykantov, MD, PhD
Professor of Medicine,	Associate Professor of Pharmacology
Division of Cardiology	and Medicine
Dissertation Supervisor	Graduate Group Chairperson

David E. Boettiger, PhD, Professor of Microbiology

Joel S. Bennett, MD, Professor of Medicine

Lawrence F. Brass, MD, PhD, Professor of Medicine, Pathology, and Pharmacology

Gary A. Koretzky, MD, PhD, Professor of Pathology and Laboratory Medicine

Dissertation Committee

Acknowledgments

My four years in the Kahn lab have been an incredible experience due to all the wonderful people associated with that group. Foremost, I offer the greatest thanks to my advisor, Mark Kahn, for serving as such a dedicated mentor. His exceptional insight, unbridled enthusiasm for science, and willingness to pursue exciting, if sometimes unconventional, avenues of investigation will have a lasting influence on my development as a physician scientist. I am also extremely grateful to my thesis committee—David Boettiger, Joel Bennett Skip Brass, and Gary Koretzky—for thoughtful advice and constructive criticism throughout my graduate training.

This dissertation would not have been possible without the support of valuable collaborators and colleagues. Karen Fong, Keith Neeves, Sean Maloney, and Scott Diamond assisted with microfluidic flow chamber assays. Arunas Kazlauskas and Kalle Saksela from the University of Helsinki provided SH3 domain phage display analysis (Fig. 2-8C and Table 2-I). Lori Emert-Sedlak and Thomas Smithgall from the University of Pittsburgh contributed *in vitro* kinase assays (Fig. 2-9). Satya Kunapuli from Temple University donated Fyn and Lyn knockout mice. Simon Cliche and Claude Gariépy from Agriculture and Agri-Food Canada supplied the chicken collagen preparations. Chandrasekaran Nagasami and John Weisel conducted scanning electron microscopy (Fig. 3-7). Wolfgang Bergmeier, Paul Billings, Lurong Lian, Dave Moore, Tim Stalker, Ken Wannemacher, and everyone from the Abrams, Bennett, Brass, Morrisey, Parmacek, and Patel labs provided valuable consultation and generous donations of reagents.

I want to convey sincere thanks to all members of the Kahn lab, past and present. Ziying Zou has been an amazing teacher, a fearless experimenter, and a wonderful bench mate, whose patience and devotion to teaching me lab techniques are greatly appreciated. Patricia Mericko has been the irreplaceable lab mother, and her attention to all the little details that keep things running has consistently helped me out over the last four years. To my fellow grad students, past and present—Dena Alpert, Cara Bertozzi, Chiu-Yu Chen, Lili Gou, Paul Hess, Ben Kleaveland, Niraj Shanbhag, and Dave Rawnsley—thank you for making lab a friendly place, for your advice (or commiseration) with science, and for always being prepared with a "lunch plan." I am particularly indebted to Cara and Paul for their close readings of this dissertation. Mei always offered sound advice for life's bigger issues as well as a helping hand for restraining chickens. To all current and former Kahn lab members— Arindam Basu, Dave Enis, John Lee, Eric Sebzda, Shawn Sweeny, Chong Xu, Lijun Yu, and Xiangjian Zheng—your presence has made it a joy to come into lab each day, and Nina Maschak and has always been a dependable source of administrative help and know-how. Tyrone Branson deserves high praise for his dependable work with animal husbandry and knowledge of Philadelphia sports.

I am exceedingly grateful to Skip Brass, Maggie Krall, Mary Tiedeman, and Maureen Osciak their for brilliant organization of the Penn MD/PhD program and for maintaining a never-ending supply of cookies. I offer sincere thanks to Vladimir Muzykantov and the Penn GGPS for their support throughout my graduate school years, as well as to Barb Zolotorow and the Heme/Onc T32 Training Grant for keeping my coffers full.

To Lauren, I am deeply grateful for your enduring love, support and encouragement throughout the grad school process. To Bub and Grandma, your leading by example has inspired me to achieve my best. To Dad, it has been wonderful to share with you the details of this project, be your roommate at conferences, and receive your sage advice. To Mom, your strength, wisdom, and tireless support has been invaluable to me. Thank you for keeping me focused and warming my heart.

ABSTRACT

THE EVOLUTION OF PLATELET RESPONSES TO COLLAGEN UNDER CONDITIONS OF HEMODYNAMIC FLOW

Author: Alec A. Schmaier

Supervisor: Mark L. Kahn

Collagen activates platelets through the immune-type GPVI receptor, but the mechanism by which this receptor has adapted to function in platelets under conditions of rapid blood flow is unclear. Additionally, it is unknown if responses to collagen are conserved in nucleated thrombocytes found in non-mammalian vertebrates, which do not express GPVI. Here we show that the GPVI proline-rich domain accelerates GPVI signaling kinetics and is required for maximal adhesion to collagen under flow. The proline-rich domain accelerates signaling through binding and directly activating the Src-family kinase Lyn. Chicken thrombocytes are potently activated by collagen but do not form 3-dimensional aggregates under arterial flow conditions, a profound contrast to platelet function. Despite selective expression of most platelet-specific genes, thrombocytes contain a significantly lower density of $\alpha_{2b}\beta_3$ integrin on the cell surface. These studies identify a novel molecular mechanism by which GPVI accelerates immune signaling kinetics and demonstrate partial conservation of hemostatic cell responses to collagen under flow.

Table of Contents

List of Tables

List of Figures

Chapter 1—Introduction: Platelet responses to collagen and the role of GPVI

Summary

Platelets are essential for normal hemostasis, but their activation also underlies the disease mechanisms of heart attack and stroke. This introductory chapter focuses on the role of collagen in platelet-mediated thrombus formation following vessel injury and the role of GPVI as the primary activator of platelets in response to collagen.

Overview of platelets and collagen in hemostasis and thrombosis

Warm-blooded organisms, including mammals and birds, circulate blood at high pressures to perfuse organs at a level commensurate with tissue metabolism. Since an adequate amount of blood perfusion is required to maintain tissue oxygenation and removal of CO_2 and waste products, highly evolved mechanisms exist within each species to prevent excess blood loss. Hemostasis, the cessation of bleeding, involves the coordination of both a cellular component made up of platelets and a plasma protein system consisting of coagulation factors present in circulating blood (Fig. 1-1)[1]. In its extreme form, excess hemostasis leads to thrombosis, the occlusion of a blood vessel, which is physiologic in preventing catastrophic hemorrhage following traumatic vessel injury but is pathophysiologic during injury in diseased arteries, leading to acute myocardial infarction and stroke.

Blood vessel injury exposes pro-thrombotic material, such as tissue factor and collagen, to circulating blood. Tissue factor exposure leads to the generation of thrombin

through coagulation cascade activation, and thrombin activates platelets and cleaves fibrinogen into fibrin to promote clot formation. Collagen is the major protein component of the extracellular matrix (ECM) that lies beneath the endothelial cell layer lining the blood vessels. Exposure of subendothelial collagen initiates two processes: (1) rapid platelet activation and (2) factor XII autoactivation with factor XIa formation leading to thrombin formation[2]. Both activities, along with thrombin generation, contribute to the formation of a platelet plug, resulting in further coagulant activity and the production of a fibrin-containing thrombus. Determining how platelets adhere and are activated by exposure of ECM components is essential to understanding the pathogenesis of acute thrombotic cardiovascular disease.

Platelets in human cardiovascular disease

The primary physiologic function of platelets is to stop hemorrhage after tissue trauma and vessel injury and to initiate an inflammatory response to repair the injury. The importance of platelets in hemostasis is evident by the increased risk of bleeding in patients who are thrombocytopenic, taking anti-platelet agents such as aspirin or clopidogrel, or lack critical platelet receptors such as in Glanzmann's thrombasthenia or Bernard-Soulier syndrome. However, platelets have a causal role in the pathologic thrombosis of cardiovascular disease. Cardiovascular disease, both coronary and cerebrovascular, is the leading cause of death in the United States and worldwide and, as a chronic condition, is predominantly associated with atherosclerosis[3]. Coronary atherosclerosis is unquestionably the leading cause of acute coronary syndromes,

including unstable angina, acute myocardial infarction and sudden cardiac death[4]. The primary event mediating athero-thrombosis is believed to be rupture of an unstable, non-stenotic atherosclerotic plaque, which exposes pro-thrombotic material and leads to platelet-mediated occlusive thrombus formation[5,6]. A major goal in the study of platelet biology is aimed at better understanding the mechanisms underlying acute thrombosis in the setting of atherosclerotic disease. Anti-platelet agents that target major components of platelet function are first-line in treatment of cardiovascular disease. However, the association of these drugs with bleeding complications underlies the importance for development of more refined platelet inhibitors that specifically target athero-thrombotic pathophysiology without interfering with physiologic hemostasis.

Platelet and thrombocyte biology

Platelets are uniquely suited to serve as hemostatic cells in mammalian physiology. They are the smallest cell type found in circulating blood, averaging a diameter of 2.0 to 3.0 μm and a thickness of 0.5 μm, and they lack a nucleus[7]. Platelets are produced from megakaryocytes, large polyploid cells found primarily in the bone marrow, by protrusion of long, beaded cytoplasmic extensions called proplatelets into the bone marrow sinusoids where they can be released to enter the bloodstream[8]. Once in the blood, platelets may circulate for a lifespan of 7-10 days before being destroyed by the reticuloendothelial system of the spleen. Platelets are extremely numerous in the circulation—a normal platelet count is 150-450,000 per μL in humans and can be greater than 1×10^6 per μL in mice—making them excellent surveyors of vascular integrity,

ready to respond immediately, in large numbers, at the site of vessel injury. However, platelets are not found in all warm-blooded species with a high-pressure vascular system. Platelets are unique to mammals, whereas non-mammalian vertebrates contain thrombocytes—larger, nucleated cells, tenfold less numerous than platelets, that are believed to serve an analogous hemostatic function. Much less is known about the biology of thrombocytes, their protein expression, or their function *in vivo*. Chapter 3 will compare the biology of mammalian platelets to that of avian thrombocytes to determine if responses to collagen in cellular hemostasis are conserved throughout evolution.

Effects of blood rheology on platelet interaction with the vessel wall

Blood rheology is an important component for platelet activation under arterial conditions. Blood flow is considered to be laminar, meaning that layers of blood pass each other at different velocities, resulting in a flow gradient where the velocity is highest in the middle of the vessel and almost zero at the vessel wall[9]. The flow velocity gradient is highest near the edge of vessel and very small near the middle of the vessel. As a result of this velocity gradient, shear rate (γ), the rate at which flow velocity changes (expressed as s^{-1}), and shear stress (τ), the tangential force per unit area exerted in the direction of flow (expressed as dynes/cm^2), are greater at the vessel wall than in the middle of the vessel. Areas of increased shear rate and shear stress, such as the edge of the vessel wall, have a positive effect on platelet adhesion[9,10].

The shear rates are very low in large vessels but increase to 1500 s^{-1} in small arteries and can increase dramatically to 40,000 s^{-1} in stenosed arteries[11]. This increased vessel shear rate in the setting of atherosclerosis is certainly an important factor contributing to pathologic activation and adhesion of platelets. The presence of red blood cells, which normally occupy 38-48% of blood volume, also has a profound effect on platelet distribution within a vessel. As shear rates increase, red blood cells are found toward the center of the vessel, and the smaller platelets are pushed toward the vessel edge, further facilitating platelet interaction with the vessel wall[12]. Increased blood viscosity also exerts a positive effect on platelet deposition[13]. The higher shear rate and shear stress of stenosed arteries and the role of blood viscosity are all contributing factors in the setting of arterio-thrombotic cardiovascular disease. Chapters 2 and 3 will examine the adhesion and aggregation of platelets in response to collagen, using flow chambers that reproduce arterial flow conditions.

Platelet activation

Several aspects of platelet cell biology allow for an efficient response to vascular injury. Upon encountering subendothelial ECM components such as von Willebrand Factor (vWF) or collagen and being exposed to soluble activators such as thrombin, adenosine diphosphate (ADP), serotonin (5-hydroxytryptamine or 5-HT), or thromboxane (TXA_2), platelets undergo a rapid and coordinated process of shape change associated with the transition from a quiescent to an activated state. Platelet activation is associated with cell spreading, which allows platelets to flatten and cover a damaged surface through

lamellipodia formation. Activation and recruitment of additional platelets is facilitated by filopodia extension. These spreading processes involve dynamic reorganization of the actin cytoskeleton and expansion of platelet surface area through recruitment of extensive membrane infoldings called the open canalicular system. The ability of platelets to rapidly change from a discoid shape to a flattened, spread shape is crucial to their functioning effectively as hemostatic cells. In Chapter 3, the ability of avian thrombocytes to perform these spreading processes will be examined to determine if this element of cellular hemostasis is conserved through evolution.

Platelet responses to collagen under arterial flow conditions

Thrombus formation at the sites of arterial injury requires the coordinated process of platelet adhesion, activation, degranulation, and aggregation. These events occur within seconds in the high-flow environment of the arterial system, and an individual platelet has only nano- to microseconds during which to interact with a site of vascular injury. Fibrous collagens, especially types I and III, constitute up to 40% of the proteins of the vessel wall, and these are the major ECM proteins that support robust platelet adhesion and activation[14]. Along with thrombin generation, collagen exposure to the rolling platelet is a primary event in platelet-mediated thrombosis (Fig 1-1). Platelets express two receptors, glycoprotein VI (GPVI) and the $\alpha_2\beta_1$ integrin, which have significant roles in the interaction of platelets with collagen[15,16]. Chapter 2 will discuss a unique element of GPVI signal transduction. Chapter 3 will consider collagen-induced cellular

hemostasis in the chicken, which does not have platelets but instead has larger, nucleated thrombocytes that do not express GPVI.

GPVI is a platelet receptor for collagen

The role of GPVI as a platelet collagen receptor was initially based on the observation that patients deficient in this protein exhibit a bleeding tendency and defective platelet aggregation in response to collagen[15,17]. GPVI is mapped to a gene cluster known as the leukocyte receptor complex (LRC, on chromosome 19 in humans) which includes killer-inhibitory receptors (KIRs), leukocyte Ig-like receptors (LILRs), and the IgA receptor FcαRI, among other Ig-domain containing receptors[18,19]. As an LRC gene, GPVI is a member of the paired immunoglobulin (Ig) receptor superfamily but is expressed exclusively on platelets and megakaryocytes[20]. The closest homolog of GPVI is FcαRI, expressed on neutrophils, eosinophils, monocyte/macrophages, and interstitial dendritic cells, and both GPVI and FcαRI require association with the adaptor protein FcRγ via transmembrane arginines on the receptor for normal surface expression and signal transduction[18,21,22].

The absence of 11 consecutive amino acids in the sequence of GPVI, compared to that of FcαRI, creates a shallow hydrophobic groove on the surface of the distal Ig domain that forms a putative collagen-binding site[23]. GPVI is believed to exist as a dimer where two GPVI Ig domains form parallel collagen binding grooves[23,24]. GPVI only recognizes fibrillar, not monomeric, collagen and binds to glycine-proline-hydroxyproline (GPO) triplets that constitute about 10% of the primary sequence of

collagens type I and III[25]. While the heterogeneity of collagen ligand makes it difficult to determine an absolute affinity, GPVI appears to be a relatively low-affinity collagen receptor, with the estimated K_d of GPVI and collagen being 57 μM[24,26]. Additionally, GPVI is capable of binding and activating platelets in response to laminin, another subendothelial basement membrane protein that adopts a similar triple helical structure[26,27]. This finding suggests that GPVI may function less as a highly specific collagen receptor and more as a sensor for the presence of ECM proteins. Chapter 3 will consider whether chicken thrombocytes express collagen receptors capable of signal transduction and thrombocyte activation.

The study of GPVI has been aided by the existence of high-affinity GPVI-specific ligands that readily induce GPVI clustering on the cell surface and subsequent platelet activation. Synthetic collagen-related peptide (CRP) contains multiple runs of the GPO motif cross-linked to recapitulate the quaternary structure of collagen[28,29], and the C-type lectin convulxin (CVX), isolated from the venom of the *crotalus durissus terrificus*, forms a hexamer that binds the proximal Ig domain of the receptor[30].

$\alpha_2\beta_1$ integrin is a high-affinity collagen receptor

The $\alpha_2\beta_1$ integrin was the first collagen receptor to be identified on platelets and is expressed at copy numbers roughly equal to that of GPVI[31]. The α_2 subunit of this integrin contains an I ("inserted") domain which binds collagen with relatively high affinity compared to GPVI (K_d = 35-90 nM) in a Mg^{2+}-dependent manner. $\alpha_2\beta_1$ recognizes the Gly-Phe-[hydroxy]Pro-Gly-Glu-Arg (GFOGER) motif, found in various

collagen subtypes but constituting only about 0.02% of the primary collagen sequence[32]. A role for $\alpha_2\beta_1$ in platelet activation has not been well established, although the integrin has the potential to transduce signal that could function in concert with GPVI signaling[33-35]. However, collagen-induced platelet activation responses such as aggregation, degranulation, and fibrinogen binding are almost completely normal in $\alpha_2\beta_1$-deficient platelets[34,36].

Like the well-characterized $\alpha_{IIb}\beta_3$ platelet integrin, one factor complicating the study of $\alpha_2\beta_1$ is its strict dependence on "inside-out" signals to activate the integrin from a low- to high-affinity state where it is capable of binding ligand[37,38]. Platelet integrins, including $\alpha_2\beta_1$, can be activated by G-protein coupled agonists such as thrombin and ADP. However, the absolute dependence on GPVI signaling in *ex vivo* collagen assays suggests that when collagen is the sole activator, GPVI is required to stimulate $\alpha_2\beta_1$ before the integrin is able to bind ligand. Regardless of how it is activated, $\alpha_2\beta_1$ is required for firm adhesion to collagen under hemodynamic flow, serving as a high-affinity collagen receptor that, once activated, arrests platelet translocation along the vessel wall[39-41]. This dissertation will not focus on $\alpha_2\beta_1$ directly, but it is important to consider its role in platelet adhesion to collagen under flow, which will be discussed in depth in Chapters 2 and 3.

GPVI activates platelets through an immune-receptor signaling pathway

Structure-function studies in platelets and cell lines have established that GPVI signal transduction mechanisms are analogous to immune receptor pathways seen in other

hematopoietic cells. Like other immune cell receptors, GPVI is believed to exist on the membrane within lipid rafts, and ligands that induce receptor clustering initiate GPVI signal transduction through colocalization of effector proteins[42,43]. Upon receptor ligation, GPVI signal transduction is initiated as follows: the GPVI-bound FcRγ adaptor, which contains an immunoreceptor tyrosine-based activation motif (ITAM), is phosphorylated by membrane-bound Src-family kinases (SFKs), specifically Lyn and Fyn, leading to recruitment and activation of the tyrosine kinase Syk (Fig. 1-2). Syk activation initiates assembly of a signaling complex via phosphorylation of the adaptor proteins linker for activated T-cells (LAT), Gads, and Src homology (SH)2 domain-containing leukocyte phosphoprotein of 76 kD (Slp-76) (Fig. 1-2). Assembly of this signaling complex leads to activation of phospholipase C (PLCγ2). PLCγ2 cleavage of phosphatidylinositol 4,5-bisphosphate (PIP_2) culminates in activation of protein kinase C (PKC) and generation of Ca^{2+} flux, a common endpoint for platelet activating signals (Fig. 1-2)[16,22,44-53]. GPVI also employs signal transduction mechanisms that are unique compared to other FcRγ-coupled immune receptors, and these observations will be described in Chapter 2.

GPVI is required for collagen-induced platelet activation

Genetic and pharmacologic studies have demonstrated that GPVI is both necessary and sufficient to activate platelets in response to collagen. GPVI- or FcRγ-deficient mouse platelets do not aggregate, degranulate, or activate integrins in response to collagen[36,54,55]. Deficiency of GPVI signaling effectors such as SFKs Lyn and Fyn, Syk, LAT, Slp-76,

and PLCγ2 also abolishes collagen-induced platelet activation[47,48,50,51,56,57]. In the absence of the other major platelet collagen receptor, α2β1, discussed later, GPVI is capable of inducing normal platelet activation in response to collagen[34,36]. Additionally, expression of GPVI in cell line systems that express immune-type signaling effector molecules is sufficient for collagen-induced signal transduction[58,59].

Using various blood perfusion chamber approaches for both mouse and human platelets, GPVI-FcRγ has been shown to be crucial for platelet adhesion to collagen under arterial shear conditions, an *ex vivo* response that most closely represents that function of platelets *in vivo*[36,40,60-62]. Chapter 2 will address whether and how GPVI has adapted this immune receptor signaling pathway to accelerate platelet activation kinetics required for adhesion to collagen under flow.

The role of GPVI in models of thrombosis and hemostasis

Atherosclerosis involves pathological changes to the vessel wall, such as an increase in ECM deposition, especially that of collagen[63]. Prothrombotic material exposed following plaque rupture induces strong platelet activation that is GPVI-dependent, thereby suggesting a role for GPVI in athero-thrombotic disease[64,65]. Studies in the mouse aimed at establishing the importance of GPVI in mediating arterial thrombosis have produced varying results, likely due to the different types of arterial injuries produced by experimental models. GPVI deficiency has little effect on thrombosis following laser injury to the cremasteric muscle arteriole, believed to be due to the fact that thrombosis in this model is thrombin-dependent and subendothelial collagen is not exposed[66-68].

However, more extensive injury model systems can be employed, such as a ferric chloride ($FeCl_3$)-induced injury to the cremasteric arterioles or mesenteric and carotid arteries, where reactive oxygen species destroy the endothelium and expose basement membrane collagen[69]. In more substantial injury models, including $FeCl_3$, GPVI-induced platelet activation is a requirement for thrombosis[67,70-72]. Tail bleeding times of GPVI-deficient mice are either normal or only slightly prolonged, however, suggesting that GPVI may not be essential for normal platelet function following minor trauma[54,55,73,74]. The role of GPVI in hemostasis and thrombosis *in vivo* will not be directly examined in this work. However, the mechanism by which GPVI is able to rapidly activate platelets under hemodynamic flow conditions, a requirement for normal hemostasis and pathologic arterial thrombosis, which will be considered in Chapter 2. Chapter 3 will address whether this fundamental mechanism of thrombus formation following collagen exposure is present in organisms that contain thrombocytes instead of platelets.

The role of GPVI in human cardiovascular disease

Increased expression of GPVI or $\alpha_2\beta_1$ on platelets is associated with increased risk of athero-thrombotic disease and implicated as a negative prognostic biomarker in patients with cardiovascular disease[75-80]. It has been difficult to determine a role for GPVI in hemostasis in humans since most cases of GPVI deficiency are seen in patients with anti-GPVI auto-antibody production associated with some degree of immune thrombocytopenia[81]. Isolated deficiency of GPVI by compound heterozygosity, although extremely rare, is associated with only a mild bleeding diathesis[82,83]. Together, the

finding that GPVI deficiency confers a protection from thrombosis, while not producing a bleeding phenotype, has generated interest in pharmacologic targeting of GPVI for therapeutic potential. GPVI inhibition may help prevent the formation of pathologic thrombi associated with the coronary and cerebral arteries[70,84]. Continued investigation of GPVI and collagen-induced cellular hemostasis as a fundamental mechanism of arterio-thrombotic disease and as a potential therapeutic target in humans is warranted.

A model for platelet responses to collagen under flow and the role of GPVI

Extensive work has demonstrated that, on a collagen-coated surface under hemodynamic flow in the absence of thrombin activity, platelets will translocate, or "roll," along collagen, activate, firmly adhere, and form 3-dimensional aggregates[85]. This process is initiated by platelet receptor GPIba/IX/V contact with collagen-bound vWF that is linearized by high shear forces on the vessel wall[10,86]. The platelet-vWF interaction results in platelet translocation along the vessel edge and allows GPVI to interact with collagen and transduce signals that activate the platelet (Fig. 1-3). GPVI binds collagen with low affinity and is therefore unlikely to directly mediate firm adhesion to collagen. However, GPVI signaling through FcRγ, Syk, Slp-76, and PLCγ2 is crucial for activation of high-affinity integrins, such as $\alpha_2\beta_1$, which mediate firm adhesion to collagen, and $\alpha_{2b}\beta_3$, which binds fibrinogen in plasma to cross-link platelets for aggregate formation (Fig. 1-3). The fact that some platelet adhesion is observed in the absence of GPVI suggests that integrins can be activated to some degree through alternative pathways, perhaps through GPIb/V/IX signaling or shear force-induced conformational change of

integrins[87,88]. GPVI signaling also results in platelet degranulation, releasing ADP and TXA_2 that activate platelet G-protein coupled receptors in an autocrine and paracrine fashion to augment platelet activation and promote aggregate growth (Fig. 1-3). Furthermore, platelet activation through GPVI and positive-feedback pathways results in flattening of the platelet shape, another requirement for efficient aggregate formation.

In vivo, platelet responses to collagen operate in conjunction with thrombin generation by the coagulation cascade and contributions from endothelial cells, becoming an increasingly complex process (Fig 1-1). Chapter 2 will address how GPVI signaling has been adapted to efficiently transition the platelet from the rolling phase to the firmly adherent phase. Chapter 3 will consider whether this model of collagen-induced activation under hemodynamic flow holds true for avian species that have thrombocytes instead of platelets.

Conclusions and outstanding questions

Platelet-mediated thrombus formation following atherosclerotic plaque rupture is the leading cause of cardiovascular death. Studies aimed at understanding this pathophysiology should focus on platelet activation and aggregation under conditions of hemodynamic flow. Collagen is a primary activator of platelets and the Ig-domain superfamily receptor GPVI is a platelet-specific receptor responsible for activation in response to collagen and platelet-mediated thrombosis. While much progress has been made in describing the function of GPVI, many questions remain. Those that will be addressed in this dissertation include:

How does GPVI, an immune-type receptor, function effectively to activate platelets under hemodynamic flow conditions?

GPVI signal transduction utilizes a signal transduction pathway analogous to that of immune receptors found on T-cells and B-cells. Receptor ligation induces clustering that results in phosphorylation of ITAM-containing adaptor molecules—FcRγ in the case of GPVI—initiating a Syk, Slp-76, and PLCγ2-dependent signaling cascade. A major difference between immune cells and platelets is that signaling in immune cells is designed to take place over the course of hours, through immune synapse formation and results in gene transcriptional regulation. GPVI must activate the platelet extremely rapidly to coordinate collagen-induced activation under conditions of hemodynamic flow. Whether and how GPVI has adapted this immune receptor signaling pathway to better suit the unique context of platelet physiology will be examined in Chapter 2.

Is collagen-induced platelet activation a conserved element of cellular hemostasis?

The ability of platelets to be activated by collagen is a fundamental aspect of platelet biology, and collagen-induced activation is mediated through GPVI. Unlike other platelet-specific receptors that are extremely well conserved, GPVI is unique to non-egg-laying mammals. As an abundant and universal component of the subendothelial ECM in all species, collagen is well suited to serve as a hemostatic activator, yet the presence of GPVI appears to be a more recent product of evolution. In the nucleated thrombocyte, a potential evolutionary precursor to the platelet, the ability to respond to collagen has not been thoroughly examined and will be discussed in Chapter 3.

Is occlusive thrombus formation universal to cellular hemostasis?

Upon contact with collagen under hemodynamic flow, platelets form thrombi, and this process can lead to vessel occlusion. The ability of platelets to mediate this response may be advantageous to mammals as a response to traumatic injury, in order to prevent catastrophic hemorrhage. Unfortunately, this platelet response contributes to pathologic thrombosis in humans and is a major contributor to morbidity and mortality from cardiovascular disease. Nucleated thrombocytes in avian species, which are larger and less numerous than platelets in mammalian species, may respond differently under hemodynamic flow conditions. The ability of thrombocytes to form 3-dimensional aggregates under arterial flow conditions is unknown and will be examined in Chapter 3. Determining whether avian thrombocytes are capable of this function will be informative in understanding whether occlusive thrombus formation in response to vessel injury is a conserved element of hemostasis in other warm-blooded organisms with a high-pressure vascular system. Studying this phenomenon in avian species will provide insight into the pathological mechanisms of mammalian platelet thrombosis that lead to human disease.

Figure 1-1. A model for coagulation system and platelet activation following vascular injury in flowing blood.

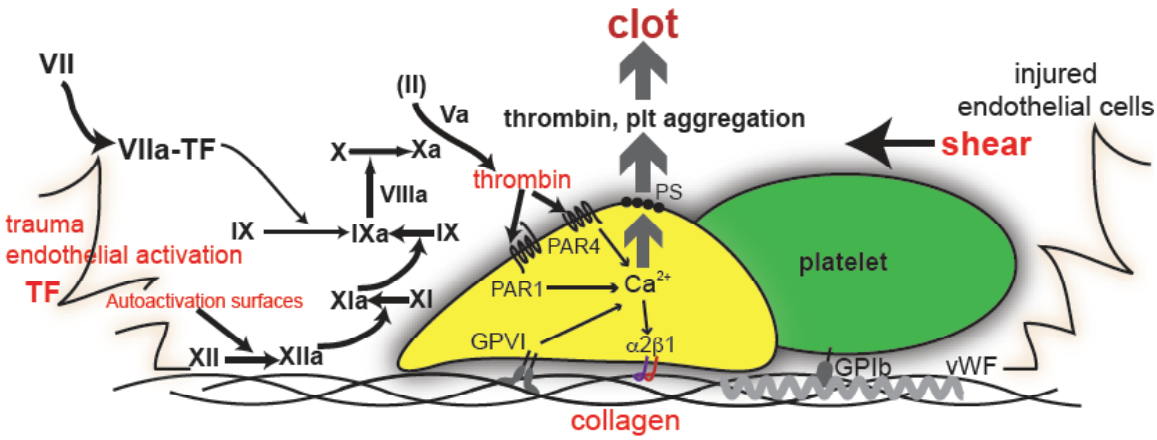

Figure 1-1. A model for coagulation system and platelet activation following vascular injury in flowing blood. Flowing blood generates shear forces that promote platelet translocation along exposed collagen through GPIb/V/IX (GPIb) interaction with Von Willebrand Factor (vWF). Collagen stimulates platelet activation through the GPVI receptor (GPVI). Endothelial injury results in exposure of tissue factor (TF), which activates coagulation factor VII (VII to VIIa-TF) and leads to factor IX activation. Independently, exposed collagen supports factor XII (XII) autoactivation to enzymatic factor XIIa (XIIa). XIIa initiates thrombin generation through a series of proteolytic reactions involving activation of factor XI (XI to XIa), which activates factor IX (IX to IXa). Factor IXa and activated factor VIII (VIIIa) activate factor X (X to Xa), which along with activated factor V (Va) activates pro-thrombin (II) to thrombin. Thrombin then stimulates platelets by activating its receptors, protease activated receptor 1 (PAR1) and 4 (PAR4). PAR activation and GPVI signaling jointly contribute to platelet activation, which results in activation of integrins ($\alpha 2\beta 1$) to mediate firm adhesion to collagen and exposure of procoagulant phophatidylserine (PS) on the platelet surface that promotes coagulation factor assembly. These events converge to create a platelet thrombus, which amplifies into a fibrin clot and leads to arterial vessel occlusion.

Figure 1-2. GPVI signal transduction.

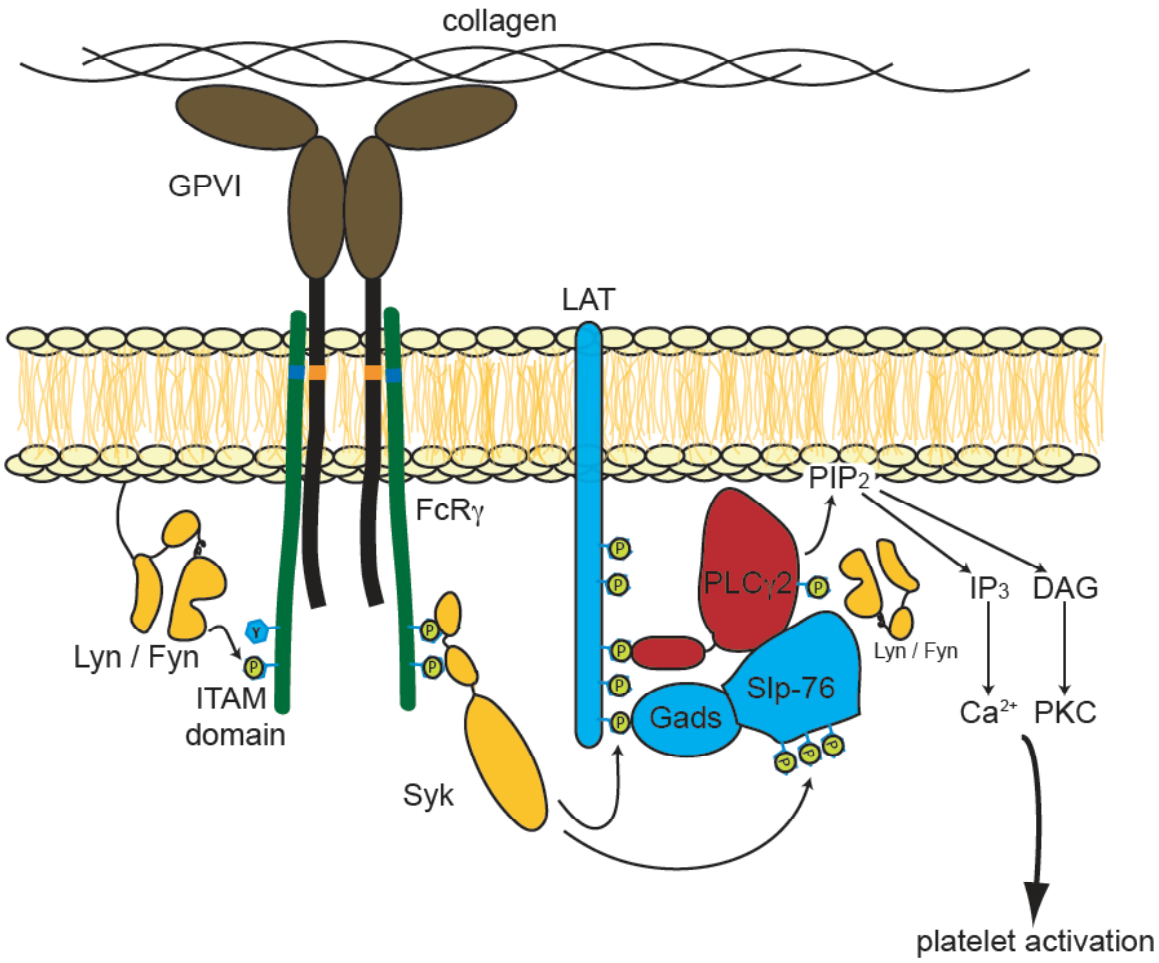

Figure 1-2. GPVI signal transduction. Collagen binding GPVI induces receptor clustering that allows SFKs Lyn and Fyn to phosphorylate tyrosine residues located on the ITAM domain of the GPVI-bound FcRγ chain. FcRγ phosphorylation results in recruitment of Syk kinase via its tandem SH2 domains. Syk phosphorylates LAT and Slp-76 to assemble a signaling complex that includes the adaptor Gads bound to Slp-76. Assembly of this complex facilitates activation of PLCγ2, which binds LAT via its SH2 domain. Throughout this process, SFKs are active in phosphorylating signaling complex components. PLCγ2 cleaves phosphatidylinositol 4,5-bisphosphate (PIP_2) to generate inositol 1,4,5-trisphosphate (IP_3) and diacylglycerol (DAG), which mobilize Ca^{2+} and activate PKC, respectively.

Figure 1-3. The role of GPVI in platelet responses to collagen under flow.

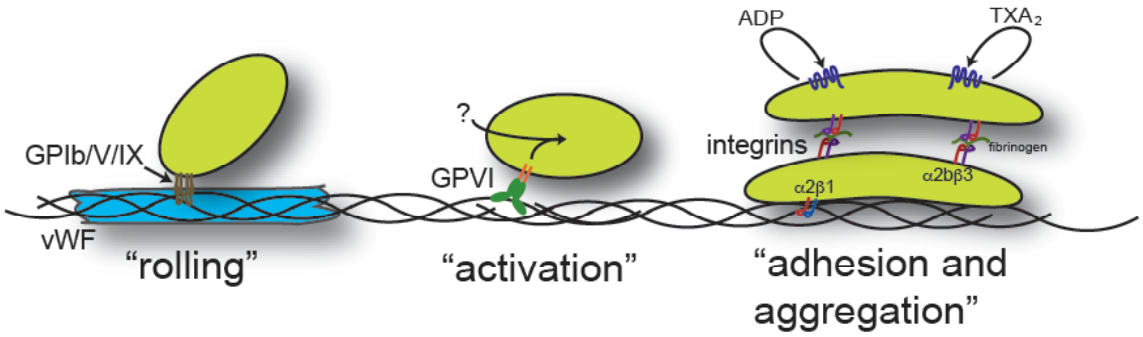

Figure 1-3. The role of GPVI in platelet responses to collagen under flow.

A model for platelet responses to collagen during hemodynamic flow in the absence of thrombin. Platelet rolling along the vessel edge is mediated by platelet GPIb/V/IX interaction with collagen-bound vWF. Platelet rolling allows for GPVI to interact with collagen and transduce signals that activate the platelet. "?" refers to additional activators that can stimulate platelets in the absence of GPVI. Platelet activation induces three essential processes: (1) shape change, which flattens the platelet profile, allowing for more efficient contact with the collagen surface; (2) degranulation, which releases soluble activators ADP and TXA_2 that increase platelet activation; and (3) activation of high-affinity integrins $\alpha_2\beta_1$ and $\alpha_{2b}\beta_3$, which mediate firm adhesion to collagen and platelet aggregation via fibrinogen binding, respectively.

Chapter 2—Molecular priming of Lyn by GPVI enables an immune receptor to adopt a hemostatic role

The data in Chapter 2 have been published in *Proceedings of the National Academy of Sciences of the United States of America*[152].

Summary

Circulating platelets use the immune receptor homolog glycoprotein VI (GPVI) to respond to collagen exposed at sites of vessel injury. In contrast to immune cell responses, platelet activation must take place within seconds to successfully form thrombi in flowing blood. In this chapter, we show that the GPVI receptor utilizes a unique intracellular proline-rich domain (PRD) to accelerate platelet activation, a requirement for efficient platelet adhesion to collagen under flow. The GPVI PRD specifically binds the Src-family kinase Lyn and directly activates it, presumably through SH3 displacement. In resting platelets, Lyn is constitutively bound to GPVI in an activated state, and platelets lacking Lyn exhibit defective collagen adhesion like that of platelets with GPVI receptors lacking the PRD. These findings define a molecular priming mechanism that enables an immune-type receptor to adopt a hemostatic function. These studies also demonstrate that active kinases can constitutively associate with immune-type receptors without initiating signal transduction before receptor ligation.

Introduction

Platelets circulate in a quiescent state but are rapidly activated at sites of vessel injury, a response essential for hemostasis in a high-pressure vascular system. Platelet activation requires the generation of rapid and coordinated intracellular signals that culminate in cell-matrix and cell-cell adhesion and thrombus formation within seconds[10,85]. Collagen, the most abundant and thrombogenic subendothelial matrix protein exposed by vessel injury, provides both a primary activating stimulus and an adhesive surface for the initiation of platelet thrombi in the arterial system. Molecular and genetic studies have established that collagen-induced platelet activation is triggered by the platelet-specific surface receptor glycoprotein (GP)VI. GPVI is a low affinity collagen receptor and is not capable of mediating direct adhesion to collagen under flow, but is required to signal in response to collagen in order to mediate activation of the high-affinity integrin $\alpha_2\beta_1$, which mediates firm adhesion to collagen. The molecular mechanisms by which circulating platelets respond to collagen are of intense interest because of collagen's primary role in arterial thrombosis.

GPVI is an immunoglobulin (Ig)-like domain-containing receptor that is structurally and functionally homologous to immune receptors but is expressed exclusively on platelets and megakaryocytes[18,20]. Extensive pharmacologic and genetic studies have demonstrated that GPVI signaling in response to collagen is highly analogous to that of the related multi-subunit T-cell receptor and the IgE and IgA receptors[46]. GPVI ligands such as collagen or the snake venom toxin convulxin induce receptor clustering that facilitates the phosphorylation of the tandem tyrosines found in

the immunotyrosine activating motif (ITAM) of the non-covalently associated FcRγ chain adaptor by Src-family tyrosine kinases (SFKs), specifically Lyn and Fyn. ITAM phosphorylation stimulates the recruitment and activation of the intracellular tyrosine kinase Syk and assembly of an immune signaling complex (see Chapter 1). This pathway, like the established G protein-coupled signaling pathways that mediate platelet activation by thrombin and ADP, results in the elevation of intracellular calcium levels and platelet activation responses, including granule release and integrin conformational changes. In contrast to immune receptors that form stable immune synapses and transmit signals which generate cellular responses over several hours, platelet activation by GPVI takes place within seconds, allowing circulating platelets to firmly adhere to exposed collagen[36,89]. Whether and how platelets have adapted the immune receptor homologue GPVI to meet the accelerated temporal requirements inherent in hemostasis is unknown.

The signaling machinery of GPVI and other immune-type receptors is encoded by their short transmembrane and intracellular domains. GPVI, like homologous immune receptors, contains a conserved transmembrane arginine that is required for its association with the FcRγ chain, the essential signal transducing component of the receptor complex[21,90-92,93]. However, a feature of GPVI that is unique among FcRγ-coupled receptors is a conserved intracellular class I (R/K)xxPxxP proline-rich domain (PRD) of the amino acid sequence K/RPLPPLP that constitutes a core binding motif for SH3 domains such as those found on SFKs[94] (Fig. 2-1A). Biochemical studies in cell lines have demonstrated that the GPVI PRD mediates binding to the SFKs Lyn and Fyn[95,96]. These studies have demonstrated variable degrees of reduced signaling by GPVI

receptors lacking this motif[59,95]. Suzuki-Inoue et al. demonstrated reduced phosphorylation of the FcRγ chain following stimulation of GPVI lacking the PRD in COS-7 cells transfected with GPVI constructs and FcRγ chain[95]. They also demonstrated an ablation of calcium mobilization in Jurkat T cells transfected with PRD-deleted GPVI, which associates with the ITAM-containing ζ-chains in this cell[95]. Jurkat T cells do not express Lyn, however. In contrast, Bori-Sanz et al. demonstrated a kinetic delay and reduced signaling strength of a GPVI truncation mutant that removed the PRD and distal C-terminal residues in rat basophilic leukemia (RBL)-2H3 cells that endogenously express FcRγ chain and Lyn[59]. The ability of cell line systems to accurately reproduce platelet biology is severely limited and cannot be used for studies under hemodynamic conditions. The role of the GPVI PRD in platelets and hemostasis has not been defined.

To study the function of the GPVI PRD, we generated mice with platelets that expressed wild-type GPVI or GPVI lacking the PRD. Our studies reveal that the PRD does not alter the strength of sustained GPVI signaling but instead accelerates platelet activation kinetics, a feature required for the efficient adhesion of platelets to collagen under flow conditions. Molecular studies to explain the basis for signal acceleration by the GPVI PRD reveal that this domain specifically binds the SH3 domain of Lyn. We find that GPVI PRD binding directly activates Lyn and that GPVI-bound Lyn in resting platelets is in an active state prior to receptor ligation. These studies provide insight into the molecular mechanism by which platelets have adapted the immune receptor signaling pathway to function under the temporal constraints of the hemostatic system.

Results

GPVI receptors lacking the intracellular PRD are expressed on mouse platelets through retroviral transduction of hematopoietic progenitors.

The proximity of the genes encoding GPVI and the homologous human FcαRI and paralogous murine PIRa in the genome and their coupling to the FcRγ transmembrane adaptor support a common evolutionary origin for these Ig-like domain-containing receptors[19]. However, a feature of GPVI that is unique among these FcRγ-coupled receptors is a conserved intracellular class I (R/K)xxPxxP PRD of the amino acid sequence K/RPLPPLP. This region is a binding motif for SH3 domains such as those of Lyn and Fyn, which phosphorylate the FcRγ ITAM (Fig. 2-1A)[47,95,97,98]. The fact that this proline-rich sequence is restricted to the GPVI receptor suggests that it confers a platelet-specific signaling function.

To examine the role of the GPVI PRD in platelet signaling, we used retroviral vectors to express wild-type human GPVI (WT GPVI) and a mutant lacking the PRD (PD GPVI) in GPVI-deficient hematopoietic progenitors that were subsequently transferred to irradiated host mice. The sequence of the cytoplasmic tail of human PD GPVI lacked 7 amino acid residues unique to the PRD and was identical to that shown by Suzuki-Inoue et al. to no longer bind SFK SH3 domains (Fig. 2-1B)[95]. Fetal liver cells from GPVI-deficient embryos were infected with retrovirus driving the expression of GFP only, or GFP with either WT GPVI or PD GPVI, and these cells were used to reconstitute lethally irradiated wild-type host animals as previously described[99]. In chimeric animals reconstituted with vectors that encoded WT or PD GPVI, GFP+ platelets co-expressed

surface GPVI (Fig. 2-1C). As expected, these chimeric animals also contained a population of GFP-/GPVI- platelets derived from GPVI-deficient donor cells that were not successfully transduced with retrovirus (Fig. 2-1C). The level of surface GPVI expression was constant and did not vary with the level of GFP expression (Fig. 2-1C), most likely because surface expression of GPVI receptors requires, and is limited by, the expression of endogenous FcRγ co-receptors[100]. The levels of GPVI expression were similar for WT GPVI and PD GPVI, indicating that both receptors are stably expressed on the platelet surface, and these levels were comparable to those found on human platelets (Fig. 2-1C and D).

Loss of the GPVI PRD does not alter sustained GPVI signaling in platelets.

Previous studies of GPVI signaling using cell lines have reported that GPVI receptors lacking the PRD signal more weakly than wild-type receptors, with virtually no signaling detected in the Jurkat T cell line and reduced signaling detected in the rat basophilic leukemia (RBL)-2H3 mast cell line[59,92,95]. To test the role of the GPVI PRD in platelets, we exposed platelets from reconstituted animals to varying concentrations of the GPVI agonist convulxin for 10 min and measured platelet activation by the surface expression of P-selectin that occurs following intracellular granule release. No significant difference in platelet activation by convulxin was detected between platelets expressing WT GPVI and PD GPVI receptors under these conditions (Fig. 2-2A and B). The ability of PD GPVI platelets to spread and form lamellipodia on type-I collagen was not altered compared to that of WT GPVI platelets, whereas vector control, GPVI-deficient platelets

did not adhere well to collagen and did not spread on collagen (Fig. 2-2C and D). Together, these results indicate that the GPVI PRD is not required for sustained signaling in response to convulxin or collagen.

The GPVI PRD is required for rapid platelet activation by GPVI.

The GPVI PRD has been shown to bind the SFKs Lyn and Fyn, a finding which suggested that this domain might accelerate the initiation of GPVI signaling by facilitating the recruitment of Lyn and Fyn to the FcRγ chain[95,96]. To test the importance of the PRD in accelerating GPVI-mediated platelet activation, platelets were stimulated with convulxin, and the degree of platelet activation at varying time points was analyzed. Platelet activation was determined by the binding of the integrin $\alpha_{2b}\beta_3$ ligand fibrinogen or by the activation state-specific anti-α_{2b} antibody JON-A. Consistent with the findings illustrated in Figure 2-2B, at 45 s the degree of activation was identical for WT GPVI and PD GPVI platelets (Fig 2-3A and B). At time points of up to 30 s following convulxin stimulation, however, platelet activation was significantly impaired in platelets expressing PD GPVI receptors compared with those expressing WT GPVI receptors (Fig. 2-3A and B). A delay in activation of PD GPVI platelets was also observed in response to stimulation with collagen-related peptide (CRP), a synthetic collagen peptide specific for GPVI that activates platelets more slowly than convulxin[28], whereas sustained signaling at timepoints of 90 and 180 sec was identical (Fig. 2-3C).

P-selectin expression is an appropriate readout for measuring sustained GPVI-induced activation, whereas fibrinogen binding is preferable for measuring GPVI signaling kinetics.

We have used P-selectin expression to compare platelet responses at 10 min, but we used fibrinogen binding for kinetic analysis of platelet activation at shorter time intervals. The rationale for this approach is that P-selectin expression is slow compared to integrin activation/fibrinogen binding and does not provide as sensitive and accurate a means of kinetic analysis. There is not a statistically significant increase in P-selectin expression before 45 sec following convulxin stimulation (Fig. 2-4A). In contrast, fibrinogen binding is detectable much earlier, i.e. by 10 sec, and there is a statistically significant change between all early time points measured (Fig. 2-4B). Conversely, we have found that the degree of fibrinogen binding can vary following a long stimulation, perhaps due to late signaling that downregulates integrin affinity, while P-selectin expression reaches a stable dose-dependent plateau and is therefore a good readout of total platelet activation.

Loss of the PRD delays proximal GPVI signal transduction in RBL-2H3 cells.

The first step in signal transduction by the GPVI receptor is the phosphorylation of FcRγ intracellular tyrosines by SFKs, an event required for the binding and activation of the downstream kinase Syk[46]. Retroviral complementation of GPVI-deficient bone marrow yields a limited number of animals that are chimeric, and these reconstituted mice often have a low percentage of platelets that express GPVI receptors. Therefore, we could not

biochemically test the mechanism of delayed PD GPVI signaling in platelets. To biochemically characterize PD GPVI signaling kinetics, we used lentiviral vectors to stably express equivalent levels of WT GPVI and PD GPVI receptors in RBL-2H3 cells (Fig. 2-5A). The RBL-2H3 mast cell line expresses endogenous FcRγ chain and has been used by our lab and others to study GPVI signaling[59,92]. Following stimulation with convulxin, RBL-2H3 cells expressing PD GPVI exhibited delayed phosphorylation of Syk, the kinase activated following FcRγ ITAM phosphorylation, relative to that of WT GPVI-expressing cells (Fig. 2-5B). However, total Syk phosphorylation at later time points was unchanged (Fig. 2-5B). We attempted to measure the kinetics of FcRγ chain phosphorylation, the primary event in GPVI signaling, in WT- and PD-GPVI-expressing RBL cells. However we were unable to detect FcRγ phosphorylation in this cell line system for technical reasons (data not shown). Lastly, elevation of intracellular Ca2+ was slower following GPVI stimulation in PD-GPVI expressing cells compared to that in WT GPVI-expressing cells (Fig. 2-5C).

The GPVI PRD is required for efficient platelet adhesion to collagen under flow.

The physiologic role of the GPVI receptor is to activate circulating platelets that come into contact with collagen at sites of vessel injury *in vivo*. Under experimental conditions of blood flow over a collagen-coated surface, GPVI signaling is essential for the transition from platelet rolling, mediated by the GPIb-von Willebrand Factor interaction, to firm adhesion, mediated by activated $\alpha_2\beta_1$ integrin-collagen interaction (see Chapter 1)[10,36,40,85]. To determine the role of the GPVI PRD during GPVI-collagen signaling

under flow conditions, whole blood from reconstituted animals was flowed over a type-I collagen patch in a microfluidic chamber, and platelet rolling and adhesion were analyzed in real time. Since each reconstituted mouse is a chimeric animal containing different percentages of GFP+/GPVI+ and GFP-/GPVI- platelets, the overall amount of platelet accumulation was not representative of how efficiently individual platelets activated transition from the rolling phase to firm adhesion. Therefore, the amount of platelet accumulation could not be used to compare the function of WT GPVI and PD GPVI receptors.

To overcome this limitation and analyze platelet adhesion in a cell-autonomous fashion, each flow experiment was analyzed frame-by-frame, and all rolling platelets were tracked to determine if and when they firmly adhered to the collagen surface (Fig. 2-6). An "adhesive efficiency" for each experiment was determined by $a / (a + r)$, where a equals the number of platelets that permanently adhered and r equals the number of platelets that rolled along collagen but did not adhere. The difference in adhesive efficiency between WT GPVI-expressing platelets and vector control, GPVI-deficient platelets was profound and consistent with previous observations that GPVI-deficient platelets are unable to adhere to collagen under flow conditions (Fig. 2-7A)[36,40,70]. A majority of WT GPVI platelets that rolled along the collagen surface successfully adhered, with an adhesive efficiency of 0.65 ± 0.11, whereas only a small number of vector control GPVI-deficient platelets were able to transition from rolling to firm adhesion, with an efficiency of 0.09 ± 0.04 (Fig. 2-7A). PD GPVI-expressing platelets exhibited a markedly reduced adhesive efficiency of 0.31 ± 0.15, demonstrating that,

compared to WT GPVI, approximately half as many PD GPVI platelets were able to transition from the rolling phase to the firmly adherent phase (Fig. 2-7A).

A second measure of how efficiently platelets adhere to collagen is the time required for each adherent platelet to transition from a rolling state to one of firm adhesion, i.e. the time each adherent platelet spends in the rolling phase. Of the firmly adherent platelets, WT GPVI platelets spent a shorter time in the rolling phase compared to PD GPVI platelets (mean rolling time 711 ± 525 ms for WT GPVI versus 972 ± 674 ms for PD GPVI; $P < 0.0005$) (Fig. 2-7B and C), a finding consistent with the slower kinetics of PD GPVI signaling which results in a longer time to activate platelet integrins and mediate firm adhesion to collagen. These observations demonstrate that the GPVI PRD is required for efficient platelet adhesion to collagen under flow, the *ex vivo* response that most closely models the physiologic role of GPVI signaling in platelets *in vivo*.

The GPVI PRD preferentially binds the SH3 domains of Lyn and Hck.

To identify all the SH3 domain-containing proteins that might bind the GPVI PRD, we expressed WT GPVI and PD GPVI cytoplasmic tails as recombinant glutathione S-transferase (GST)-fusion proteins in *E. coli* (Fig. 2-8A). Incubation of these proteins with platelet lysate followed by GST pulldowns demonstrated the ability of the GPVI intracellular tail to bind Lyn and Fyn in a PRD-dependent manner (Fig. 2-8B). Next, we used these recombinant proteins to screen a human SH3 proteome phage-display library in order to identify the preferred SH3 domain binding partners for a number of proteins

containing PRDs[101]. The WT GPVI fusion protein served as an excellent SH3 domain target in this assay, binding approximately 1000-fold more SH3 domain-expressing phage than did the PD GPVI fusion protein or GST alone (Fig. 2-8C). The identity of the SH3 domains bound by GST-WT GPVI proteins was determined by sequencing the inserts of the selected phage clones after a single round of affinity selection. Of 48 SH3 domains bound by GST-WT GPVI proteins, 40 encoded the SH3 domains of SFKs (Table 2-I). Of 48 clones sequenced in 3 independent experiments, 40 encoded the SH3 domains of SFKs (Table 2-I). Remarkably, 35/40 encoded the SH3 domain of either Lyn (16/40) or Hck (19/40) (Table 2-I). These results suggest that the SH3 domains of the SFKs Lyn and Hck are specific binding partners of the GPVI PRD.

To test the results of the SH3 domain phage display screen, we determined which of the putative partner proteins could be co-immunoprecipitated with endogenous GPVI receptors in human platelets. Lyn co-immunoprecipitated with GPVI both under resting conditions and following receptor stimulation with convulxin (Fig. 2-8D). In contrast, Fyn was observed to associate with GPVI receptors following receptor stimulation but to have little or no association with GPVI in the resting platelet (Fig. 2-8D). The Fyn SH3 domain was identified in the phage display screen, although as a rare binding partner compared to Lyn or Hck (Table 2-I). As previously reported, Src did not co-immunoprecipitate with GPVI (Fig. 2-8D). Burton's tyrosine kinase (Btk), whose SH3 domain was also identified by phage display as a less frequent GPVI tail binding protein, did not associate with GPVI in platelets (Fig. 2-8D). Consistent with previous studies[96], we could not detect Hck expression in platelets (data not shown), suggesting that Hck is

not a physiologically relevant GPVI binding partner. These findings identify Lyn as a constitutive GPVI PRD binding partner in platelets.

GPVI PRD binding directly activates the Lyn and Hck kinases.

Constitutive recruitment of Lyn to GPVI via an SH3-domain/PRD interaction could accelerate GPVI signaling merely by placing the kinase in close proximity to its substrate, the FcRγ ITAM. Alternatively, since SFKs can be activated via SH3-domain displacement[102], GPVI PRD-Lyn SH3 domain binding could directly regulate the kinase activity of Lyn. Hck and Lyn are efficiently activated through SH3 binding by the HIV-1 protein, Nef[102,103], and Hck and Lyn have been identified as the preferred binding partners for the Nef SH3 domain using the same SH3 phage display screen as that described above[101]. We therefore reasoned that the GPVI PRD might activate Hck and Lyn through a mechanism similar to that of Nef.

To determine if the GPVI PRD can directly activate Hck and Lyn, we used an *in vitro* kinase assay that has previously demonstrated direct Nef activation of these kinases [103]. Recombinant Hck, Lyn, and c-Src were expressed in insect cells with a C-terminal modification that promotes autophosphorylation and confers an inactive kinase state[103]. Purified kinase activity was then assayed *in vitro* with a peptide substrate, either alone or in the presence of increasing concentrations of purified recombinant GST-WT GPVI, GST-PD GPVI, or Nef protein. WT GPVI fusion protein activated Hck to a level comparable to that of Nef at similar molar ratios (Fig. 2-9A). WT GPVI also induced strong activation of Lyn, even at low GPVI:Lyn molar ratios, to a significantly greater

extent than did Nef under the same conditions (Fig. 2-9B). PD GPVI fusion proteins were unable to activate Hck or Lyn even at high molar excess, demonstrating the requirement for the GPVI PRD to mediate kinase activation (Fig. 2-9A and B). Consistent with the binding studies described above and with previous findings[103], neither WT GPVI nor Nef were capable of inducing c-Src activation *in vitro* (Fig. 2-9C). These observations demonstrate that GPVI functions as a direct activator of Hck and Lyn kinase activity, presumably via displacement of the intramolecular negative regulatory SH3/linker interaction within these kinases by the GPVI PRD.

GPVI-bound Lyn is held in the active state in resting platelets.

To determine if GPVI-bound Lyn is found in an activated state *in vivo*, we immunoprecipitated GPVI from human platelets under resting and stimulated conditions and used phospho-specific antibodies to assess the kinase activation state. The SFK that co-immunoprecipitated with GPVI under both resting and stimulated conditions was phosphorylated at the activation loop, indicating that it was in the active state (Fig. 2-10). More strikingly, none of the GPVI-bound Lyn was found to be phosphorylated on its negative regulatory tail, despite a large amount of cellular Lyn that was found in this inactive state (Fig. 2-10). These findings indicate that GPVI-associated Lyn is exclusively in the active state even in resting platelets. The activation-loop phosphotyrosine antibody used in these experiments recognizes all SFKs, but our studies identified Lyn as the only SFK that associates with GPVI in resting platelets (Fig 2-8D). In these assays the antibody reproducibly detected a doublet at 53 kD and 56 kD that is

characteristic of Lyn (Fig. 2-10). To ensure that the detection of activated Lyn associated with GPVI in resting platelets was not due to low-level platelet activation during cell harvest, we assessed the phosphorylation state of the FcRγ ITAM tyrosines. Robust FcRγ tyrosine phosphorylation was observed following 15 s of convulxin stimulation, but none was observed in resting platelets (Fig. 2-10), although small amounts of basal FcRγ phosphorylation have been reported previously[104]. These findings demonstrate that the Lyn associated with GPVI receptors in resting platelets is held in the active state but that the FcRγ ITAM is not phosphorylated in the absence of receptor ligand.

Lyn-deficient platelets exhibit the delayed GPVI receptor signaling and defective adhesion to collagen under flow characteristic of PD GPVI platelets.

The studies described above suggest that the rapid early signal transduction conferred by the GPVI PRD is dependent upon association with active Lyn. To test the dependence of this mechanism on Lyn, we examined GPVI signaling and collagen adhesion under flow in mouse platelets lacking Lyn or Fyn. As observed for PD GPVI platelets (Fig. 2-2), the dose response of Lyn-deficient platelets stimulated with convulxin for 10 min was similar to that of wild-type platelets (Fig. 2-11A), although at the lowest dose of convulxin stimulation a gain of function was observed in Lyn-deficient platelets consistent with previous findings[47]. However, when platelet activation responses were examined at short time points following GPVI receptor stimulation, a delay in the activation of Lyn-deficient platelets similar to that of PD GPVI platelets was observed (Fig. 2-11B). In contrast, Fyn-deficient platelets did not demonstrate a significant delay in GPVI-induced

platelet activation at short time points (Fig. 2-11C). Fyn-deficient platelets, however, exhibited a defect in activation following convulxin stimulation for 10 min, as previously reported (Fig. 2-11D)[47]. Like PD GPVI platelets, Lyn-deficient, but not Fyn-deficient, platelets exhibited a significant defect in adhesion to collagen under flow (Fig. 2-12A and B). These studies reveal that rapid GPVI signals require both the GPVI PRD and Lyn kinase. Similar to loss of the GPVI PRD, loss of Lyn confers delayed GPVI receptor signaling and defective adhesion to collagen under flow.

Discussion

Immune-type receptors are expressed by non-immune cells where they have adopted new functions, but the molecular adaptations that have fostered such novel roles remain unknown. In the present study we identify the binding and direct activation of Lyn by the PRD of the GPVI receptor as a molecular mechanism by which platelets accelerate immune receptor signaling to adapt it to hemostasis, a biological response that must take place within seconds. Previous studies have demonstrated that the GPVI PRD binds SFKs and contributes to GPVI signaling in cell lines[95,96], but the molecular consequences of GPVI PRD interaction with SFKs and the functional role of this interaction in platelet responses was unknown. Our results demonstrate that the PRD is not essential for GPVI signaling, but instead primes the receptor for rapid platelet activation required for efficient adhesion to collagen in the setting of blood flow by binding and directly activating Lyn. Additionally, these findings identify a novel molecular mechanism by which an immune receptor has become a hemostatic receptor, and they provide insight into the basic mechanisms of immune receptor signal transduction.

The activation of circulating platelets by exposed vessel wall collagen must take place within seconds for effective hemostasis, and GPVI is essential in this process [10,36,40,70,85]. GPVI is an immune-type receptor that signals through a pathway characterized by sustained and progressive signaling responses that do not typically result in extremely rapid cellular responses[89,105]. A large number of molecular and genetic studies have demonstrated that GPVI signaling in platelets is similar to that of related receptors in immune cells[16,22,44-50]. While these studies have confirmed that GPVI is

functionally a *bona fide* member of the immune receptor family, they have not addressed the way in which this signaling pathway has been adapted in platelets to serve a hemostatic role. Our findings suggest that the GPVI PRD is therefore a specialized region that accelerates immune-receptor signaling to function in a non-immune, hemostatic role.

This study provides new biological insight into the molecular regulation of SFKs through identification of an unexpected mechanism by which the GPVI PRD accelerates immune receptor–induced cellular activation. The GPVI PRD selectively binds the SH3 domains of Lyn and Hck and directly activates these kinases *in vitro*. The ability of the GPVI PRD to activate Lyn directly by binding to its SH3 domain provides a striking example of how this mechanism, first described in studies of the HIV-1 Nef protein, has an important role, not previously appreciated, in endogenous biological responses[106,107]. Studies of Hck activation by Nef support a model in which binding of Nef to the SH3 domain of Hck displaces the SH3 domain from an intramolecular association with a polyproline II helix in the SFK linker that holds the kinase in an inactive state[108]. Although studies of Nef have demonstrated SH3 domain displacement to be a potent mechanism of SFK activation that likely contributes to HIV virulence[102,103], the extent and purpose to which endogenous proteins activate SFKs by this mechanism is not clear. Our studies suggest that GPVI activation of Lyn occurs through a Nef-type SH3 displacement mechanism, although structural studies comparing SFK activation by these two proline-rich polypeptides are needed to determine whether or not they are molecularly identical. Interestingly, our *in vitro* studies demonstrate that, like Nef, the

GPVI PRD can activate forms of Lyn and Hck which are phosphorylated at their negative-regulatory C-terminal tail tyrosines, suggesting that these two regulatory mechanisms can function independently[109,110]. However, our analysis of GPVI-associated Lyn in platelets reveals that virtually none is C-terminally tyrosine phosphorylated, suggesting that GPVI binding to the Lyn SH3 domain may also positively regulate kinase activity by promoting dephosphorylation at this negative regulatory site. Future studies addressing the molecular basis of Lyn activation by GPVI may reveal whether and how these two molecular mechanisms of SFK regulation are coordinated *in vivo*.

While both Lyn and Fyn are required for optimal GPVI signaling[47], our studies suggest Lyn, but not Fyn, drives the explosive GPVI signaling required for adhesion to collagen under flow. The preference of the GPVI PRD for binding Lyn over Fyn and the observation that Lyn, but not Fyn, binds GPVI receptors in resting platelets support a division of labor in which PRD-bound Lyn drives initial GPVI-induced platelet activation and Fyn participates in more sustained GPVI signaling. This model of SFK signaling downstream of GPVI is supported by biochemical studies demonstrating a delay in FcRγ, Syk and PLCγ2 phosphorylation following GPVI stimulation of Lyn-deficient platelets[111]. Consistent with this model, PD GPVI receptors exhibit delayed Syk phosphorylation and calcium signaling in RBL-2H3 cells.

A final question raised by these findings is whether GPVI-bound activated Lyn affects other Lyn substrates in the platelet. There are roughly 1500 GPVI receptors expressed on the platelet surface[58], a number that is likely to be considerably lower than

the total quantity of intracellular Lyn. We therefore speculate that GPVI-induced activation of Lyn is unlikely to significantly affect the phosphorylation of other Lyn substrates because of both physical sequestration of the activated kinase and the relatively small effect on the activation state of total Lyn.

Our studies also provide unexpected insight into ITAM activation, a primary step in all immune receptor signal transduction. An apparent paradox raised by our findings is how the GPVI receptor can constitutively associate with activated Lyn kinase yet not phosphorylate the ITAM of its co-receptor FcRγ and activate the resting platelet. A recent study of ITAM phosphorylation by the T cell receptor has revealed that the CD3ε ITAM is embedded in the lipid bi-layer of the cell membrane and sequestered from activating SFKs in unstimulated cells[112]. Through a yet undefined mechanism, T cell receptor ligation and clustering result in release of the ITAM from the membrane, exposure to SFKs, and initiation of downstream receptor signaling[112]. These findings suggest that a similar sequestration of the FcRγ ITAM in the cell membrane may allow activated Lyn to be held by GPVI in the immediate proximity of the FcRγ subunit without initiating signal transduction prior to receptor-ligand interaction (Fig. 2-13). Future studies of GPVI-FcRγ signaling in platelets, e.g., mutation of the acidic membrane proximal residues in FcRγ proposed to mediate lipid interaction and separation from the GPVI receptor tail[93,112], may be informative regarding both the basis of signal acceleration by the GPVI PRD and ITAM signaling by immune receptors.

It is intriguing to consider the appearance of the GPVI PRD in the context of platelet and immune receptor evolution. Adaptive immunity and ITAM signaling

receptors emerged over 500 million years ago with jawed vertebrates[113], while platelets appeared more recently in mammals, 300 million years ago[7]. The GPVI receptor is encoded by a gene in the leukocyte receptor complex (LRC), a region of the mammalian genome that underwent rapid evolution between egg-laying mammals, such as the platypus, and placental and marsupial mammals[114,115]. Consistent with its location within the re-organized mammalian LRC, homology-based searches reveal clear GPVI orthologs in the genome of placental and marsupial mammals but not in the platypus or avian genomes. Thus the GPVI receptor appears to have evolved with other LRC immune receptors after platelets had already appeared in mammals (see Chapter 3). Alignment of the predicted opossum and human GPVI receptor amino acid sequences reveals the presence of a highly conserved intracellular PRD that is present in all known GPVI receptors (Fig. 2-1A). These observations suggest that acceleration of immune receptor signaling by the PRD may have been instrumental in the evolution of GPVI as a platelet collagen receptor.

The identification of a molecular mechanism by which an immune-type receptor accelerates signal transduction to perform a hemostatic function in platelets may also direct new therapeutic strategies to treat cardiovascular disease. Collagen activation of platelets is a primary event in the formation of arterial thrombi that cause heart attack and stroke. Agents that target the PRD of GPVI may selectively block rapid platelet collagen responses without inhibiting overall hemostasis and non-hemostatic immune receptor signaling.

Materials and methods

Animals

GPVI-deficient and Lyn-deficient mice have been previously described[54,116]. Wild type C57/BL6 mice were purchased from Charles River Laboratories (Wilmington, MA). All of the mice used for study were maintained in the animal facility of the University of Pennsylvania in accordance with National Institute of Health guidelines and approved animal protocols.

Antibodies and reagents

Anti-human GPVI monoclonal antibodies HY101 and 6B12 were produced as previously described [58] and were conjugated with Alexa Fluor-647 using the Monoclonal Antibody Labeling Kit purchased from Molecular Probes (Eugene, OR). Convulxin, AYPGKF peptide, and PE-conjugated anti-murine CD62P (P-selectin) antibody were purchased from previously described sources[117]. Collagen-related peptide (CRP) was obtained from Dr. Richard Farndale (Cambridge, UK). FITC-conjugated polyclonal anti-rabbit Ig was purchased from BD PharMingen (Eugene, OR). JON/A, JAQ1, and Leo.H4 monoclonal antibodies were purchased from Emfret Analytics (Eibelstadt, Germany). Type-I fibrillar collagen (1 mg/mL) derived from equine tendon was purchased from Chronolog (Havertown, PA). Purified acid-soluble fibrillar collagen (PureCol™) derived from bovine hide (3 mg/mL) was purchased from Inamed (Freemont, CA). Rat anti-mouse CD41 (integrin α_{2b}) monoclonal antibody was purchased from BD Biosciences (San Jose, CA). Alexa-Fluor 488 and 647 Monoclonal Antibody Labeling Kits, Alexa-Fluor 647-

conjugated human fibrinogen, and Alexa-Fluor 594-conjugated phalloidin were purchased from Invitrogen (Carlsbad, CA). Murine stem cell factor (MSCF), IL-3 and IL-6 were purchased from PeproTech (Rocky Hill, NJ). Anti-GFP, anti-Lyn, anti-Fyn, anti-Syk, and anti-Btk rabbit polyclonal antibodies were obtained from Santa Cruz Biotechnology (Santa Cruz, CA). Anti-FcRγ chain rabbit polyclonal antibody was obtained from Abcam (Cambridge, MA). Anti-phosphotyrosine mouse monoclonal antibody 4G10 was obtained from Millipore (Billerica, MA). Anti-phospho Src family (Y416), anti-phospho Lyn (Y507), and anti-phospho Syk (Y525/526) rabbit polyclonal antibodies, and anti-Src rabbit monoclonal antibodies were obtained from Cell Signaling (Beverly, MA).

Retrovirus production

The cDNA of human GPVI was subcloned into the p-GEM-T Easy vector (Promega, Madison, WI), and site-directed mutagenesis to remove the PRD was performed using the Stratagene QuickChange site-directed mutagenesis kit (La Jolla, CA). The oligonucleotide used for site-directed mutagenesis has been previously described[95]. Wild-type and PRD deleted GPVI were subcloned into *XhoI*/*HpaI* sites of the murine stem cell virus MigR1 vector with an IRES-GFP inserted prior to the polyadenylation signal, as described previously[99]. Production and titering of retrovirus was performed as previously described[118]. For RBL-2H3 cell infections, wild-type GPVI and GPVI lacking the proline-rich domain were subcloned into *XbaI*/*EcoRI* sites the HFUW lentiviral vector (kind gift from Dr. Eric Brown from Department of Cancer Biology,

University of Pennsylvania School of Medicine). The lentiviral vectors were packaged using HEK 293T cells.

Fetal liver reconstitution

Reconstitution of lethally irradiated animals with stem cells derived from fetal liver was performed as previously described[99]. Briefly, fetal liver cells from *gp6*$^{-/-}$ embryos at E14-E16 were harvested, and mononuclear cells were isolated using Lympholyte (Cedarlane Labs, Burlington, NC) gradient and cultured overnight in IMDM (Invitrogen) with 10% fetal bovine serum in the presence of 100 ng/mL MSCF, 20 ng/mL IL-3, and 10 ng/mL IL-6. The cells were then spin-infected twice with *gp6* retroviruses at a multiplicity of infection equal to 5 virions per cell. A total of 1 x 10^6 cells (250 μL per mouse) were retro-orbitally injected into 8-10-week-old C57/BL6 donor mice that received a lethal dose of 900 cGy total body irradiation. All platelet studies were performed at least 6 weeks after transplantation.

GPVI antibody staining

For mice, a drop of blood was collected from the tail vein, whereas for humans a drop of blood was obtained from a finger-stick from a healthy donor into 100 μL of Tyrode's buffer (137 mM NaCl, 1 mM $MgCl_2$, 2.7 mM KCl, 3.3 mM NaH_2PO_4, 1 g/L BSA, 5.6 mM glucose, 20 mM HEPES, pH 7.4) containing 15 U/mL heparin. Diluted whole blood was incubated with Alexa-Fluor 647-conjugated HY101 anti human GPVI antibody at 2 μl/mL for 30 min at room temperature, and samples were analyzed using flow cytometry.

Murine blood collection

Mice were anesthetized with 16 μg/g body weight tribromoethanol, and 100 μL of whole blood was collected by retro-orbital bleeding with a heparinized capillary tube. Platelet-rich plasma (PRP) was obtained by diluting whole blood 1:2 in Tyrode's buffer and performing centrifugation at 100 *g* for 4 min.

Platelet spreading assay

Lab-Tek II chamber slides (Thermo Fischer Scientific, Rochester, NY) were coated with type I fibrillar collagen at 30 μg/mL in 50 μM acetic acid for 16 h at 4 °C, washed 3 times with PBS, and blocked with BSA 1 mg/mL in PBS for 30 min at room temperature. PRP was diluted to 2 x 10^7 platelets per mL in modified Tyrode's buffer (137 mM NaCl, 20 mM HEPES, 2.7 mM KCL, 3.3 mM NaH_2PO_4, 5.6 mM glucose, 1 g/L BSA, pH 7.4) containing 1 mM $MgCl_2$, and 5 x10^6 platelets were incubated on the collagen-coated chambers for 45 min at 37°C. Fixation, permeablizing, and staining were performed as previously reported[119]. Following 3 washes in PBS, adherent platelets were fixed with 3% paraformaldehyde in PBS for 40 min, washed 3 times in PBS, and permeablilized with 0.3% Triton X-100 in PBS with BSA 1 mg/mL for 2 h. After 3 washes in PBS, platelets were incubated with anti-GFP rabbit polyclonal antibody (10 μL/mL) for 16 h at 4°C, washed 3 times in PBS, and incubated with FITC-conjugated polyclonal anti-rabbit Ig (2 μL/mL) for 2 h at room temperature. Filamentous actin was stained with Alexa-Fluor 594-conjugated phalloidin (25 μL/mL) for 45 min at room temperature. Platelet

spreading was imaged as previously described[99], and only platelets with both GFP and actin staining were visualized. Platelet surface area was measured in pixels using Image J software (National Institutes of Health, Bethesda, MD) particle analysis. Particles of sizes from 250 to 4050 pixels, which represented those well-separated platelets, were measured.

Platelet stimulation assays

Platelet stimulation assays quantified by flow ctytometric analysis were perfomed as previously described[99]. Platelet-rich plasma (PRP) was diluted to 2.5 x 10^7 platelets per mL in modified Tyrode's buffer, and 2.5 x 10^6 platelets were stimulated with varying concentrations of convulxin for 10 min at 37°C in the presence of PE-conjugated anti-murine P-selectin antibody (2 μL/mL, BD Biosciences) and 1 mM $CaCl_2$ and $MgCl_2$. In time-course assays, 2.5 x 10^6 platelets were stimulated were stimulated with 10 nM convulxin (Alexis) or 10 μg/mL CRP for the time indicated in the presence of Alexa-Fluor 647-conjugated fibrinogen, and the reaction was stopped by addition of 1% paraformaldehyde for 5 min followed by washing. In time course assays using JON/A antibody binding, platelets were stimulated with 10 nM convulxin for the time indicated at room temperature, and the reaction was stopped by addition of 1% paraformaldehyde for 5 min followed by washing. Platelets were then stained by addition of PE-conjugated JON/A antibody (10 μL/mL) for 30 min at room temperature. Fibrinogen and antibody binding were measured with a FACSort (BD Biosciences, San Jose, CA), and the data were analyzed with FlowJo 6.3.1 software (Tree Star, Ashland, OR).

Ca^{2+} mobilization assays

RBL-2H3 cells were labeled with Fura-2 AM (Molecular Probes, Eugene OR), and calcium signaling was detected as previously described[58]. Briefly, RBL-2H3 cells transfected with lentivirus driving expression of WT or PD GPVI or vector alone were grown to confluence in a 10 cm culture dish and many cells had detached from the dish surface. These non-adherent RBL-2H3 cells are perfectly viable. Floating and adherent cells were isolated by successive aspiration, washed in RHB medium (RPMI 1640 [Invitrogen] containing 25 mM HEPES and 1 mg/mL BSA), and resuspended to a concentration of 2 x 10^7 cells per mL. Fura-2 AM was added to the cell suspension at a final concentration of 4 μg/mL and incubated at 37 °C in 5% CO_2 for 30 min. Cells were washed twice in RHB medium and resuspended in RHB medium at a concentration of 2 x 10^6 cells per mL. Aliquots of 1.4 mL of labeled cells were analyzed in a Fluorescence Spectrometer under stirring conditions following addition of agonist.

Fabrication of microfluidic devices, collagen patterning, and whole blood flow assay

Fabrication of microfluidic devices and microfluidic collagen patterning was performed as previously described [39]. Channels were initially filled with 1 mg/mL BSA in HBS to ensure that no bubbles were trapped in the channel. Whole blood from reconstituted mice was collected retro-orbitally as described above. Blood was incubated with JAQ-1 antibody at 25 μg/mL for 10 min, to block any wild-type mouse GPVI on platelets derived from host precursors that escaped bone marrow ablation, and with 5 μg/mL

Leo.H4 monoclonal antibody, to prevent aggregate formation for ease of analysis. Whole blood from *lyn*-/- or *fyn*-/- mice and wild-type controls was collected retro-orbitally in heparinized capillary tubes, labeled with Alexa-Fluor 488-conjugated CD41 antibody, and incubated with 5 μg/mL Leo.H4. A volume of 70 μL of whole blood was placed on the inlet of the device and withdrawn by a syringe pump (Harvard Apparatus PHD 2000, Holliston, MA) for up to 4 min at flow rates of 5 μL/min to achieve a full channel width-averaged wall shear rate of $\bar{\gamma}_{chan} = 1000\ s^{-1}$.

Image capture and analysis

The adhesion of GFP+ platelets or fluorescently labeled platelets was monitored continuously by epifluorescence microscopy. For blood from reconstituted animals, images were captured continuously with a 60-200 ms exposure time depending on the percentage of GFP+ platelets in each mouse at an interval of 100 ms using Slidebook software (Intelligent Imaging Innovations). Every new rolling platelet that appeared was tracked in subsequent frames to determine if it ultimately adhered firmly to the collagen surface or if it continued to roll but did not adhere. All analyses were performed with the observer blinded to the identity of the sample. All image stacks were analyzed frame-by-frame in Slidebook. Any platelet that was captured by fluorescent imaging was presumed to be rolling along the collagen surface, as non-rolling GFP+ platelets, leukocytes, and red blood cells moved too fast to be visualized. Each frame was analyzed to determine if a new platelet began to roll on the patterned collagen surface. Firmly adherent platelets were defined as ones that did not change position for at least 30 frames. Platelets that

came in contact with the wall of the flow chamber were not counted. Platelets that rolled as a pre-formed clump or adhered to pre-existing platelet clumps and not to the collagen surface directly were not counted. Each experiment was only analyzed as long as individual platelet-collagen interactions could be distinguished. In determining the number of frames each adherent platelet spent rolling, the last frame before the platelet changed position for a final time was counted. Thus, a platelet that was permanently adhered by the first frame in which it was observed was counted as rolling for zero frames, and the rolling time consisted only of the interval before the frame in which the platelet appeared. The adhesive efficiency for each image stack was determined by calculating $a / (a + r)$, where a equals the number of platelets that permanently adhere and r equals the number of platelets that roll along collagen but do not adhere. The time each adherent platelet spent in the rolling phase was calculated as $(F)(Ex) + (F + 1)(Int)$, where F equals the number of frames the platelet spent rolling, Ex equals the exposure time per frame, and Int equals the interval time between captures, which was 100 ms for all experiments.

Images were captured using a CCD camera (C9300-201 Hamamatsu, Bridgewater, NJ) mounted on an inverted microscope (Nikon Eclipse TE2000-U, Melville, NY) with a 300 W Xenon lamp (Perkin Elmer Optoelectronics, Freemont, CA) through a Lambda DG-4 high-speed filter changer (Sutter Instruments, Novato, CA) used at 470 nm Ex / 525 nm Em. For blood flow experiments from *Lyn*-/- or *Fyn*-/- mice or wild-type controls, the collagen patch was defined using Image J software (National Institutes of Health, Bethesda, MD). The average background of the upstream region was

calculated for each column and those values were subtracted from the reaction zone pixel values to correct for background gradients across the width of the channel. Surface coverage was calculated by dividing the area of pixels with a value greater than zero by the area of the collagen patch.

Production of GST-fusion proteins and expression of recombinant SFKs and Nef

GST fusion proteins of the GPVI C-tail were prepared from cDNA encoding the WT or PD GPVI sequence beginning from Glu269 to the terminal Ser residue using forward primer 5'-TAGAATTCGAGGACTGGCACAGCCGGAGGAA-3' and reverse primer 5'-TACTCGAGTCATGAACATAACCCGCGGCTGTG-3'. Fragments were subcloned into *EcoRI*/*XhoI* sites of pGEX4T-1, and proteins were expressed in *E. coli* according to manufacturer instructions, purified with glutathione agarose (Amersham Biosciences, Piscataway, NJ). Human Hck, Lyn, and c-Src were expressed in Sf9 insect cells and purified to homogeneity as previously described[103]. The C-terminal sequence of each SFK was modified to Tyr-Glu-Glu-Ile-Pro, which promotes autophosphorylation of the tail tyrosine and permits high yield purification of the downregulated form of each kinase[103]. The SF2 allele of HIV-1 Nef was expressed in bacteria and purified as previously described[103].

Phage display

The phage-displayed SH3 domain library panning onto purified target proteins was performed as previously described[101]. Briefly, 6-well tissue culture plates (Cellstar) were

coated with 20 µg/mL bacterially expressed purified GST fusion proteins of the GPVI C-tail and the GPVI C-tail lacking the PD sequence or, in control experiments, GST protein alone (1.5 mL per well) in 50 mM Na-carbonate buffer pH 9.6 overnight at 4ºC. The subsequent steps were performed at room temperature. The plates were washed 3 times with 2 mL of TBS-T buffer (Tris-buffered saline [TBS] supplemented with 0.05% Tween 20) and incubated with blocking solution (5% non-fat milk in TBS-T) for 2h, followed by incubation with the mixture of human SH3 library-displaying phages (109-1010 pfu/well) prepared in TBS-T and supplemented with 2.5% of non-fat milk for 2 h. Subsequently, the phage mixture was removed and plates were washed 4 times with 2 mL of TBS-T. The infection of TG1 bacteria by phages that remained bound to GPVI C-tail proteins or GST alone was carried out by adding 1 mL of log-phased cells (OD_{600} = 0.5-0.6) to each well followed by incubation at 37ºC for 1h. Subsequently, different dilutions of infected TG1 (1:1, 1:10, 1:100, and 1:1000) were seeded onto ampicillin-containing LB plates. The next day, the resultant colony numbers from WT GPVI C-tail and from PD GPVI C-tail were compared to the number of colonies obtained from the control (GST alone) plate. WT GPVI C-tail-interacting SH3 domains were identified by performing a sequencing reaction (sequencing primer 5'-CCTATTGCCTACGGCAGCC-3') on the SH3 domain-encoding phagemides that were isolated from individual bacterial colonies.

Immunoprecipitations from platelet or RBL-2H3 cell lysate

Blood was collected from 5 healthy donors into 30 or 60 mL syringes containing 5 or 10 mL of acid citrate dextrose. Platelets were isolated from platelet-rich plasma by

centrifugation in the presence of 1 U/mL apyrase and 1 μM prostacyclin and washed once in platelet wash buffer (10 mM HEPES, 1 mM EDTA, 150 mM NaCl, pH 6.0) before resuspending in modified Tyrode's buffer. 6×10^8 washed platelets were stimulated with 10 nM convulxin or left unstimulated at 37º C with stirring, and reactions were terminated with addition of 5x lysis buffer (1% NP-40, 50 mM Tris pH 7.4, 150 mM NaCl, 2 mM EDTA final concentration) with a 1:50 dilution of EDTA-free protease inhibitor cocktail (Roche Diagnostics, Indianapolis, IN) and a 1:100 dilution of HaltTM phosphatase inhibitor cocktail (Thermo Scientific, Rockford, IL). Transfected RBL-2H3 cells were incubated in RPMI at 37ºC for 30 min at a concentration of 1×10^7 cells per mL. 6×10^6 RBL-2H3 cells were stimulated with 1 nM convulxin or left unstimulated at 37º C with stirring, and reactions were terminated with addition of an equal volume of ice-cold 2x NP40/dodecyl maltoside lysis buffer (1.6% NP-40, 2% dodecyl maltoside, 20 mM Tris, pH 7.5, 300 mM NaCl, 4 mM EDTA, 2 mM dithiothreitol)[105], with protease and phosphatase inhibitors as described above. Samples were lysed for 1 h at 4ºC, and insoluble material was pelleted by centrifugation at 15,000 *g* for 20 min. For GST-fusion immunoprecipitation, lysate was incubated with glutathione-sepharose beads conjugated with GPVI GST-fusion protein. For GPVI immunoprecipitation, lysate was incubated with 5 μg/mL HY101 monoclonal antibody or 5 μg/mL mouse IgG for 2 h at 4ºC before addition of protein-A sepharose and overnight incubation with rocking. Sepharose beads were pelleted and washed 4 times for 5 min in 1x lysis buffer before addition of Laemmli sample buffer with 2.5% β-mercaptoethanol and boiling for 10 min. Samples were run

on 4-12% v/v gradient SDS-polyacrylamide using MOPS electrophoresis buffer, transferred to PVDF membranes, blocked, and probed with antibody.

In vitro kinase assays

Production of recombinant HIV-1 Nef and tyrosine kinase assays were performed in 384-well plates using the Z'-Lyte kinase assay system and the Tyr2 peptide substrate (Invitrogen) as previously described[103]. Briefly, to assess the effect of GPVI compared to Nef on SFK activity, Hck (20 ng), Lyn (50 ng), or c-Src (50 ng) was incubated at room temperature for 5 min with increasing molar concentrations of GST-WT GPVI, GST–PD GPVI, or Nef. Purified GST-fusion proteins were dialyzed to remove free glutathione prior to use in *in vitro* kinase assays. ATP (100 μM final) and Tyr2 substrate (1 μM final) were then added to the reaction, and samples were incubated for 1 h (45 min for Hck). Development reagent, which contains a protease that digests non-phosphorylated peptide, was then added, and samples were incubated for an additional 60 min before termination of the reaction with stop reagent. Fluorescence was assayed, based on FRET between coumarin and fluorescein in the phosphorylated (uncleaved) substrate peptide only. Raw fluorescence values were corrected for background, based on a 0% phosphorylation (no ATP) negative control, and reaction endpoints were calculated as emission ratios of coumarin fluorescence divided by the fluorescein FRET signal. These ratios were then normalized to the ratio obtained with a 100% phosphorylation control peptide. Each condition was assayed in quadruplicate, and results are presented as the mean ± SD.

Statistics

P values were calculated using an unpaired two-tailed Student's *t* test assuming unequal variance.

Figure 2-1. Expression of wild-type GPVI receptors and GPVI receptors lacking the intracellular PRD in GPVI-deficient mouse platelets using retroviral vectors.

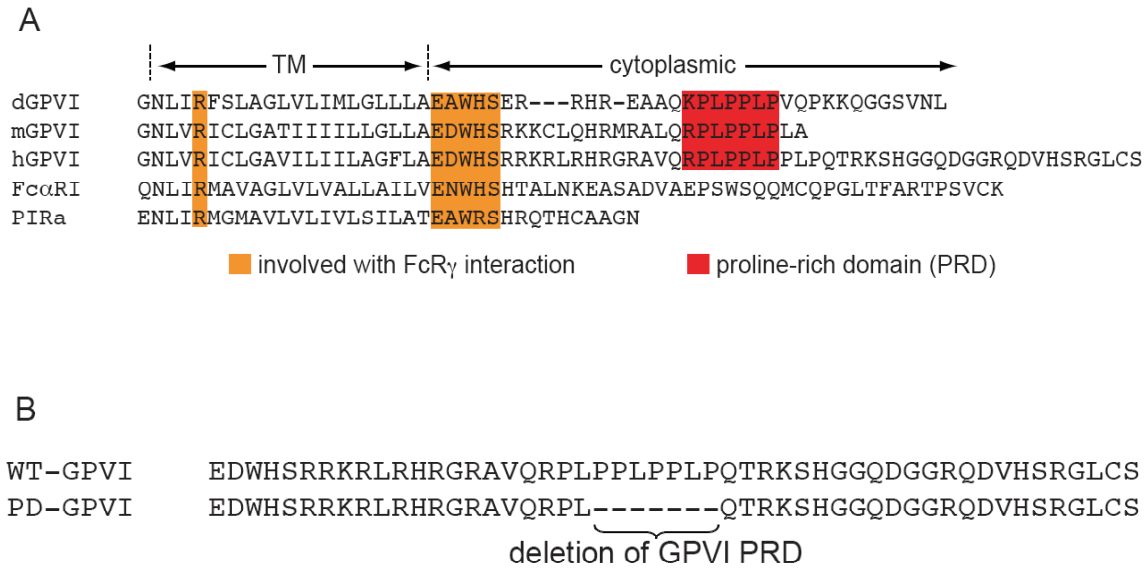

Figure 2-1 (cont'd). Expression of wild-type GPVI receptors and GPVI receptors lacking the intracellular PRD in GPVI-deficient mouse platelets using retroviral vectors.

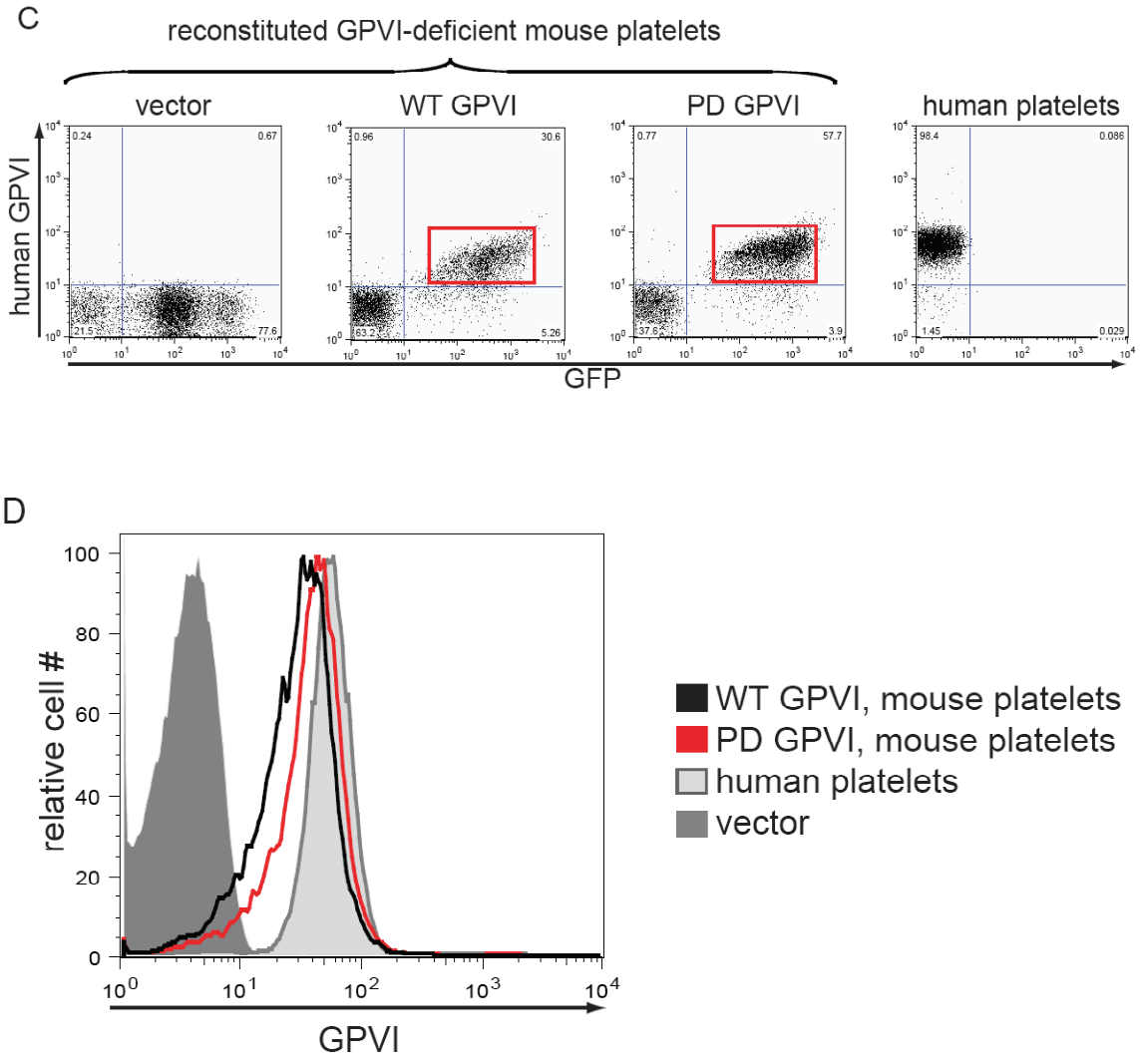

Figure 2-1. Expression of wild-type GPVI receptors and GPVI receptors lacking the intracellular PRD in GPVI-deficient mouse platelets using retroviral vectors. A. Alignment of the predicted transmembrane and intracellular amino acid sequences from opossum (d), mouse (m), and human (h) genes encoding the GPVI receptor, the homologous and paralogous human Fc alpha receptor (FcαRI), and the mouse paired Ig-like receptor (PIR)a. The amino acids shown in orange are involved in coupling of the receptor to the transmembrane signaling adaptor FcRγ. The amino acids shown in red constitute a binding motif for SH3 domains. Note the lack of the GPVI PRD in homologous immune receptors. B. The amino acid sequences of the cytoplasmic tails of the wild-type human GPVI (WT GPVI) and mutant GPVI lacking the proline-rich region of the cytoplasmic tail (PD GPVI) are shown. The sequence of the cytoplasmic tail of human PD GPVI lacked 7 amino acid residues unique to the PRD and was identical to that shown by Suzuki-Inoue et al. to no longer bind SFK SH3 domains[95]. C. Retroviral co-expression of GPVI receptors and GFP in GPVI-deficient mouse platelets. Retroviral vectors were used to co-express GFP only (vector), or GFP with either WT GPVI or PD GPVI, in GPVI-deficient fetal liver cells that were subsequently used to reconstitute lethally irradiated mice. Shown are GFP and surface GPVI expression in the platelets of animals reconstituted with cells exposed to empty vector (vector), vector driving expression of WT GPVI, vector driving expression of PD GPVI, and human platelets. GFP+ platelets expressing surface WT GPVI and PD GPVI are shown in red boxes. D. Expression levels of human GPVI on mouse platelets. Shown are histograms of

surface GPVI in GFP-positive platelets from the indicated reconstituted mice compared to GPVI on human platelets.

Figure 2-2. Loss of the GPVI PRD does not alter sustained GPVI receptor signaling in platelets.

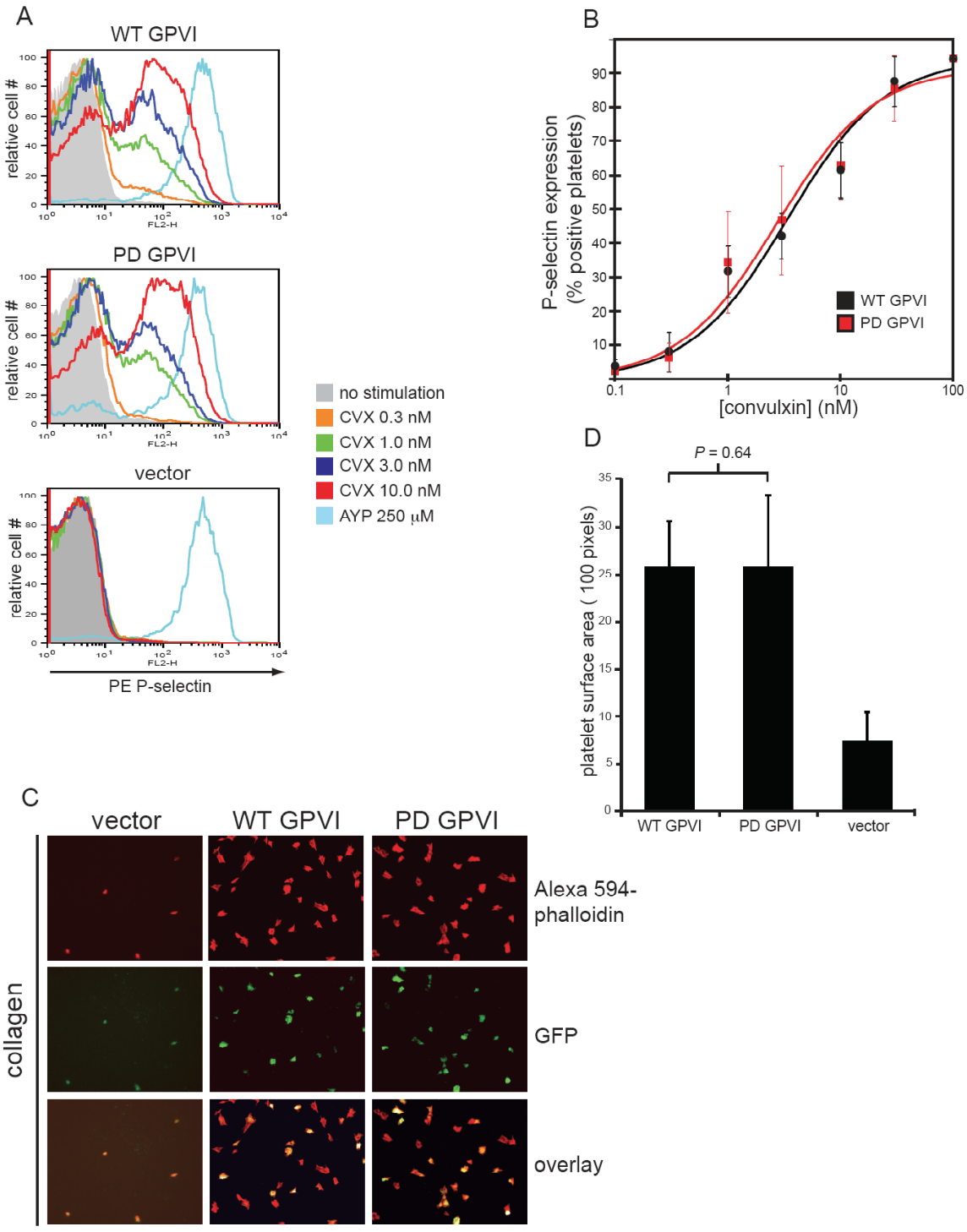

Figure 2-2. Loss of the GPVI PRD does not alter sustained GPVI receptor signaling in platelets. A. Platelet activation mediated by WT and PD GPVI signaling. Platelets from GPVI-deficient mice expressing WT GPVI or PD GPVI receptors were stimulated with the indicated concentrations of convulxin for 10 min, and activation was measured using flow cytometry to detect the expression of surface P-selectin in GFP+, GPVI-expressing platelets. AYP indicates exposure to the PAR4 agonist peptide AYPGKF. B. Dose-response curve of platelet activation mediated by WT and PD GPVI signaling. C. Platelet spreading on collagen mediated by WT or PD GPVI. Platelets from the indicated mice were incubated for 45 min on immobilized type-I collagen, and spreading was visualized by staining with Alexa-Fluor 594-conjugated phalloidin to detect cellular actin. GFP expression was simultaneously measured to identify platelets derived from vector-transduced precursors. D. Quantitation of platelet spreading driven by WT GPVI or PD GPVI, depicted in panel C. The area occupied by adherent platelets was measured using the Image J program. n = 100-300 individual platelets from 2-3 different animals analyzed for WT or PD GPVI or vector control.

Figure 2-3. The intracellular PRD is required for rapid platelet activation by GPVI receptors.

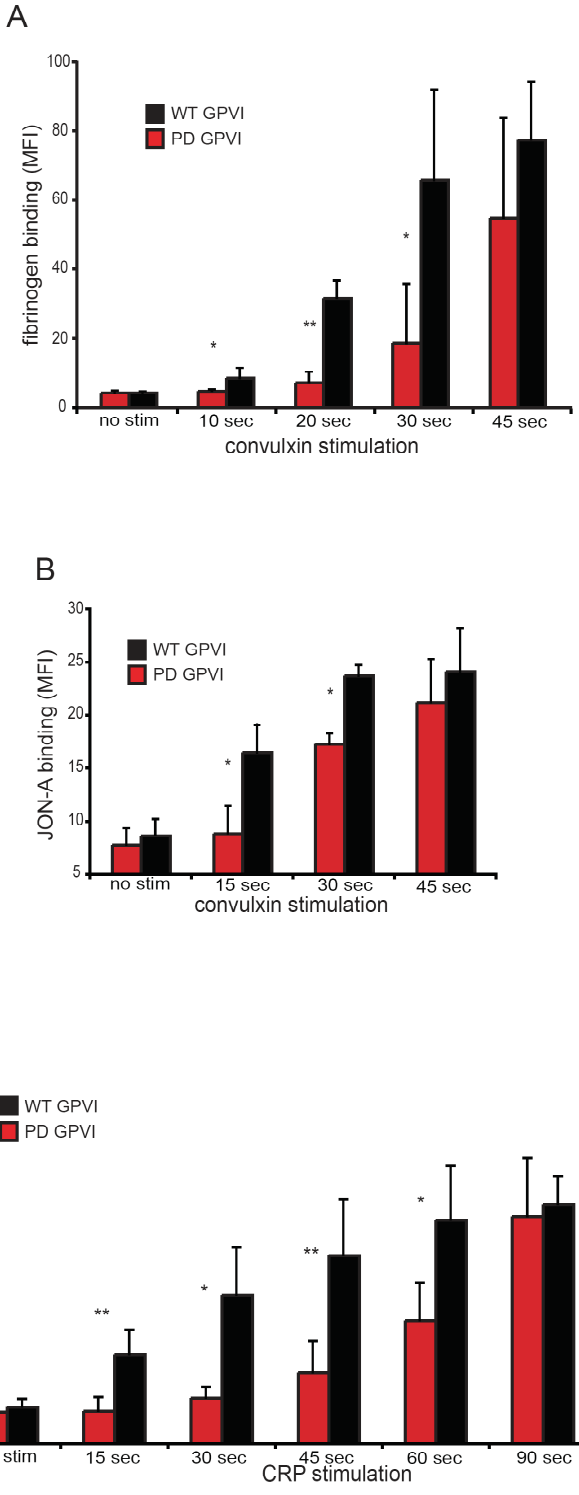

Figure 2-3. The intracellular PRD is required for rapid platelet activation by GPVI receptors. A. Time course of platelet fibrinogen binding by WT and PD GPVI-expressing platelets following convulxin stimulation. Platelets were stimulated with 10 nM convulxin in the presence of Alexa-Fluor 647-conjugated fibrinogen for times indicated, fixed, and analyzed by flow cytometry. B. Time course of JON-A binding following 10 nM convulxin stimulation. C. Time course of fibrinogen binding following stimulation with 10 μg/mL CRP. In all experiments only GFP+, GPVI-expressing platelets were analyzed. * = P <0.05, ** = P <0.01; error bars indicate mean ± SD; n = 3-6 experiments for each time point indicated, using 4 animals for WT or PD GPVI.

Figure 2-4. Time course analysis of P-selectin expression and fibrinogen binding following convulxin stimulation in wild-type platelets.

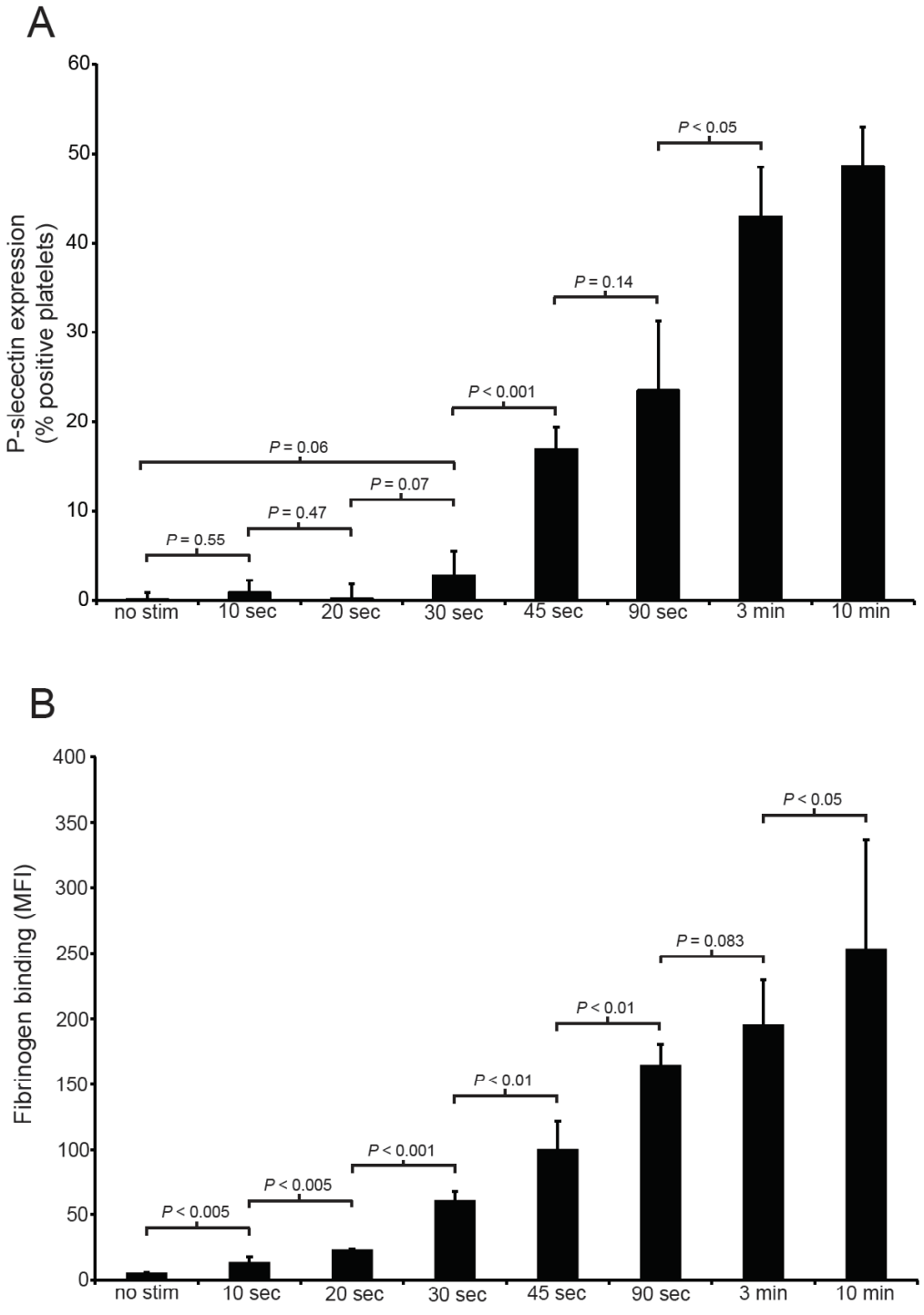

Figure 2-4. Time course analysis of P-selectin expression and fibrinogen binding following convulxin stimulation in wild-type platelets. A. Time course of P-selectin expression following convulxin stimulation. Wild-type mouse platelets were stimulated with 10 nM convulxin for times indicated in the presence of antibody against P-selectin, and P-selectin expression was determined by flow cytometry. B. Time course of platelet fibrinogen binding following convulxin stimulation. Platelets were stimulated with 10 nM convulxin in the presence of Alexa-Fluor 647-conjugated fibrinogen for times indicated, fixed, and analyzed by flow cytometry. *P* values were calculated between time points indicated; error bars indicate mean ± SD; n = 4-8 experiments for each time point indicated, using 4 animals.

Figure 2-5. PD GPVI receptors exhibit delayed Syk phosphorylation and calcium signaling.

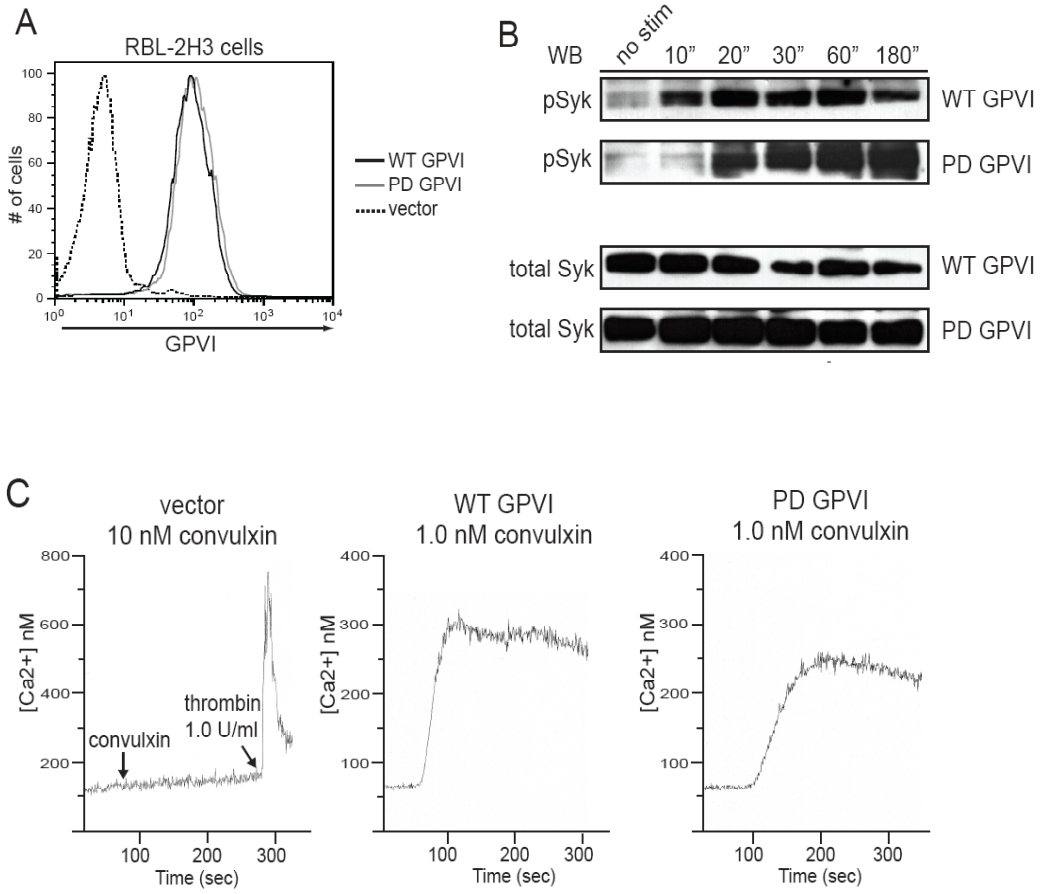

Figure 2-5. PD GPVI receptors exhibit delayed Syk phosphorylation and calcium signaling. A. Lentiviral vectors were used to express WT GPVI or PD GPVI or vector alone (vector) in RBL-2H3 cells, and surface expression of GPVI was detected by flow cytometry. B. Time course of GPVI-mediated activation of Syk following convulxin stimulation in WT GPVI and PD GPVI-expressing RBL-2H3 cells. GPVI-expressing RBL-2H3 cells were stimulated with convulxin for the time periods indicated, and whole cell lysate was analyzed by immunoblotting (WB) with antibodies against activated Syk (pSyk) and total Syk. C. Ca2+ mobilization in RBL-2H3 cells expressing WT and PD GPVI and vector control. Cells were loaded with the Ca2+-sensitive fluorophore Fura-2 AM and stimulated with 1 nM convulxin. Intracellular Ca2+ mobilization was measured by the ratio of Fura-2 emissions in a fluorimeter. Curves from representative experiments are shown; $n = 3$ measurements.

Figure 2-6. Tracking rolling and adhesion of GFP+/GPVI+ platelets to collagen under flow.

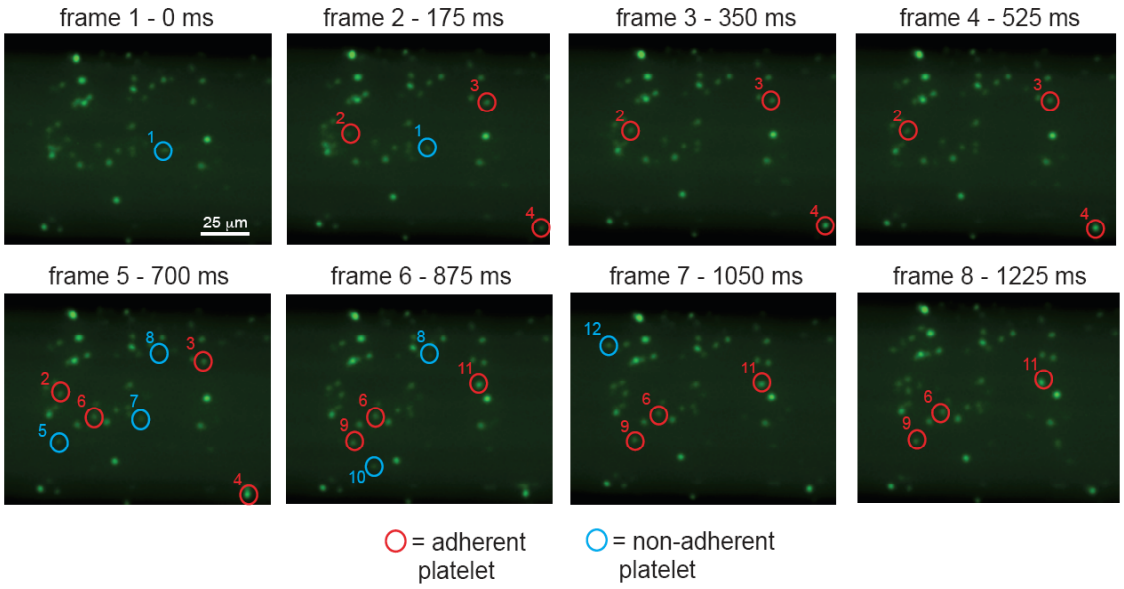

Figure 2-6. Tracking rolling and adhesion of GFP+/GPVI+ platelets to collagen under flow. Measurement of platelet adhesion efficiency during flow over a collagen coated surface. Shown is an example of sequential images taken with a 75 ms exposure time during flow of whole blood containing WT GPVI-expressing platelets over a type-I collagen-coated surface. Blood from reconstituted mice was flowed over a patterned type-I collagen strip at a shear rate of 1000 s^{-1}, and fluorescent images were taken every 100 ms to follow the interaction of GFP+ platelets with collagen under flow. Each platelet that appears on the collagen strip was tracked to determine if it remained adherent (red circles) or did not remain adherent (blue circles). Adhesive efficiency was determined by $a / (a + r)$, where a = # of platelets that permanently adhere and r = # of platelets that roll along collagen but do not adhere. The direction of flow and translocation of platelets is from left to right.

Figure 2-7. The GPVI PRD is required for efficient platelet adhesion to collagen under flow.

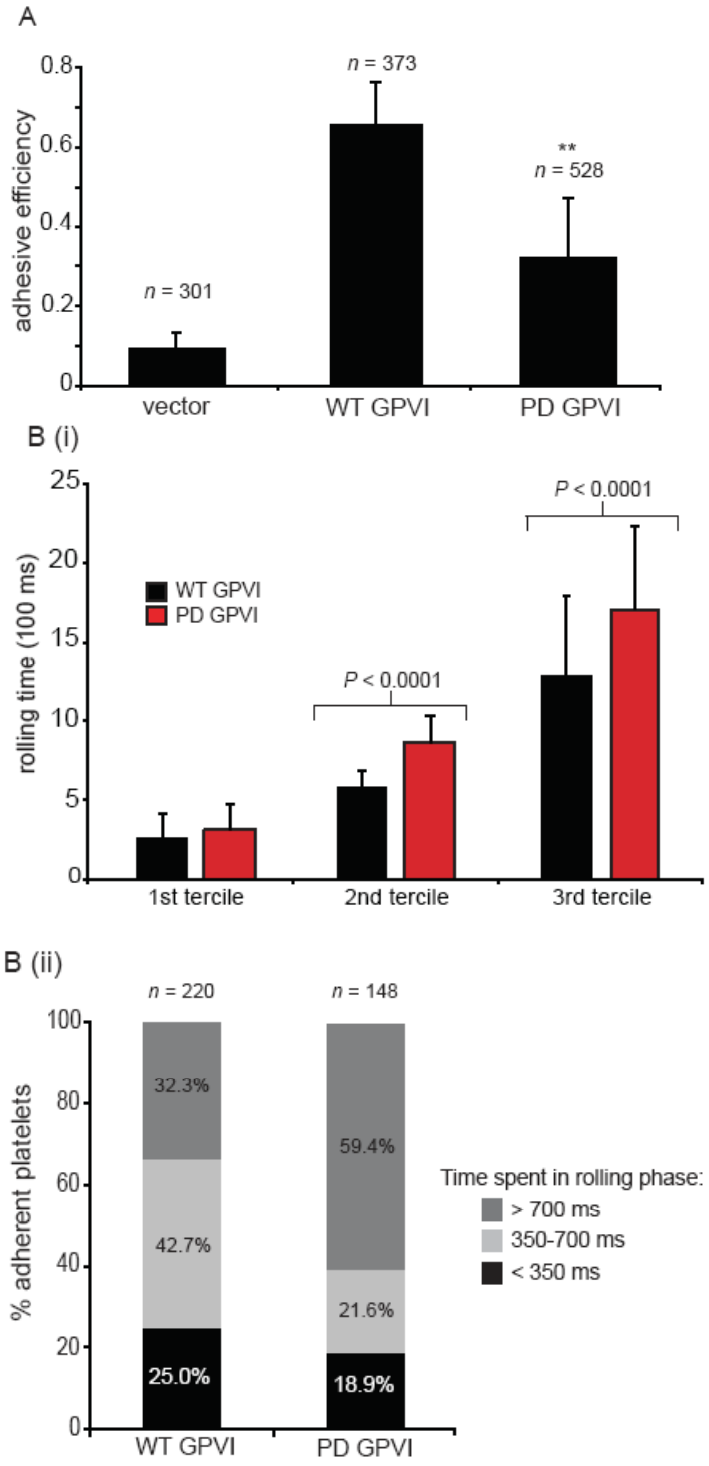

Figure 2-7. The GPVI PRD is required for efficient platelet adhesion to collagen under flow. A. Adhesive efficiency to collagen under flow of WT or PD GPVI-expressing platelets or vector control platelets. B. Rolling times on collagen for WT or PD GPVI platelets. The time each adherent platelet spent in the rolling phase was calculated based on the number of frames during which each platelet changed position. B. (i) Rolling times are shown divided into terciles (1st, shortest third of rolling times in each group; 2nd, middle third of rolling times in each group; 3rd, longest third of rolling times in each group). B. (ii) Percentage rolling times < 350 ms, 350–700 ms, and > 700 ms. The same adherent platelets were analyzed in panels (i) and (ii). ** = $P < 0.01$; error bars indicate mean ± SD; 3-5 movies using 3-4 animals for each GPVI variant or vector control were analyzed in a blinded fashion; *n* = total number of adherent platelets analyzed.

Figure 2-8. The GPVI PRD preferentially binds the SH3 domains of the SFKs Lyn and Hck.

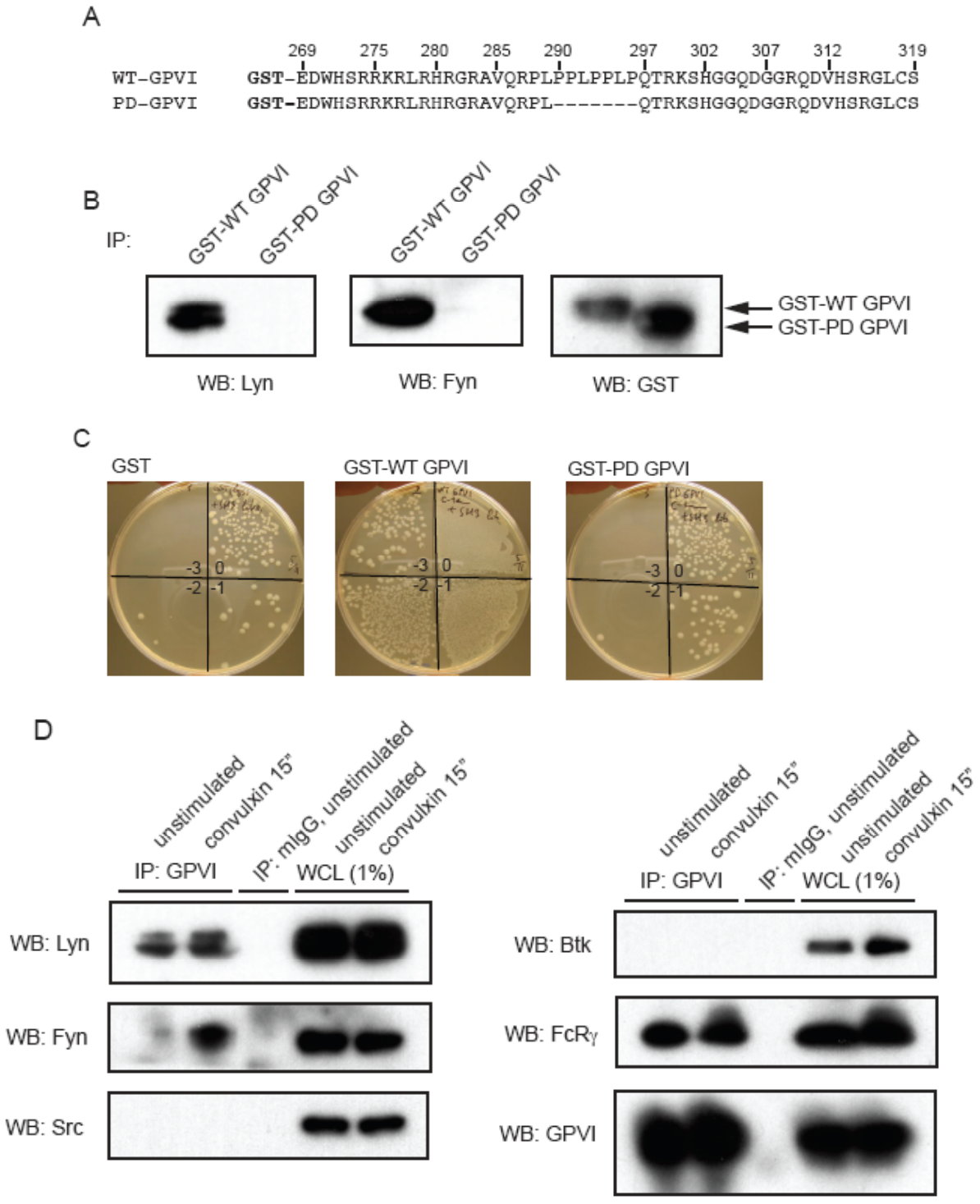

Figure 2-8. The GPVI PRD preferentially binds the SH3 domains of the SFKs Lyn and Hck. A. Shown are the amino acid sequences of the cytoplasmic tail of WT GPVI and PD GPVI expressed as GST-fusion proteins. B. Binding of SH3 domain-containing proteins from platelet lysate is dependent on the GPVI PRD. Washed human platelets were lysed, and platelet proteins were precipitated with either GST-WT GPVI or GST-PD GPVI bound to glutathione beads, resolved by SDS-PAGE, and analyzed by immunoblotting (WB) for Lyn, Fyn, or GST. C. Phage display screening of WT or PD GPVI GST-fusion protein binding to human SH3 domains, an unbiased method in which all SH3 domains compete with each other for binding to the target protein. SH3 domain-expressing phages captured by GST-GPVI constructs or plain GST were used to infect *E. coli* TG1 cells and plated as 10-fold dilutions onto ampicillin plates. Enrichment of SH3 displaying phages bound to the WT GPVI receptor was approximately 1000-fold compared to that bound to PD GPVI or GST alone. D. Lyn constitutively associates with GPVI in unstimulated platelets. Washed human platelets were left unstimulated or stimulated with 3 nM convulxin for 15 s, lysed, and proteins immunoprecipitated (IP) with GPVI were resolved by SDS-PAGE and analyzed by immunoblotting (WB) for Lyn, Fyn, Src, Btk, FcRγ, or GPVI. An immunoblot of whole cell lysate (WCL), loaded at 1% of GPVI IP input, and one of mouse IgG control IP are also shown. Blots depicted are representative of 3 independent experiments.

Table 2-I. The GPVI cytoplasmic tail preferentially binds the SFKs Lyn and Hck.

	# of clones			
SH3 domain	**Screen #1**	**Screen #2**	**Screen #3**	**Total**
Lyn	4/8 clones	10/24 clones	2/16 clones	16/48 clones
Hck	1/8 clones	10/24 clones	8/16 clones	19/48 clones
Fyn	1/8 clones	1/24 clones	0/16 clones	2/48 clones
Btk	1/8 clones	1/24 clones	2/16 clones	4/48 clones
Yes	1/8 clones	0/24 clones	2/16 clones	3/48 clones
Src	0/8 clones	0/24 clones	0/16 clones	0/48 clones
CrkL	0/8 clones	1/24 clones	0/16 clones	1/48 clones
Intersectin 1 3rd SH3 domain	0/8 clones	1/24 clones	2/16 clones	3/48 clones

Table 2-I. The GPVI cytoplasmic tail preferentially binds the SFKs Lyn and Hck.

The identity of the SH3 domains bound by GST-WT GPVI proteins was determined by sequencing the inserts of the selected phage clones after a single round of affinity selection. Shown are sequencing results of bacterial clones containing the phagemide encoding the corresponding SH3 domain bound to WT GPVI. Results demonstrate GPVI intracellular tail binding preference for SFKs, specifically Lyn and Hck

Figure 2-9. GPVI directly activates Lyn and Hck in a PRD-dependent manner.

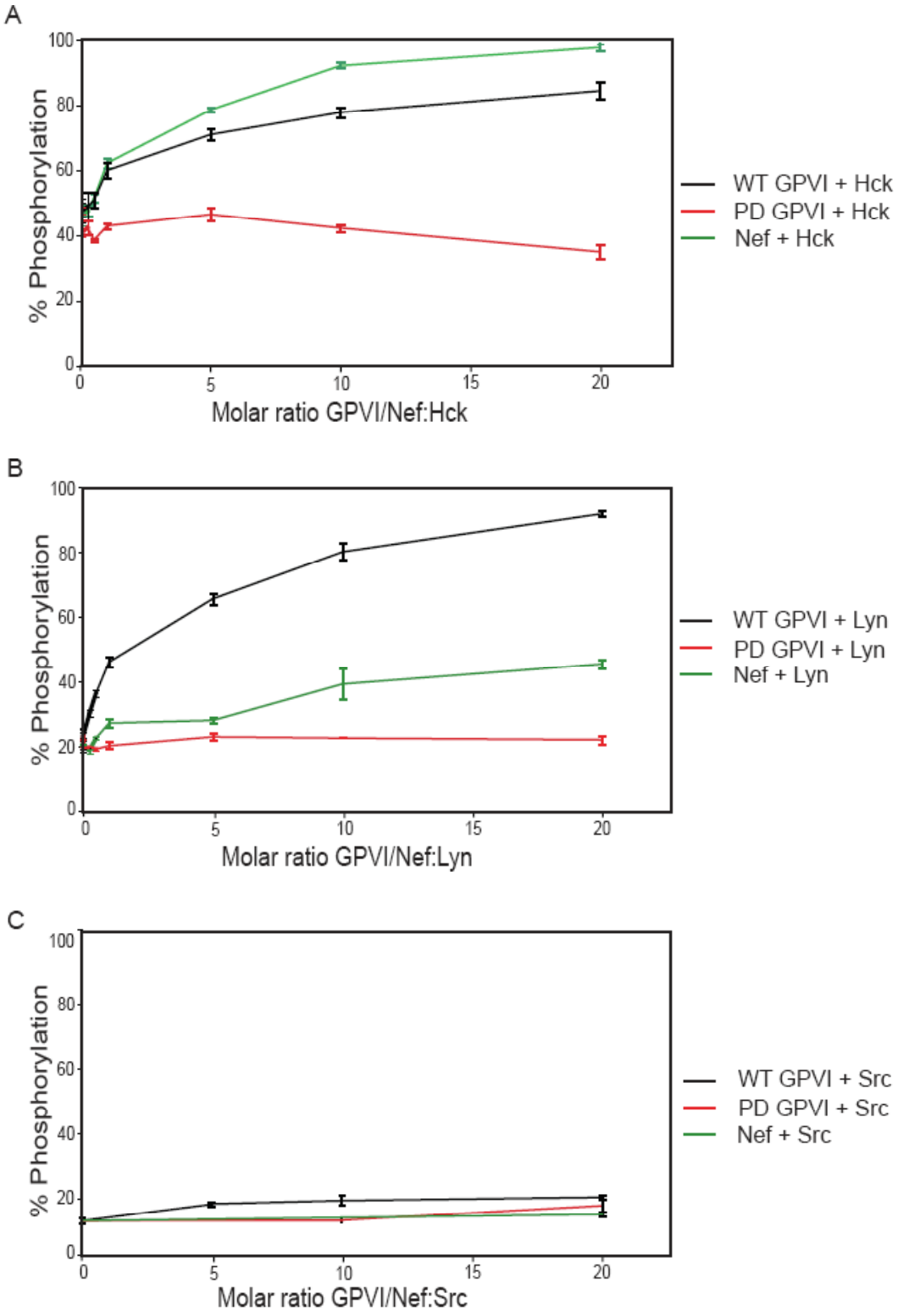

Figure 2-9. GPVI directly activates Lyn and Hck in a PRD-dependent manner. Recombinant Hck (panel A), Lyn (panel B), and c-Src (panel C) were purified from Sf9 insect cells in an inactive state and assayed for kinase activity with a peptide substrate *in vitro* in the presence of increasing concentrations of purified GST-WT GPVI, GST-PD GPVI, or recombinant HIV-1 Nef. Each condition was repeated in quadruplicate, and the extent of phosphorylation is expressed as mean percent phosphorylation relative to a control phosphopeptide ± SD. The results shown are representative of 2 independent experiments.

Figure 2-10. GPVI-bound Lyn is held in the active state in unstimulated platelets.

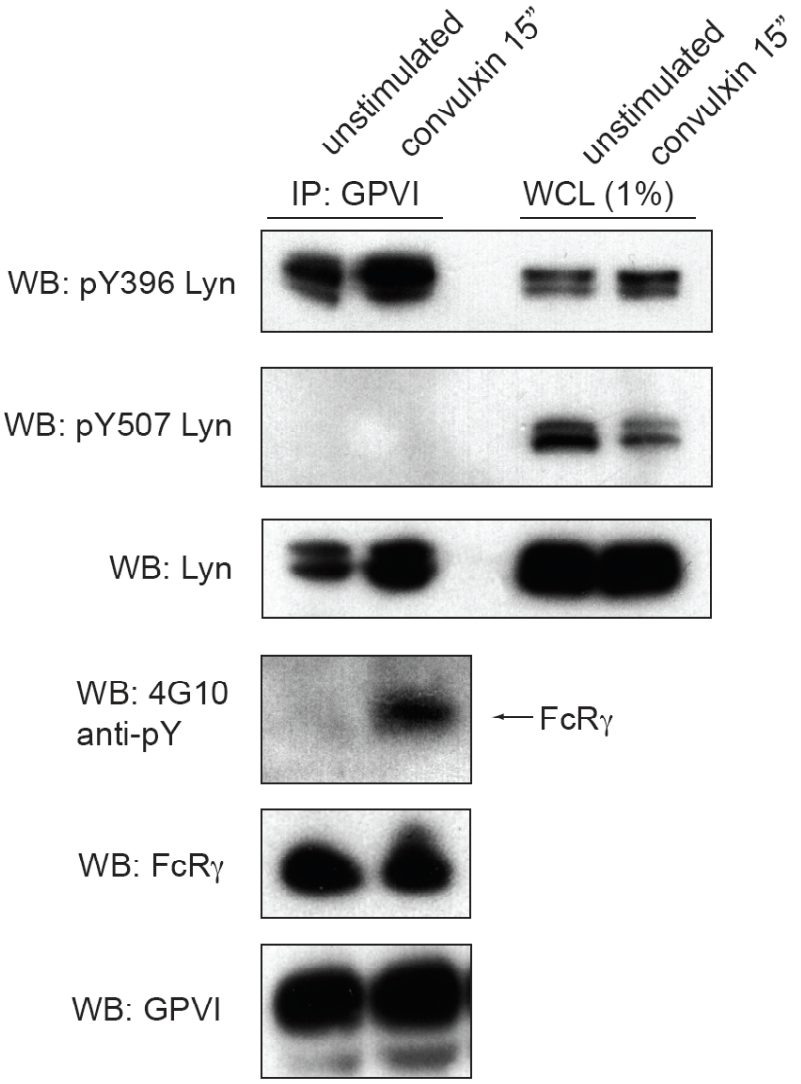

Figure 2-10. GPVI-bound Lyn is held in the active state in unstimulated platelets. Washed human platelets were left unstimulated or stimulated with 3 nM convulxin for 15 s, lysed, and proteins immunoprecipitated (IP) with GPVI were immunoblotted (WB) with phosphospecific antibodies for Lyn. pY396 indicates Lyn phosphorylated at the activation loop, and pY507 indicates Lyn phosphorylated at the negative regulatory site. Phospho-Lyn Y396 antibody reacts with other SFKs phosphorylated at their activation loop, but the characteristic doublet at 53 kD and 56 kD identifies Lyn as the predominant species. Probing with 4G10 was used to detect phosphorylated FcRγ chain, compared to total FcRγ chain, that co-immunoprecipitated with GPVI. An immunoblot of whole cell lysate (WCL), loaded at 1% of GPVI immunoprecipitation input, is also shown. Blots depicted are representative of 3 independent experiments.

Figure 2-11. Lyn- and Fyn-deficient platelet activation following convulxin stimulation.

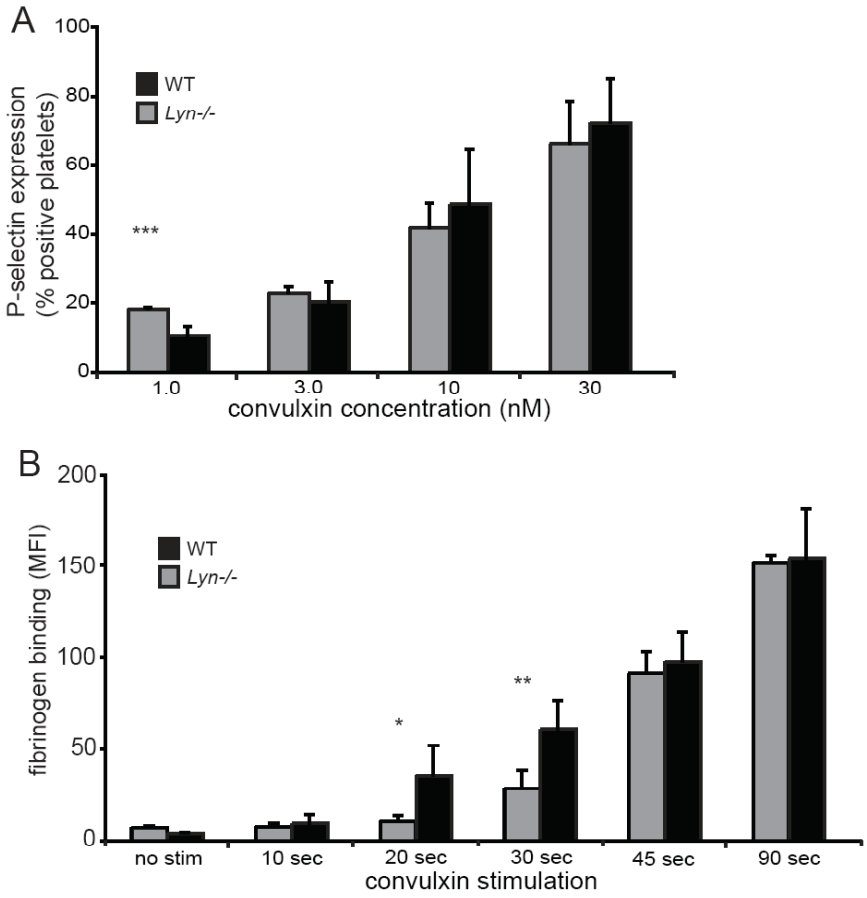

Figure 2-11 (cont'd). Lyn- and Fyn-deficient platelet activation following convulxin stimulation.

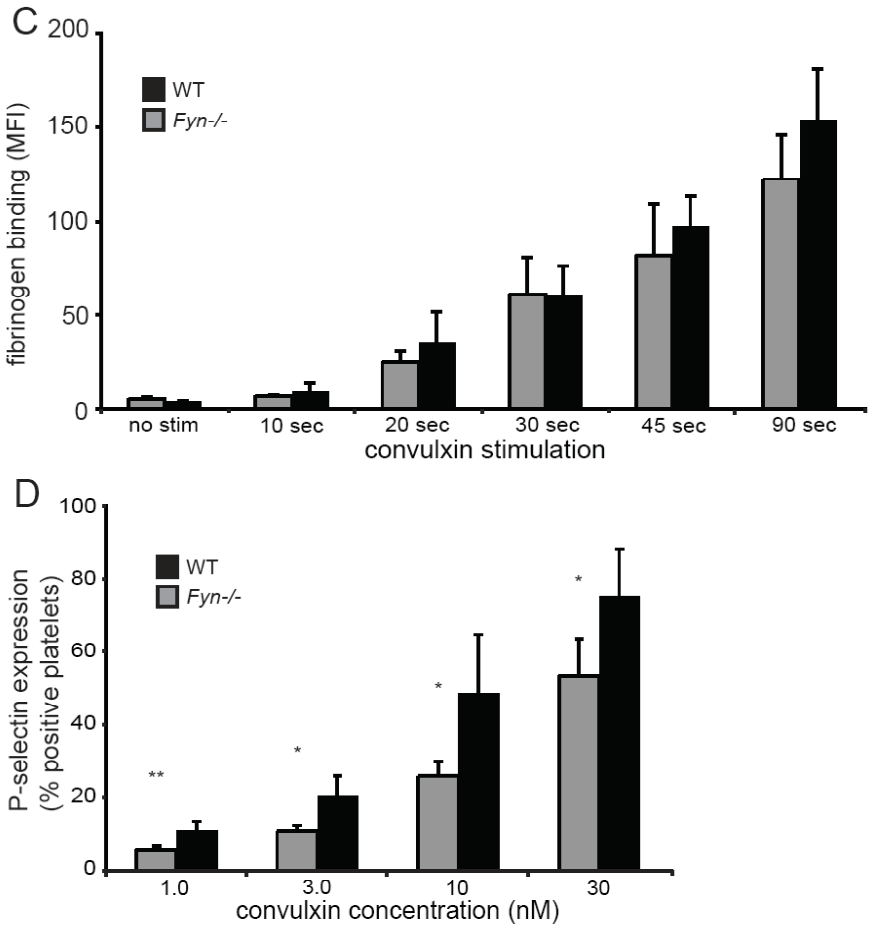

Figure 2-11. Lyn- and Fyn-deficient platelet activation following convulxin stimulation. A. Platelets from *Lyn*-/- mice or wild-type littermate controls (WT) were stimulated with the indicated concentrations of convulxin for 10 min, and P-selectin expression was determined by flow cytometry. B. Time course of platelet fibrinogen binding following convulxin stimulation. Platelets were stimulated with 10 nM convulxin in the presence of Alexa-Fluor 647-conjugated fibrinogen for times indicated, fixed, and analyzed by flow cytometry. * = P <0.05, ** = P <0.01, *** = P <0.005; error bars indicate mean ± SD; n = 4-6 experiments using 3 mice of each genotype for each concentration of convulxin or time point. C. Platelets from *fyn*-/- mice or wild-type littermate controls (WT) were stimulated with the indicated concentrations of convulxin for 10 min, and P-selectin expression was determined by flow cytometry. Bars indicate % P-selectin positive platelets. D. Time course of platelet fibrinogen binding following convulxin stimulation. Platelets were stimulated with 10 nM convulxin in the presence of Alexa-Fluor 647-conjugated fibrinogen for times indicated, fixed, and analyzed by flow cytometry. Bars indicate mean fluorescent intensity (MFI) of fibrinogen binding. * = P <0.05, ** = P <0.01, *** = P <0.005; error bars indicate mean ± SD; n = 4-6 experiments using 3 mice of each genotype for each concentration of convulxin or time point.

Figure 2-12. Lyn-deficient platelets exhibit defective adhesion to collagen under flow.

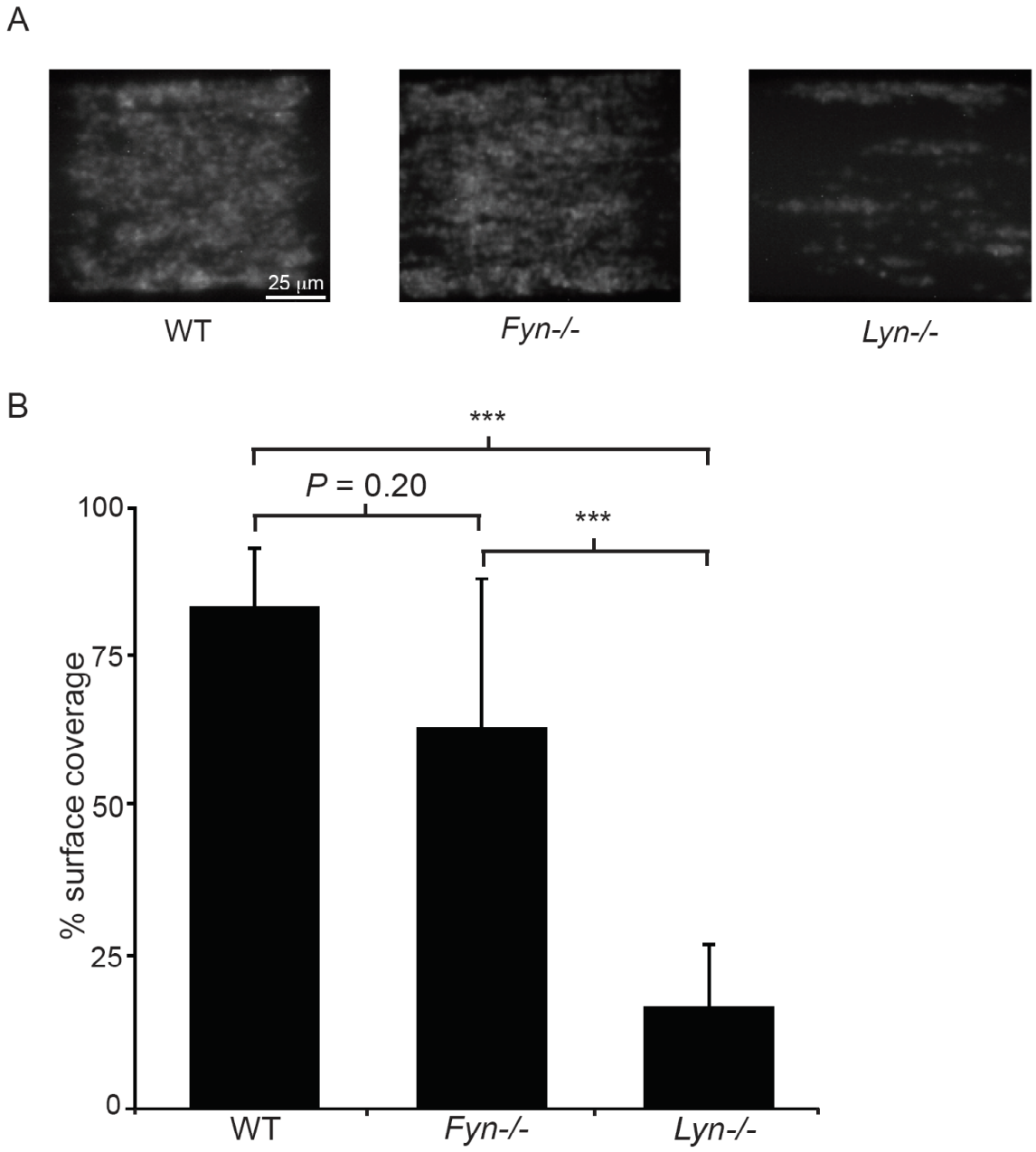

Figure 2-12. Lyn-deficient platelets exhibit defective adhesion to collagen under flow. A. Blood from *Lyn*-/-, *Fyn*-/-, or wild-type control animals was flowed over a patterned type-I collagen strip at a shear rate of 1000 s^{-1}. Images depict adhesion of fluorescently labeled platelets after 5 min of flow. The direction of flow is from left to right. B. Quantitation of percent of surface area coverage following 5 minutes of flow. *** = $P < 0.005$ for surface area coverage between WT and *Lyn*-/- platelets and between *Fyn*-/- and *Lyn*-/- platelets; error bars indicate mean ± SD; n = 6-8 experiments using 4 mice of each genotype.

Figure 2-13. Priming of Lyn by the GPVI PRD drives rapid signal transduction following receptor ligation.

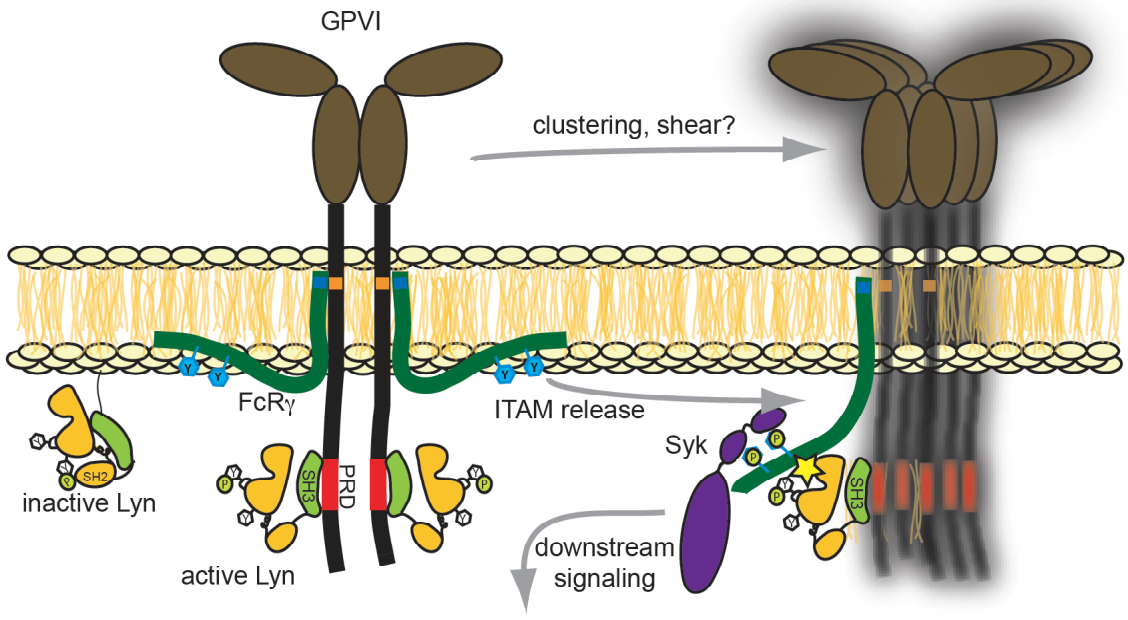

Figure 2-13. Priming of Lyn by the GPVI PRD drives rapid signal transduction following receptor ligation. In this model, Lyn is held in an activated state when constitutively bound to GPVI through displacement of the Lyn SH3 domain (light green) by the GPVI PRD (light red). Premature, ligand-independent receptor signaling is prevented by sequestration of the GPVI-associated FcRγ chain (dark green) within the lipid bi-layer, keeping ITAM domains (light blue) inaccessible to activated Lyn prior to receptor ligation[112]. Following GPVI-collagen binding, the FcRγ chain is released from the membrane by clustering or mechanical shear forces, allowing GPVI-bound, activated Lyn to phosphorylate the FcRγ ITAM. ITAM phosphorylation results in recruitment of Syk (purple) and initiation of the downstream GPVI signaling cascade.

Chapter 3—In contrast to mammalian platelets, avian thrombocytes do not form aggregates on collagen under arterial flow conditions

Summary

Specific cellular and molecular mechanisms exist within platelets to orchestrate the coordinated action of aggregate formation over collagen during hemodynamic flow. Both mammals and birds have high-pressure vascular systems, with similar flow rates and fluid shear forces. In birds, nucleated thrombocytes that are 3-5 times the diameter of platelets, and approximately 10-fold less numerous, are believed to play a hemostatic role analogous to that of platelets. However, it is unknown whether avian thrombocytes mediate aggregate formation under high shear in a manner similar to platelets. Using transcriptional profiling, we find that avian thrombocytes express most of the signaling receptors and pathways described in platelets. Flow of PPACK-anticoagulated chicken whole blood over chicken collagen at high shear results in thrombocyte rolling and firm adhesion, but thrombocytes covered significantly less surface area compared to human platelets and failed to form 3-dimensional aggregates. We describe molecular differences between platelets and thrombocytes that may explain the inability of thrombocytes to form aggregates under flow and suggest that vaso-occlusive arterial thrombosis may be a uniquely mammalian phenomenon that provided an evolutionary advantage in response to trauma but now underlies the basis of human cardiovascular disease and death.

Introduction

Acute myocardial infarction results from coronary artery occlusion by a platelet thrombus formed under high shear, most often following rupture of a nonstenotic atherosclerotic plaque[5,6]. Platelet-driven thrombosis is especially important in the arterial system, particularly in the high shear environment of stenotic coronary arteries [1,120]. Platelet aggregate formation under hemodynamic shear is highly efficient, and inhibiting this process is a basis for treatment of cardiovascular disease. Improved understanding of the pathological mechanisms underlying platelet aggregate formation at the site of vessel injury will advance our knowledge and treatment of cardiovascular disease.

The mechanisms by which platelets adhere and aggregate under hemodynamic conditions are essential for mammalian hemostasis and thrombosis and have been exceptionally well studied[85]. Hemostasis, the cessation of bleeding, is a requirement of any organism that utilizes blood circulation for tissue oxygenation and removal of waste products. All essential mammalian blood coagulation factors are conserved in primitive non-mammalian vertebrates such as zebrafish[121]. While hemostasis is a necessity to mammalian and non-mammalian species alike, megakaryocytes and non-nucleated platelets are exclusive to mammals. All other vertebrates have nucleated thrombocytes, instead of platelets, as hemostatic effector cells. Significantly less is understood of the function of thrombocytes, compared to that of platelets.

Thrombocytes found in non-mammalian vertebrates are nucleated, ovoid-shaped, and formed from diploid precursors in the bone marrow. Unlike more primitive vertebrates, such as the zebrafish or reptilian species, avian species have a highly

developed cardiovascular system with a high cardiac output and blood pressures that can exceed those in mammalian systems[122]. Therefore, the hemodynamic forces that necessitate efficient hemostasis in mammals must also be present in birds. Circulating thrombocytes are larger than platelets and similar in size to lymphocytes, about 6-8 μm in diameter. In chicken blood, there are approximately 20-60,000 thrombocytes per μL, a significantly lower concentration than that of mammalian platelets[123,124].

The function of thrombocytes in serving as specialized hemostatic cells is believed to be analogous to that of platelets, but evidence in support of this claim is limited and consists almost entirely of *in vitro* data. Avian thrombocytes express $\alpha_{2b}\beta_3$ integrin and aggregate through binding plasma fibrinogen in response to thrombin and 5-HT stimulation[125-127]. In contrast to platelets, thrombocytes have not been demonstrated to aggregate in response to ADP or epinephrine, although ADP may cause thrombocyte shape change[125,128]. Thrombocytes secrete granule contents, including 5-HT, following stimulation and contain a surface-connected canalicular system membrane component, also found in platelets[129-131]. Additionally, thrombocytes actively phagocytose Gram-positive and -negative bacteria and have been proposed to serve a broader immunologic function compared to that of platelets[124,132].

The fact that megakaryocytes and platelets are unique to mammals suggests there is some important aspect of mammalian biology and evolution—perhaps the need for more efficient hemostasis in response to trauma—that benefitted from the use of platelets, compared to thrombocytes, as hemostatic cells. However, if this hypothesis is correct—that platelets confer a superior hemostatic response to the organism—then what

functions of platelets are exceptional and cannot be performed by thrombocytes? It is intriguing that platelets are not required for any known element of hemostasis that is only found in mammals.

The existence of thrombocytes in avian species with high-pressure vascular systems presents an opportunity to test the conservation of basic elements of cellular hemostasis between platelets and thrombocytes. Our initial interest in avian thrombocyte biology began from the finding that thrombocytes do not contain an ortholog of the platelet collagen receptor glycoprotein (GP) VI detectable by BLAST search (see Chapter 2), while many other platelet-specific receptors have definitive chicken orthologs. We were surprised to discover studies demonstrating that chicken thrombocytes aggregate in response to collagen, a GPVI-dependent process in mammals[127,130]. Through collagen-induced platelet activation, GPVI is required for the transition of a rolling platelet to a firmly adherent platelet during flow on a collagen surface (see Chapter 1). Our findings in the previous chapter demonstrate that GPVI is molecularly specialized to rapidly activate platelets under conditions of hemodynamic flow. Can thrombocytes also activate and firmly adhere to collagen under arterial shear conditions?

Using transcriptional profile analysis, we determine that thrombocytes specifically express the receptors associated with hemostatic function and shear-resistant adhesion in platelets. Signaling studies confirm that thrombocytes are potently activated by collagen. Collagen signaling in the thrombocyte uses an immune receptor pathway analogous to that of GPVI. During flow of chicken whole blood in the presence of thrombin inhibition, we observe thrombocyte rolling and integrin-dependent firm

adhesion. However, there is significantly less surface coverage compared to that exhibited by platelets and a striking absence of 3-dimensional aggregate formation. We demonstrate that specific molecular mechanisms that have been adopted by the platelet to promote aggregate formation under shear, such as a high density of $\alpha_{2b}\beta_3$ integrin, are absent in the thrombocyte. These studies suggest that the ability to rapidly form 3-dimensional aggregates under arterial shear is exclusive to platelets. Platelet-mediated occlusive thrombus formation may represent a distinct quality of mammalian hemostasis not present in other species that also have a high-pressure system.

Results

Chicken thrombocytes specifically express genes associated with platelet function. Thrombocytes in avian species are believed to express many platelet-specific proteins and function analogously to platelets in mammalian systems, yet a thorough transcriptional profile analysis has not been performed. We wished to complete a gene-expression profile analysis of chicken thrombocytes to determine if they contain transcripts associated with hemostatic function and if this expression is restricted only to thrombocytes. Based on their expression of $\alpha_{2b}\beta_3$ integrin, thrombocytes could be isolated from chicken plasma preps by staining with AP-2 mAb, which cross-reacts with both chicken and human $\alpha_{2b}\beta_3$[123] (Fig. 3-1A). On average, chicken plasma preps contained about 50-70% thrombocytes, with the rest presumably representing leukocytes (Fig. 3-1A). Using cell sorting based on positive and negative cell markers, we isolated pure populations of chicken thrombocytes and lymphocytes (Fig. 3-1B). Gene-expression analysis on the Affymetrix chicken chip revealed that thrombocytes, and not lymphocytes, significantly upregulate genes that are known to have a specific role in platelet function, including the VonWillebrand factor receptors GPIb and GPIX, integrins β_1, β_3, α_2, and α_V, the thrombin receptor protease-activated receptor (PAR) 1, the ADP receptors P_2X_1 and P_2Y_1, and the serotonin receptor HTR_{2A} (Table 3-I). The fact that this list was not exhaustive for platelet genes is at least partially due to incomplete annotation of the chicken genome and/or lack of representation on the Affymetrix chicken gene chip. These limitations notwithstanding, transcriptional profile analysis confirms that chicken

thrombocytes are specialized among hematopoietic cells to serve a hemostatic function in the organism.

Chicken thrombocytes are strongly activated by thrombin and collagen.

In vivo, following vessel injury, thrombin from tissue factor release and collagen exposure in the subendothelium are the two primary activators of platelets (see Fig. 1-1). We sought to determine if thrombocytes are capable of activation in response to these agonists and how the thrombocyte response compares to that of platelets. Due to a lack of species-specific activation markers for chicken thrombocytes, we performed [^{3}H] serotonin (5-HT) secretion assays under non-stirring conditions as a means to directly compare the activation response of platelets and thrombocytes. Chicken thrombocytes readily take up 5-HT from the plasma and release it upon activation, presumably through a degranulation mechanism similar to that of platelets[129,130]. Thrombin stimulated [^{3}H]5-HT release in a concentration-dependent manner, although this stimulation was less potent than that of human platelets (Fig. 3-2A). The thrombin used in this assay was purified from a bovine source, and it is not clear if species-specific differences account for the lower sensitivity of chicken thrombocytes.

A gene encoding the platelet-specific collagen receptor GPVI was absent from our gene-expression analysis, and a BLAST search revealed no GPVI orthologs in the chicken genome. However, it has been documented that chicken thrombocytes are capable of aggregating in response to collagen, although the relative strength of collagen as a thrombocyte agonist is unclear[130]. Fibrillar equine type-I collagen induced [^{3}H]5-HT

release from thrombocytes in a concentration-dependent manner, and this response was even more sensitive than that of human platelets (Fig. 3-2B). However, consistent with the apparent lack of GPVI on chicken thrombocytes, thrombocytes were not activated by convulxin and only very weakly activated by collagen-related peptide (CRP), both of which are GPVI-specific agonists that induced potent activation of platelets (Fig. 3-2C).

It has been unclear the extent to which ADP or thromboxane, both of which are well characterized platelet agonists, can activate avian thrombocytes. ADP did not induce any [^{3}H]5-HT release in either thrombocytes or platelets (Fig. 3-2C), consistent with data demonstrating a lack of ADP-induced secretion in platelets in the absence of aggregation, when assays are performed in non-stirring conditions[133]. Thrombocyte activation was also determined by the ability of agonists to induce aggregation of thrombocytes in thrombocyte-rich blood plasma. Collagen induced thrombocyte aggregation, whereas ADP and the thromboxane analog U-46619 at high pharmacologic concentrations induced only transient and weak thrombocyte aggregation (Fig. 3-2D). 5-HT, which has been reported to induce duck thrombocyte aggregation, did not induce any aggregation response in chicken thrombocytes at high pharmacologic doses (Fig. 3-2D)[127]. Annexin V and human fibrinogen binding following stimulation of washed thrombocytes was analyzed by flow cytometry but could not produce a readout of thrombocyte stimulation (data not shown).

Collagen-induced signaling in the thrombocyte requires Src-kinases and Syk.

Unlike most activating receptors on the platelet surface, which are G-protein coupled, GPVI is a member of the immunoglobulin (Ig) domain-containing superfamily and utilizes tyrosine kinase signaling through Src-family kinases (SFKs) and Syk kinase (see Fig. 1-2)[46]. To determine if collagen-induced thrombocyte activation is also dependent on these tyrosine kinases, we measured the ability of the SFK inhibitor PP2 and the Syk-inhibitor piceatannol to inhibit collagen-induced [^{3}H] 5-HT release. Both PP2 and piceatannol inhibited collagen-induced thrombocyte [^{3}H] 5-HT release in a dose-dependent fashion (Fig 3-3A and B) and were more selective for inhibiting collagen-induced, but not thrombin-induced, secretion (Fig. 3-3C). Interestingly, PP2 was observed to partially inhibit thrombin-induced [^{3}H] 5-HT release in the thrombocyte, whereas it had no affect on thrombin activation of platelets (Fig. 3-3C).

Thrombocytes do not form aggregates on a collagen surface under arterial shear conditions.

The ability of platelets to adhere and form aggregates when exposed to collagen under high shear and the cellular and molecular mechanisms underlying this process have been thoroughly characterized (see Fig 1-3). It is unknown whether thrombocytes, which would be subject to much greater shear forces proportional to the square of their diameter—9-25 times the forces on platelets—are capable of this function. The fact that thrombocytes express the GPIb/V/IX complex and the high-affinity collagen receptor integrin α_2 suggested that vWF-mediated rolling and integrin-mediated adhesion may be

conserved. To test whether thrombocytes are capable of rolling, adhering, and aggregating on a collagen surface under high shear, we perfused chicken and human whole blood anticoagulated with the direct thrombin inhibitor PPACK over a chicken collagen surface. Chicken type-I and III collagen was purified from chicken skin and the resultant collagen-coated slides had a more heterogeneous collagen distribution than slides coated with the commercially available Chronolog type-I collagen derived from equine tendon (Fig 3-4). We used chicken collagen for the hemodynamic flow assays to avoid any possible species-specific effects of the collagen type on thrombocyte adhesion under flow.

These flow assays reproduce a critical element of platelet-collagen interaction *in vivo*—the need to adhere firmly to immobilized collagen under hemodynamic shear—but isolate the function of collagen-induced platelet activation by excluding thrombin generation and endothelial cell contribution (see Fig. 1-3). To allow for real-time fluorescent imaging of adherent cells, platelets and thrombocytes were labeled with the mouse mAb AP-2, which binds both human and chicken $\alpha_{2b}\beta_3$[123]. AP-2 blocks fibrinogen binding by up to 50% in human platelets when used at high concentrations but appears to have only a minor effect on thrombocyte-fibrinogen binding[129,134]. AP-2 does not inhibit thrombocyte aggregation in response to thrombin[123,126]. During flow of human blood over collagen, platelets rolled and firmly adhered, and after 5 min of perfusion, large 3-dimensional aggregates had formed on the collagen surface (Supplemental movie 3-1). Perfusion of chicken whole blood revealed thrombocytes rolling and firmly adhering to the collagen surface, and membrane tethers could be

observed (Supplemental movie 3-2). After 5 min of perfusion, a large number of thrombocytes had firmly adhered but covered a much smaller total collagen surface area compared to platelet coverage (Fig. 3-5). Most profoundly, thrombocytes were not observed to form any aggregates on the collagen surface, whereas platelets formed large aggregates in a shear-dependent fashion, consistent with previous findings (Fig. 3-5B-D)[40].

To determine if thrombocytes are capable of aggregate formation if given more time to set down adherent cells, chicken blood was perfused over collagen for 15 min. Remarkably, after 15 min, a monolayer composed of more thrombocytes than observed in 5-min perfusion experiments had formed on the collagen surface, but virtually no 3-dimensional aggregates had formed (Fig. 3-6). The lack of 3-dimensional aggregate formation by thrombocytes was most evident in DAPI-stained images that detect each thrombocyte nucleus. While thrombocytes might be closely approximated to one another, and in some cases were in direct contact with one another, there was no overlap of individual nuclei, suggesting that no cells were stacked on top of each other (Fig. 3-6B). Together, these results suggest that thrombocytes have a conserved mechanism to adhere to collagen under arterial shear, but unlike platelets, they do not cover a collagen surface as efficiently and do not form aggregates under hemodynamic flow conditions.

Thrombocytes are fully activated despite a lack of aggregate formation under hemodynamic flow.

Platelet adhesion and aggregate formation under flow are associated with a flattening of the platelet shape and formation of filopodia and lamellipodia. The spreading of fully activated platelets presumably facilitates aggregate formation by allowing for more efficient stacking of platelets on top of each other. To determine if thrombocytes are fully activated and undergo a similar shape change during aggregate formation, we performed scanning electron microscopy of platelets and thrombocytes following a 5-min perfusion of whole blood over chicken collagen through the parallel plate flow chamber. High-power imaging confirmed that thrombocytes covered significantly less surface area compared to platelets and did not form 3-dimensional aggregates (Fig. 3-7A and B). Large, 3-dimesnsional aggregates were readily observed for platelets following whole blood perfusion under the same conditions (Fig. 3-7A and B). Individual thrombocytes and platelets appeared fully activated, as evidenced by cell spreading, accompanied by filopodia and lamellipodia formation and cell vacuolization, which suggested thrombocyte degranulation (Fig. 3-7C). Occasional cell-cell contacts between thrombocytes could be observed, presumably a result of membrane extensions and fibrinogen-mediated thrombocyte cross-linking (Fig. 3-7B and E). In contrast, platelet cross-linking was extremely robust, resulting in large aggregates and creation of a platelet lattice (Fig. 3-7D).

Pharmacologic inhibition of integrin function or collagen signaling decreases thrombocyte adhesion to collagen under flow.

Integrin activation is required to mediate firm adhesion to collagen under flow. To assess the requirement for integrins to mediate adhesion of thrombocytes, we used EDTA to chelate cations required for integrin function. EDTA inhibited thrombocyte and platelet adhesion to collagen, suggesting that collagen-induced activation of integrins under shear is a conserved process (Fig. 3-8A).

Collagen-induced platelet activation through GPVI signaling is required for normal platelet adhesion to collagen under hemodynamic flow, and pharmacologic inhibition or genetic deletion of GPVI significantly reduces platelet adhesion under shear[40]. To test whether collagen-induced thrombocyte activation is required for adhesion under shear, we used PP2 to inhibit collagen-mediated signaling. Following 5-min perfusion of whole blood pre-treated with PP2, both platelet and thrombocyte surface coverage of collagen was reduced to a similar degree (Fig. 3-8B and Supplemental movies 3-3 and 3-4). Following PP2 treatment, both platelets and thrombocytes demonstrated an increased amount of rolling along the collagen surface, with delayed or absent firm adhesion to collagen (Supplemental movies 3-3 and 3-4). These results suggest that for both platelets and thrombocytes, collagen-induced signaling under hemodynamic flow is required for cellular activation and efficient transition from a rolling state to a firmly adherent state.

Thrombocytes express fewer $\alpha_{2b}\beta_3$ integrin receptors than do platelets and are not affected by $\alpha_{2b}\beta_3$ inhibition during adhesion to collagen under flow.

The observation that thrombocytes do not form aggregates under hemodynamic flow could be expected if thrombocytes were to express significantly lower levels of $\alpha_{2b}\beta_3$ integrin on the cell surface. $\alpha_{2b}\beta_3$ is the most abundant platelet surface receptor, expressed at a copy number of approximately 50-80,000 receptors per cell, and, as a result, is found at an extremely high density on the cell surface[135]. To compare the levels of $\alpha_{2b}\beta_3$ on the surface of human platelets to that on the surface of chicken thrombocytes, we compared staining with AP-2 mAb by flow cytometry. Remarkably, the expression of $\alpha_{2b}\beta_3$ on the platelet surface was significantly greater than that on the thrombocyte surface (MFI 653 on platelets compared to 322 on thrombocytes; $P = 0.018$) (Fig. 3-9A). Taking into account a conservative estimate of thrombocyte versus platelet size—assuming a platelet diameter of 2 μm and a thrombocyte diameter of 6-7 μm—and assuming a spherical shape for both cells, a thrombocyte could be expected to have a surface area at least 9-12.25 times that of a platelet. This difference in surface area would result in an 18.2-24.8 times greater density of $\alpha_{2b}\beta_3$ on the platelet compared to the thrombocyte.

To test the importance of $\alpha_{2b}\beta_3$ in platelet and thrombocyte responses to collagen under hemodynamic flow, we pharmacologically inhibited $\alpha_{2b}\beta_3$ with eptifibatide, a cyclic lys-gly-asp peptide that prevents $\alpha_{2b}\beta_3$ binding to fibrinogen[136]. Eptifibatide inhibited collagen-induced aggregation of thrombocytes (Fig. 3-9B). After 5 min of perfusion of eptifibatide-treated whole blood, platelet surface coverage of collagen was

dramatically reduced at high shear forces of 1300 and 1150 s^{-1} yet was paradoxically increased at lower shear forces of 700-350 s^{-1} (Fig. 3-9C*i*). Eptifibatide treatment had no effect on thrombocyte adhesion to collagen under flow (Fig. 3-9C*ii* and Supplemental movie 3-6). By blocking platelet aggregation, eptifibatide treatment resulted in deposition of single platelets only and the absence of platelet aggregates (Fig. 3-9D and Supplemental movie 3-5). Pharmacological inhibition of $\alpha_{2b}\beta_3$ on platelets resulted in a monolayer formation on the collagen surface analogous to normal thrombocyte adhesion following whole blood perfusion. These results demonstrate that at high shear forces, platelets are dependent on aggregate formation to maximize surface coverage of collagen, whereas thrombocytes do not utilize aggregate formation to enhance surface coverage under hemodynamic flow.

Platelets, but not thrombocytes, utilize ADP signaling to enhance adhesion and aggregate formation under hemodynamic flow.

ADP, released from platelet dense granules during collagen activation under flow, promotes aggregate formation through autocrine and paracrine activation of P_2Y receptors[137,138]. While ADP treatment only resulted in weak and transient thrombocyte aggregation, this response was inhibited with the small molecule P_2Y_{12} antagonist MesAMP (Fig. 3-10A). Consistent with previously published findings, treatment of whole blood with MesAMP decreased platelet surface coverage and aggregate size following 5-min perfusion over collagen (Fig. 3-10B). MesAMP did not decrease collagen surface coverage of thrombocytes under flow (Fig. 3-10C), consistent with

thrombocytes' apparent lack of a robust ADP-mediated activation response. These findings confirm that platelets utilize ADP signaling to enhance aggregate formation and surface coverage on collagen under flow, while they suggest that thrombocytes do not employ this positive-feedback mechanism to enhance shear-resistant adhesion.

Discussion

The aggregation of platelets in response to collagen exposure following vascular injury allows for an efficient hemostatic response but also underlies the thrombotic pathophysiology of acute cardiovascular disease. While anuclear platelets are responsible for cellular hemostasis in mammals and pathological thrombosis in humans, avian species circulate larger, nucleated thrombocytes, which are believed to serve a similar hemostatic function in birds. The ability of thrombocytes to respond to collagen under hemodynamic flow has not been studied. In this chapter, we demonstrate that while thrombocytes are capable of potent activation by collagen and firm adhesion to collagen under flow, thrombocytes, in contrast to platelets, do not form 3-dimensional aggregates under arterial flow conditions. We provide evidence that this profound difference is due to the relatively low density of $\alpha_{2b}\beta_3$ receptors on the thrombocyte surface and the lack of additional positive-feedback pathways that are required for maximal platelet surface coverage and aggregate formation.

True anuclear platelets first appeared in early mammalian species. The monotreme order, most closely related to primitive mammalian ancestors, consists of egg-laying mammals such as the duck-billed platypus and the echidna (spiny anteater). These species contain platelets of size and number similar to those found in mice and humans, although monotreme platelets may occasionally be larger than human or mouse platelets—up to 8 μm in diameter, similar in size to a thrombocyte[7]. Marsupial species such as the opossum have platelet counts that are comparable to those of placental mammalian species. One common misconception is the idea that placental birth was the

driving force behind the evolution of platelets. The fact that monotremes, which are egg-laying, and marsupials, which have a nonplacental pregnancy, both have platelets suggests that platelets did not evolve to facilitate placental birth.

There is functional evidence that, as the major constituent of circulating cells after red blood cells, thrombocytes function as the hemostatic effector cells in non-mammalian vertebrates. However, gene expression profiling of thrombocytes has not been performed to demonstrate that thrombocytes specifically upregulate platelet-specific genes associated with hemostatic function. Our results show that, compared to lymphocytes, thrombocytes specifically express genes that have a distinct role in platelet function. The fact that we limited our comparison of thrombocytes solely to lymphocytes does not eliminate the possibility that other blood cells such as granulocytes or monocytes could express hemostatic effector genes. However, the fact that the K55-negative / AP-2 negative population was relatively minor suggests that this cell population could not be contributing in large numbers to avian hemostasis. Additionally, all adherent cells following flow on the collagen surface expressed $\alpha_{2b}\beta_3$, as determined by AP-2 binding, suggesting that only thrombocytes are capable of this specialized shear-resistant behavior. In summary, our results demonstrate that avian thrombocytes have a gene expression profile associated with hemostatic function.

Results from parallel plate flow chamber experiments suggest that thrombocytes do not effectively form shear-resistant aggregates during flow over a collagen surface. This finding represents a fundamental difference from the behavior of platelets, which, even in the absence of thrombin generation, form large 3-dimensional aggregates on

collagen in a shear-dependent fashion. What are the mechanisms that underlie this distinction? In flowing blood, thrombocytes are subject to greater forces due to their larger cell size, proportional to the square of their diameter. A thrombocyte of 7 μm in diameter could be subject to 12.25 times greater force compared to a platelet of 2 μm in diameter. This increased force could negatively affect the ability of thrombocytes to build a growing aggregate in the setting of flowing blood.

We attempted to address cellular and molecular mechanisms underlying this distinction in shear-resistant aggregate formation. Thrombocytes have a ~50% reduction in $\alpha_{2b}\beta_3$ copy number on the cell surface, which results in an approximately 10-20-fold decrease in $\alpha_{2b}\beta_3$ density, after taking the larger thrombocyte size into account. The fibrinogen receptor, integrin $\alpha_{2b}\beta_3$, is expressed at approximately 80,000 copy numbers on the platelet surface, resulting in a high density which accounts for 17% of the platelet membrane protein mass[139]. Thrombocytes have sufficient $\alpha_{2b}\beta_3$ density to mediate aggregation under stirring conditions, but greater densities, such as those found on platelets, may be required for aggregation under the more stringent conditions of hemodynamic flow at arterial shear rates. This difference in integrin density between platelets and thrombocytes could underly the major distinction in aggregation behavior during flow over collagen. It would be intriguing to overexpress $\alpha_{2b}\beta_3$ in the chicken thrombocyte to see if increased integrin expression at densities similar to that of the platelet could allow for shear-resistant thrombocyte aggregation in whole blood flow. Although they are nucleated cells, thrombocytes are reported to be extremely difficult to

culture, posing an impediment to gene transfection and reconstitution of chicken blood with cultured thrombocytes[140].

Similar to platelets, thrombocytes appear fully activated, spread, and degranulated in response to collagen under flow, a prerequisite for platelet aggregation under these conditions. The difference in cell size is the only major distinction between these two cell types as seen under high-power scanning electron microscopy analysis. Thrombocytes engage in robust cell spreading behavior, characterized by filopodia and lamellipodia formation, in a manner almost identical to platelets, suggesting evolutionary conservation of this response and an essential role for it in normal hemostatic function.

It appears that thrombocytes may have a less extensive and/or less sensitive repertoire of agonists involved in potentiating thrombocyte activation. While thrombin and collagen are both primary activators of thrombocytes and platelets, platelets utilize positive feedback via thromboxane and 5-HT signaling to maintain activation, and, most notably, they absolutely require ADP signaling to maximize adhesion to collagen under flow[137,138]. Thrombocytes do not appear to have evolved a potent response to any of these agonists. The possible existence of additional agonists, perhaps unique to thrombocytes and not platelets, cannot be ruled out. Such agonists may serve to augment thrombocyte activation following thrombin or collagen stimulation. However, in the absence of a high density of $\alpha_{2b}\beta_3$ integrin and the potential for aggregation under high shear, robust autocrine and paracrine signaling during adhesion under flow may not have any additional effect. It is possible that the adaptations that facilitate platelet aggregation under arterial blood flow conditions—small cell size, increased cell number, high $\alpha_{2b}\beta_3$

density—co-evolved with positive-feedback pathways, such as a robust response to ADP, that potentiate platelet aggregation.

The finding that chicken thrombocytes do not form aggregates over collagen following blood flow at arterial shear rates raises the question of what happens in birds following vascular injury. It has been repeatedly demonstrated in mammalian injury model systems, most well characterized in the mouse, that vascular injury of a sufficient degree results in the formation of a platelet-mediated thrombus that occludes vessel flow. Our results from chicken thrombocyte studies raise several questions. Is cell-mediated thrombosis strictly a platelet, and therefore, mammalian phenomenon? Do birds form thrombi following vessel wall injury, and, if so, are there alternate mechanisms for this response other than thrombocyte aggregation, such as a robust coagulation response? Finally, is occlusive thrombus formation absolutely necessary to prevent hemorrhage following vascular injury, or is a cell monolayer sufficient for hemostasis in this setting? Thrombocytes appear capable of monolayer formation following adhesion to collagen under flow, and perhaps this response is suitable for hemostasis in avian species. The mammalian adaptation of platelet-driven occlusive thrombus formation is most likely an adaptive response to significant vessel trauma designed to prevent catastrophic hemorrhage. However, this response is also the driving force behind pathologic thrombosis that occurs in the setting of cardiovascular disease. To answer these questions, comparative thrombosis experiments need to be designed in an avian model to determine the response of thrombocytes to vessel injury *in vivo* in the arterial system.

The hemodynamics and cardiovascular physiology of many non-mammalian species, such as reptiles and fish, is vastly different from that of mammals, making it difficult to predict the requirement for an efficient cellular hemostatic response. Avian species, however, are warm-blooded, with a large cardiac output and higher blood pressures than mammalian species[122]. In this sense, the presence of high-shear arterial flow reproduces a hemodynamic environment very similar to that of a mammalian system. Some of the most recently characterized thrombocytes are those present in zebrafish and have been shown to activate in response to collagen and weakly activate in response to ADP—an activation profile similar to that of chicken thrombocytes[141-143]. Additionally, laser injury models of the caudal artery in 3- to 4-day post-fertilization zebrafish larvae demonstrate generation of thrombocyte aggregates, and, in some cases, occlusive thrombi[143,144]. However, the arteries in these zebrafish models are small and have relatively low shear compared to large arteries found in avian or mammalian species. Morpholino-injected knockdown of α_{2b} only resulted in a 50% reduction in thrombus surface area in this model, whereas at arterial shear rates of 1300 s^{-1}, eptifibatide-treated human platelets show a >90% reduction in aggregate surface area (Fig. 3-8D)[144].

Our finding that potent collagen-induced activation of hemostatic cells is conserved from platelets to thrombocytes indicates the importance of subendothelial collagen as a primary activator in hemostasis. However, our studies suggest some fundamental differences between collagen-induced thrombocyte activation and GPVI-induced platelet activation in response to collagen. Thrombocytes are not activated by

the GPVI-specific ligands CRP, a collagen peptide mimetic, or convulxin, a snake venom toxin that binds a site of GPVI not required for collagen interaction. CRP is a synthetic peptide consisting of 10 gly-pro-hydroxypro (GPO) repeats, cross-linked to create a quaternary structure[28]. CRP is believed to specifically activate GPVI through coordination with certain basic residues exposed within an apical groove in the GPVI D1 ectodomain and is believed to recapitulate the primary mechanism by which GPVI interacts with collagen[23,25,145,146]. The fact that CRP does not activate chicken thrombocytes suggests that the primary means by which collagen interacts with its receptor(s) on thrombocytes is fundamentally different from that of the collagen-GPVI interaction. It should be noted, however, that there are residues implied in collagen binding that have no effect on CRP binding, suggesting the GPVI binding sites for collagen and CRP are not entirely identical.

The use of tyrosine kinase signaling for collagen-induced activation appears to be conserved from avian thrombocytes through mammalian platelets. A thrombocyte-specific Ig-receptor that couples to the immunotyrosine activating motif-containing FcRγ subunit through a transmembrane arginine has been identified that binds chicken IgY[147]. It remains to be seen whether there is a single Ig-receptor or multiple receptors that are responsible for collagen-induced thrombocyte activation and if unique extra- or intracellular features of such receptors are conserved through mammalian GPVI.

The lack of a chicken GPVI ortholog is consistent with our understanding that monotremes (egg-laying mammals), which diverged from therian (marsupial and placental) mammals approximately 150 million years ago and whose genome is

particularly well annotated, also do not contain a GPVI ortholog. Furthermore, the leukocyte-receptor complex (LRC), the gene cluster that encodes mammalian GPVI and other immunoglobulin (Ig) superfamily members, has undergone dramatic rearrangement from avian to monotreme to placental mammals[114,148-150]. Chicken and mammalian paired Ig-receptors share basic structural similarities and ITAM-coupling mechanisms, but no direct chicken orthologs exist for mammalian LRC genes[114,151]. It will be informative to determine the array of thrombocyte-specific Ig receptors and their role in hemostatic function.

Materials and methods

Antibodies and reagents

Mouse AP-2 mAb was a generous gift from Thomas Kunicki[123]. Mouse K55 mAb was a generous gift from Hyun Lillehoj[152]. Convulxin, type-I fibrillar collagen derived from equine tendon, and ADP were obtained from previously described sources[153]. Collagen-related peptide (CRP) was generous gift from Debra Newman. Thrombin from bovine plasma (40-300 NIH units/mg protein) was purchased from Sigma-Aldrich (St. Louis, MO). PP2 and piceatannol were purchased form Calbiochem (San Diego, CA). Eptifibatide was purchased from Merck (Whitehouse Station, NJ). MesAMP was purchased from Axxora (San Diego, CA). Alexa-Fluor 488 and 647 Monoclonal Antibody Labeling Kits and Alexa-Fluor 594-conjugated phalloidin were purchased from Molecular Probes (Carlsbad, CA).

Blood collection and preparation

Chicken studies

Blood was collected from the wing vein of healthy female Rhode Island red pullet chickens, aged approximately 6 months, from a commercial source using a 19-gauge butterfly needle into 10-mL or 30-mL syringes anticoagulated with either 1:10 (v/v) 93μm D-phenylalanyl-L-prolyl-L-arginine chloromethyl ketone (PPACK) or 1:6 (v/v) acid/citrate/dextrose (65 mM Na_3citrate•$2H_2O$, 70 mM citric acid•H_2O, 100 mM dextrose, pH 4.4) or 1:9 (v/v) sodium citrate (130 mM Na_3citrate•$2H_2O$, pH 7.4). Whole blood was diluted 1:1 in modified Tyrode's buffer (137 mM NaCl, 20 mM HEPES, 2.7

mM KCL, 3.3 mM NaH_2PO_4, 5.6 mM glucose, 1 g/L BSA, pH 7.4) containing 1 mM $MgCl_2$, and 12-mL aliquots were spun at 50 *g* for 5 min. The thrombocyte-rich plasma layer was isolated by aspiration pipetting. For preparation of washed thrombocytes, 1 U/mL apyrase and 1 μM prostacyclin were added to thrombocyte-rich plasma, and samples were washed once in platelet wash buffer (10 mM HEPES, 1 mM EDTA, 150 mM NaCl, pH 6.0) before resuspending in modified Tyrode's buffer. Cells were counted using a hemocytometer, and the larger, ovoid red blood cells were deliberately not counted.

Human studies

Blood was collected from 6 healthy donors using a 19-gauge butterfly needle into 10 mL or 30 mL syringes anticoagulated as described above. Washed platelets were prepared are described for thrombocytes above.

Chicken plasma cell transcriptional profiling

Washed thrombocyte-rich plasma from 3 separate chicken blood collections was co-stained with Alexa-Fluor 488-conjugated K55 mAb and Alexa-Fluor 647-conjugated AP-2 mAb for 30 min, washed with phosphate-buffered saline, and resuspended in Dulbecco's Modified Eagle Medium (Invitrogen, Carlsbad, CA) at 40 x 10^7 cells per mL. 2 x 10^6 K55 positive, AP-2 negative cells (lymphocytes) and K55 negative, AP-2 positive cells (thrombocytes) were collected via cell sorting, and RNA was isolated using Trizol (Invitrogen) and RNAEasy Kit (Qiagen, Valencia, CA). Thrombocyte and lymphocyte cDNA was produced using the Superscript® First Strand Synthesis Kit (Invitrogen).

Transcriptional profiling was performed by the University of Pennsylvania Microarray Facility using the GeneChip Chicken Genome Array (Affymetrix, Santa Clara, CA).

[^{3}H] 5-HT secretion assays

Thrombocyte-rich plasma or platelet-rich plasma was incubated with [^{3}H] 5-HT (2 μCi [0.074 MBg]/mL) at 37 °C for 30 min. Thrombocyte or platelet suspensions were washed and resuspended to final concentration of 2 x 10^7 cells per mL or 2 x 10^8 platelets per mL, respectively, in modified Tyrode's buffer plus 1 μm imiprimine and 1 mM $CaCl_2$. Cell aliquots of 500 mL were stimulated under non-stirring conditions at 37 °C for 10 min. In certain cases, inhibitors were added and cells were incubated at 37 °C for 10 min prior to stimulation. Reactions were stopped by addition of equal volume 2% paraformaldehyde and 0.1 mM EDTA followed by centrifugation at 10,000 *g* for 5 min. [3H] counts were measured from the supernatants of stimulated samples and unstimulated controls, which were used as background. To determine total loading, [3H] counts were measured in an equal volume of loaded cells following lysis in an equal volume of fixing buffer plus 2% Triton X-100. Percent serotonin release was represented as ([^{3}H] sample – [^{3}H] background) / ([^{3}H] total – [^{3}H] background) x 100. Percent inhibition was represented as (% release with inhibitor) / (% release without inhibitor) x 100.

Thrombocyte aggregation assays

Thrombocyte-rich plasma collected from blood anticoagulated in sodium citrate was diluted to a concentration of 2 x 10^7 cells per mL. 5 x 10^6 cells were used for each stimulation. Aggregation assays were performed as previously described[58].

Preparation of chicken collagen-coated slides

An acid-soluble chicken collagen types-I and –III prep was prepared as described previously[154]. Reconstitution of fibrilar chicken collagen was performed as previously indicated[155]. Briefly, the collagen was dissolved in 0.5 M acetic acid at 1.5 mg/mL and dialyzed against 2 changes of 50 mM Tris HCl, pH 7.5 at 4 °C over 48 h. After dialysis, the gelatinous white collagen precipitate was resuspended with a repeated aspiration through a 22-gauge needle and then sonicated with a steel probe sonicator (Branson 450 Digital Sonifer®, Danbury, CT) on ice for 3 pulses of 5 sec at 10% amplitude with at least 15 sec between pulses. Coating of microscope slides was performed as described previously [40]. Briefly, 300 µL of fribrillar chicken collagen was placed in a flexiperm well that was attached to an EtOH-washed 25 x 75 mm glass (Fisher, Pittsburgh, PA) or Permanox™ (Nunc, Rochester, NY) microscope slide, for scanning electron microscopy assays, and incubated at 4 °C overnight. Slides were then washed 2 times with PBS and blocked with 1% denatured BSA for at least 1 h at room temperature prior to use.

Whole blood flow assays

The tapered-wall parallel plate flow chamber was assembled as previously described[40,156]. The assembled chamber was then placed on the stage of an inverted microscope (Nikon Eclipse TE2000-U, Melville, NY). Blood collected in PPACK was warmed at 37 °C for 10 min, along with inhibitors, and 2.5 μg/mL fluorescently labeled Alexa-Fluor 488-conjugated AP-2 mAb was added, which binds both human and chicken $\alpha_{2b}\beta_3$ to label platelets or thrombocytes[123]. Whole blood was perfused over the collagen-coated glass slide at a flow rate of 0.428 mL/min using a syringe pump (Model '11' Plus; Harvard Apparatus) for 5 min. After whole blood perfusion, chambers were rinsed with modified Tyrode's buffer at the same flow rate for 5 min prior to static image collection.

Whole blood flow image capture and analysis

During whole blood flow, platelet or thrombocyte adhesion was monitored continuously by epifluorescence microscopy. Images were captured using a CCD camera (C9300-201 Hamamatsu, Bridgewater, NJ) mounted on an inverted microscope with a 300 W Xenon lamp (Perkin Elmer Optoelectronics, Freemont, CA) through a Lambda DG-4 high-speed filter changer (Sutter Instruments, Novato, CA) used at 470 nm Ex / 525 nm Em. For real-time fluorescent microscopy during blood flow, images were captured continuously with a 300 ms exposure time at an interval of 100 ms using Slidebook software (Intelligent Imaging Innovations) as previously described[153]. Static image collection was obtained using epifluorescence microscopy at different axial positions along the flow chamber that correspond to a given shear rate. Platelet or thrombocyte percent surface

coverage and average aggregate size were quantified using ImageG software (National Institutes of Health). Both results were reported as the mean plus or minus standard error of the mean (SEM).

Fluorescent microscopy of collagen slides following whole blood flow

Slides were removed from the flow chamber and fixed in 1% paraformaldehyde for 5 min and washed 3 times in PBS. Slides were then permeabilized in 0.02% Triton X-100 in PBS with BSA 1 mg/mL for 5 min followed by 3 washes in PBS. Filamentous actin was stained with Alexa-Fluor 594-conjugated phalloidin (25 μL/mL) for 45 min at room temperature. Slides were imaged with fluorescent microscopy as previously described[99].

Scanning electron microscopy of collagen slides following whole blood flow

Permanox™ (Thermo Fisher Scientific, Rochester, NY) slides were coated with chicken collagen as described for glass slides. Permanox was used to facilitate slide cutting for microscopy preparation. Following whole blood perfusion, slides were removed from the flow chamber, washed 3 times in PBS, and fixed in 2% glutaraldehyde until microscopy analysis. Slide sections were analyzed on a Philips XL20 scanning electron microscope.

Flow cytometric analysis

Washed platelets or thrombocytes were diluted to a concentration of 2.5×10^7 platelets per mL or 2×10^7 cells per mL, respectively, and 2.5×10^6 platelets or 2.5×10^6 thrombocytes were stained with Alexa-Fluor 488-conjugated AP-2 mAb at room

temperature for 1 h and analyzed by flow cytometry. Mean fluorescent intensity of AP-2-positive cells was quantified for platelets and thrombocytes.

Thrombocyte spreading assay

Lab-Tek II chamber slides (Thermo Fischer Scientific, Rochester, NY) were coated with type I fibrillar collagen (Chronolog) at 30 μg/mL in 50 μM acetic acid for 16 h at 4 °C, washed 3 times with PBS, and blocked with BSA 1 mg/mL in PBS for 30 min at room temperature. Thrombocyte-rich plasma was diluted to 2 x 10^7 cells per mL in modified Tyrode's buffer containing 1 mM $MgCl_2$ and 1 mM $CaCl_2$, and 500 μL of cells were incubated on the collagen-coated chambers for 45 min at 37°C. Fixation, permeablizing, and staining were performed as previously reported[153].

Figure 3-1. Analysis of chicken plasma preps by flow cytometry.

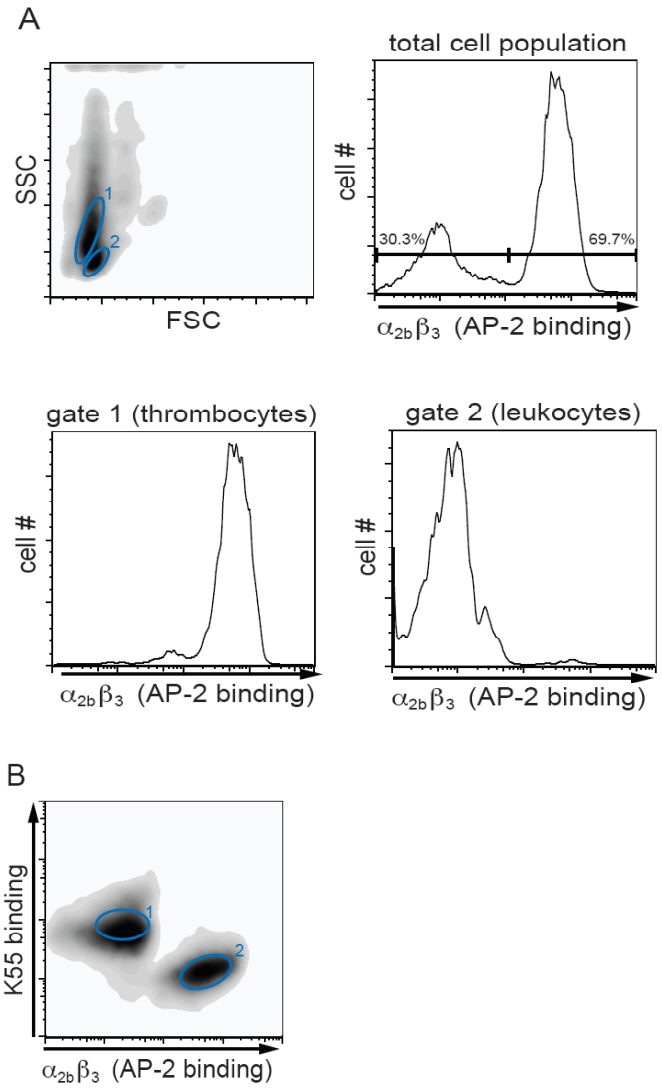

Figure 3-1. Analysis of chicken plasma preps by flow cytometry. A. Washed chicken thrombocyte-rich plasma was stained with Alexa-Fluor 488-conjugated AP-2 mAb and analyzed by flow cytometry. Thrombocytes could be detected at a distinct forward and side scatter from leukocytes (compare gate 1 to gate 2) and were readily identified by expression of the thrombocyte-specific marker $\alpha_{2b}\beta_3$ (AP-2-positive cells).
B. Thrombocyte-rich plasma cells were sorted for transcriptional profiling based on positive and negative selection markers using the lymphocyte-specific mAb K55, which excludes thrombocytes, and the thrombocyte-specific mAb AP-2. Gate 1 was specific for lymphocytes while gate 2 was specific for thrombocytes.

Table 3-I. Detection of platelet-specific gene expression in thrombocytes by transcriptional profiling.

Gene	Ratio (T/L)	Fold Change	P value
MPL	422.0	821.2	3.5E-05
GP9	892.4	6.7	3.8E-04
ITGB3	612.8	597.6	5.3E-05
ITGB1	2.2	1.07	0.002
ITGA6	5.2	1.02	0.004
ITGA2	215		1.3E-06
ITGAV	24.3	9.5	3.1E-04
PAR1	26.3	1.36	0.001
PAR4	7.0	1.005	0.007
P2RX1	823.7	38.2	2.0E-04
P2RY1	15.0	29.0	2.2E-04
HTR2A	467.1	209.4	1.0E-04
CD36	1027.5	4.03	5.0E-04
TBXAS1	74.8	42.5	2.0E-04

Table 3-I. Detection of platelet-specific gene expression in thrombocytes by transcriptional profiling. Thrombocytes and lymphocytes were sorted by positive and negative selection for cell-specific markers, and gene expression analysis was performed using the Affymetrix chicken gene chip. The gene expression ratio of thrombocytes to lymphocytes (T/L), fold change, and P values for genes of known platelet specificity present in the chicken chip are shown.

Figure 3-2. Activation of chicken thrombocytes by collagen and thrombin.

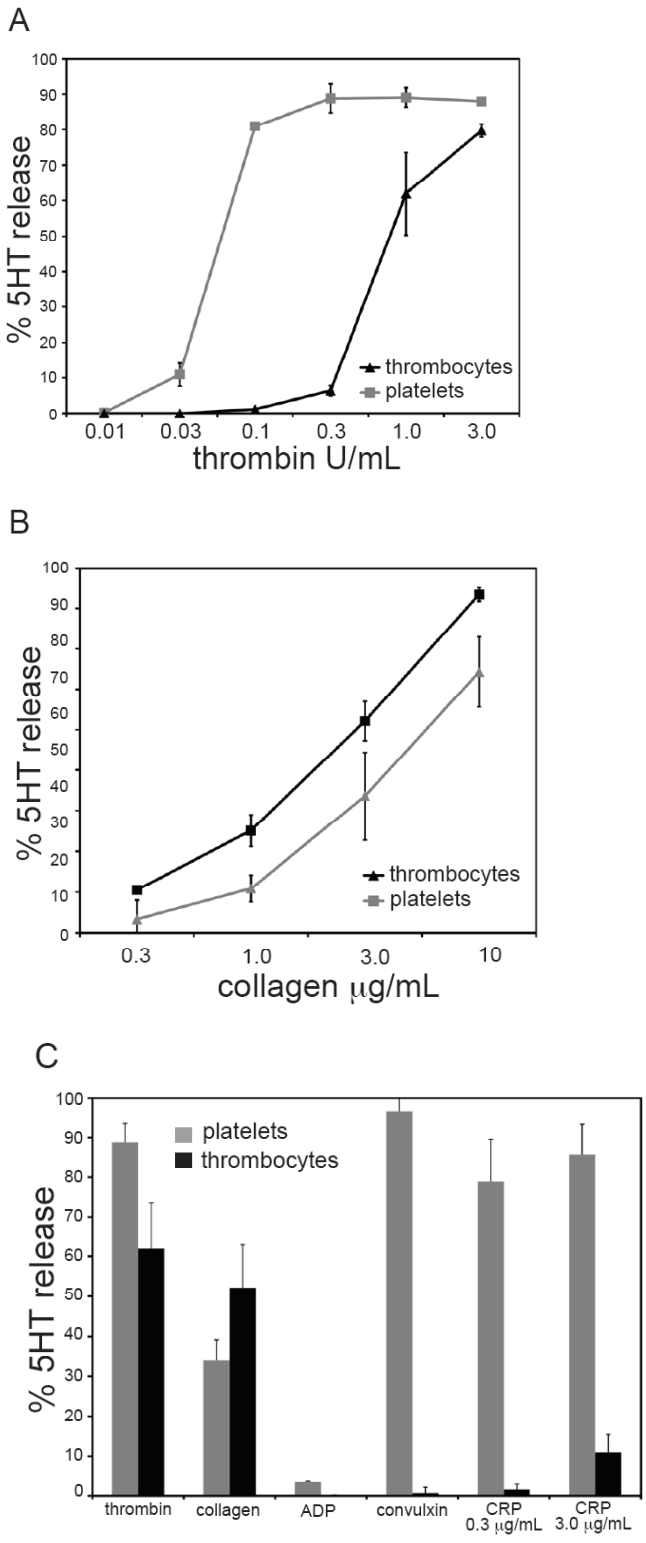

Figure 3-2 (cont'd). Activation of chicken thrombocytes by collagen and thrombin.

D

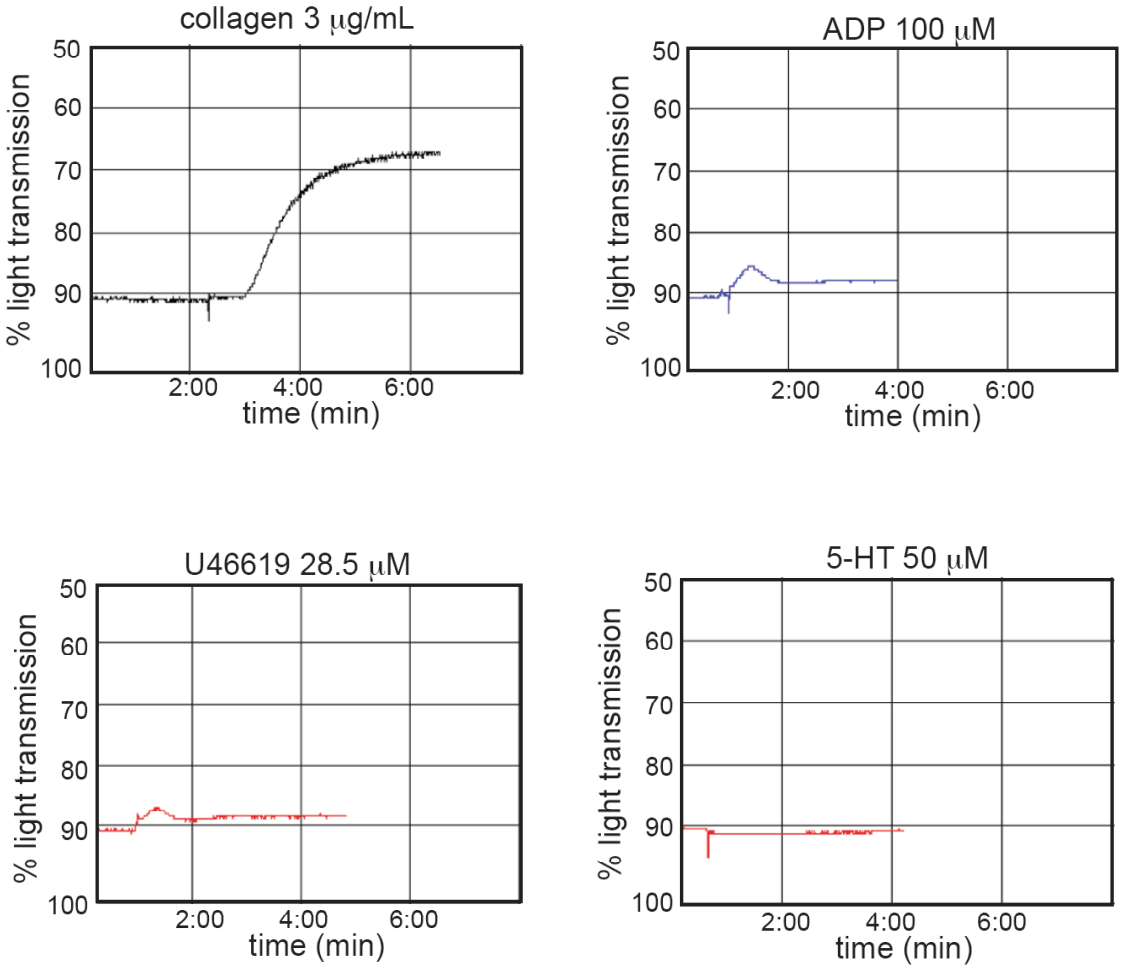

Figure 3-2. Activation of chicken thrombocytes by collagen and thrombin. 5-HT release from platelets or thrombocytes was measured following loading with [^{3}H] 5-HT. Cells were stimulated with increasing doses of bovine thrombin (A) or equine type-I collagen (B) or various agonists (C). In panel C, thrombin, collagen, and ADP were used at concentrations of 1 U/mL, 3.0 μg/mL, and 10 μM, respectively. D. Aggregation of chicken thrombocytes in response to various agonists. Thrombocyte-rich chicken plasma was stimulated with indicated agonists, and aggregation was measured by percent light transmittance in a luri-aggregometer.

Figure 3-3. PP2 and piceatannol inhibit collagen-induced 5-HT secretion in thrombocytes in a dose-dependent manner.

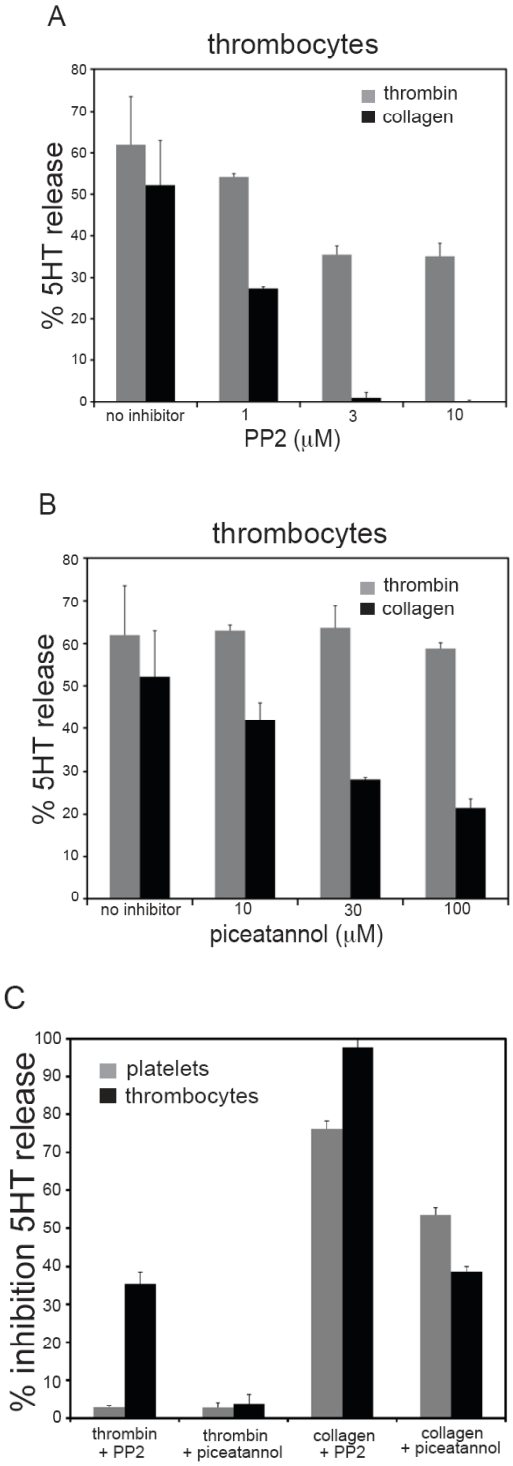

Figure 3-3. PP2 and piceatannol inhibit collagen-induced 5-HT secretion in thrombocytes in a dose-dependent manner.

5-HT release from platelets or thrombocytes was measured following loading with [^{3}H]-5-HT. Chicken thrombocytes were stimulated with either thrombin (1 U/mL) or collagen (3 μg/mL) in the presence of increasing doses of PP2 (A) or piceatannol (B). C. PP2 (3 μM) and piceatannol (30 μM) were used to inhibit 1 U/mL thrombin- or 3.0 μg/mL collagen-induced 5-HT release in either human platelets or chicken thrombocytes. In all panels, shown is the mean ± SD; *n* = 3 experiments per condition.

Figure 3-4. Chicken collagen type-I and –III coated on glass slides.

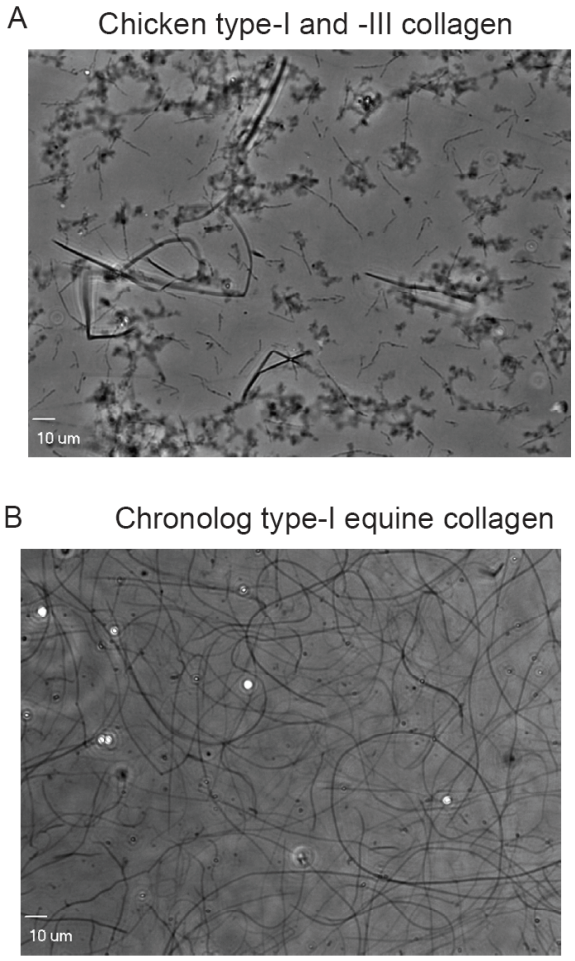

Figure 3-4. Chicken collagen type-I and –III coated on glass slides. Chicken collagen type-I and –III was purified from chicken skin and dialyzed against 0.05 M Tris-HCl pH 7.5 to create a fibrillar peptide. A. Chicken collagen was coated on glass slides overnight at 4 ºC. B. Glass slides coated with Chronolog type-I equine collagen are shown for comparison.

Figure 3-5. Thrombocytes cover less surface area and fail to form aggregates during adhesion to collagen under whole blood flow.

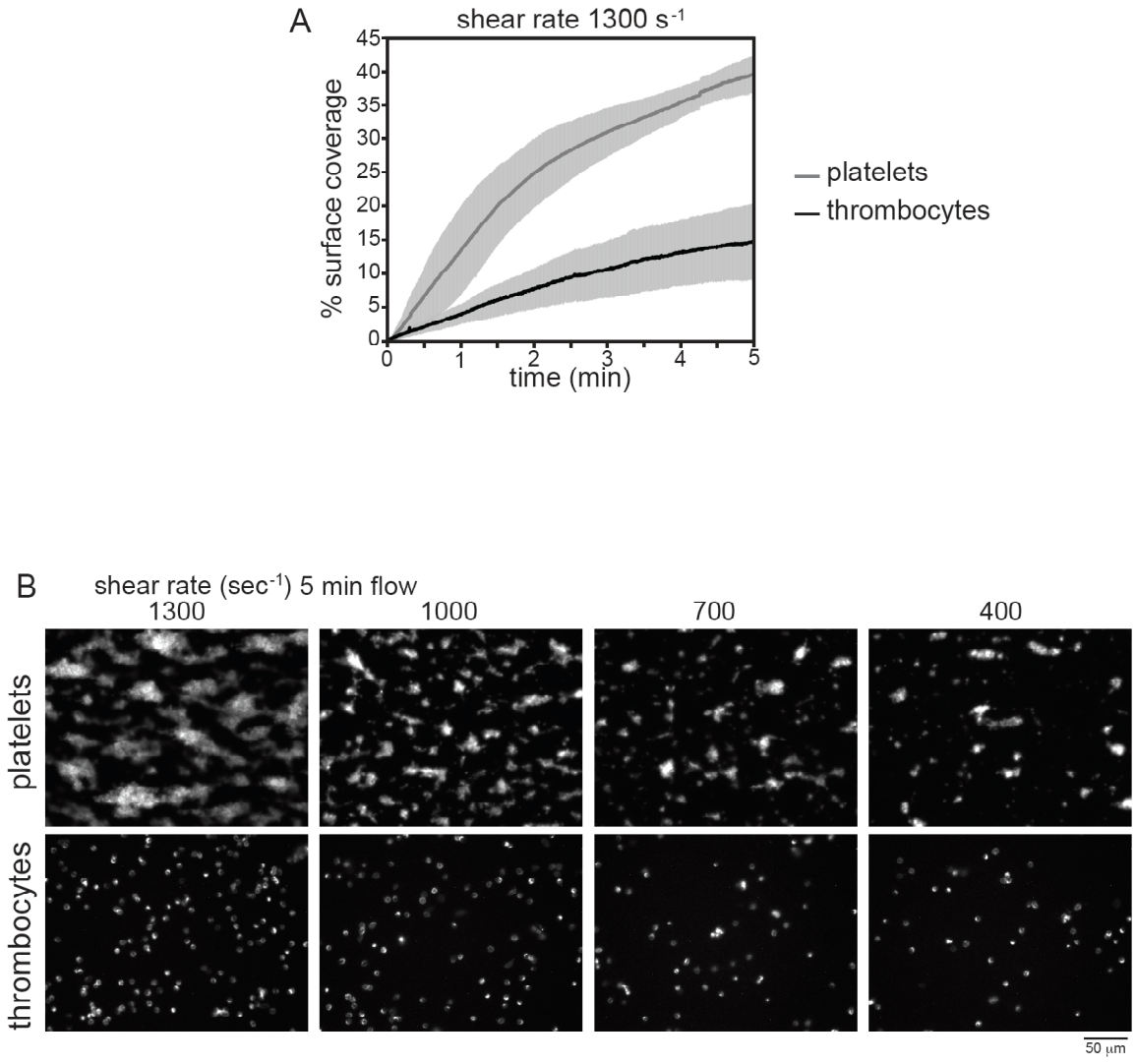

Figure 3-5 (cont'd). Thrombocytes cover less surface area and fail to form aggregates during adhesion to collagen under whole blood flow.

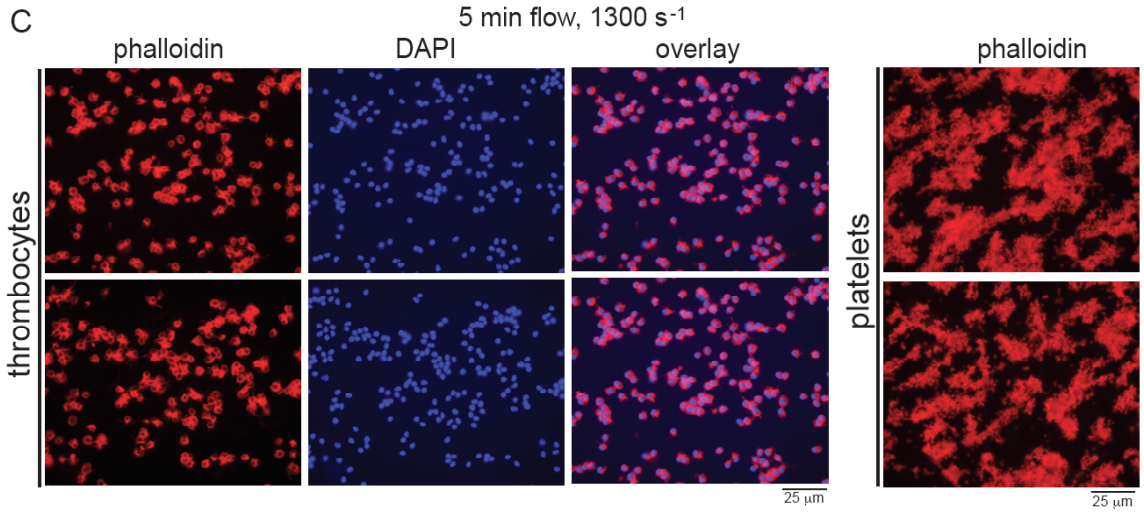

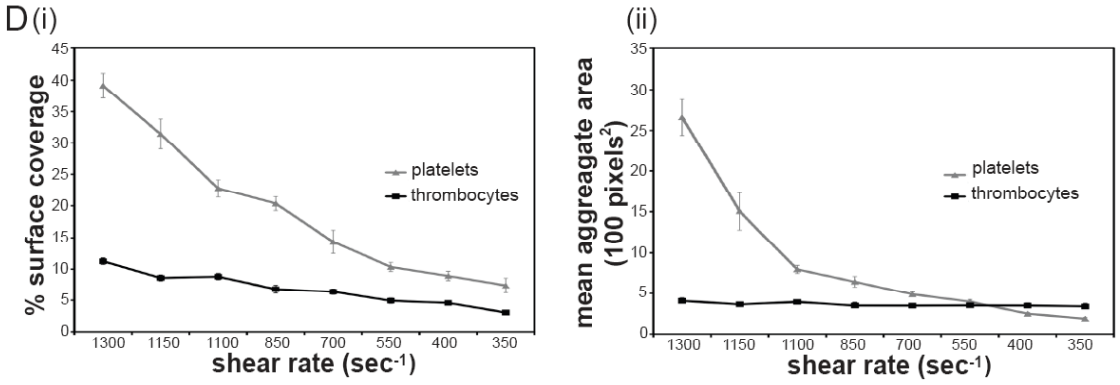

Figure 3-5. Thrombocytes cover less surface area and fail to form aggregates during adhesion to collagen under whole blood flow. PPACK-anticoagulated human or chicken whole blood was labeled with AP-2 mAb and perfused through a tapered-wall parallel plate flow chamber for 5 min over a chicken collagen-coated glass slide. A. Time traces of percent surface coverage of collagen surface by platelets or thrombocytes. Shown is mean ± SD; n = 7-10 for each condition. B. Representative fluorescent images captured at areas corresponding to shear rates of 1300, 1100, 700, and 400 s^{-1} after 5 min perfusion of whole blood. C. Representative images of thrombocyte or platelet adhesion to collagen following whole blood flow for 5 min at 1300 s^{-1}. Slides were fixed, permeabilized, and stained with Alex-Fluor 594-conjugated phalloidin to detect actin filaments. Nuclear staining of thrombocytes with DAPI is also shown. D. Percent collagen surface area coverage (i) and mean aggregate area (ii) of human platelets or chicken thrombocytes following perfusion of whole blood for 5 min was determined by analysis of fluorescent images. Shown are the mean ± SEM; n = 7-10 experiments for each condition.

Figure 3-6. Chicken thrombocytes do not form aggregates after extended flow of whole blood.

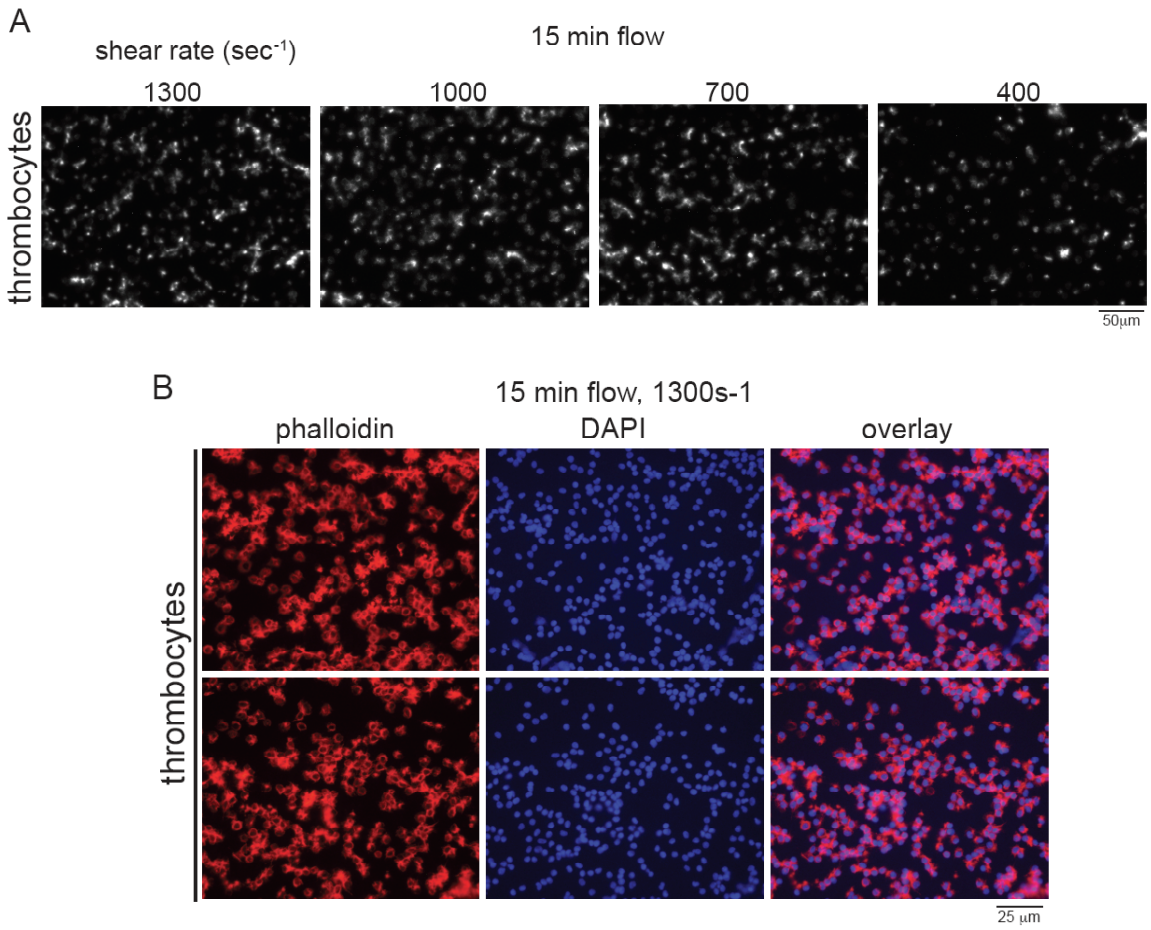

Figure 3-6. Chicken thrombocytes do not form aggregates after extended flow of whole blood. A. Representative fluorescent images captured at areas corresponding to shear rates of 1300, 1100, 700, and 400 s^{-1} after 15 min perfusion of chicken whole blood. B. Representative images of thrombocyte adhesion to collagen following whole blood flow for 15 min at 1300 s^{-1}. Slides were fixed, permeabilized, and stained with phalloidin and DAPI. Note that each adherent thrombocyte can be distinctly visualized by DAPI staining, demonstrating an absence of 3-dimensional aggregation.

Figure 3-7. Scanning electron microscopy of platelets and thrombocytes following adhesion to collagen under whole blood flow.

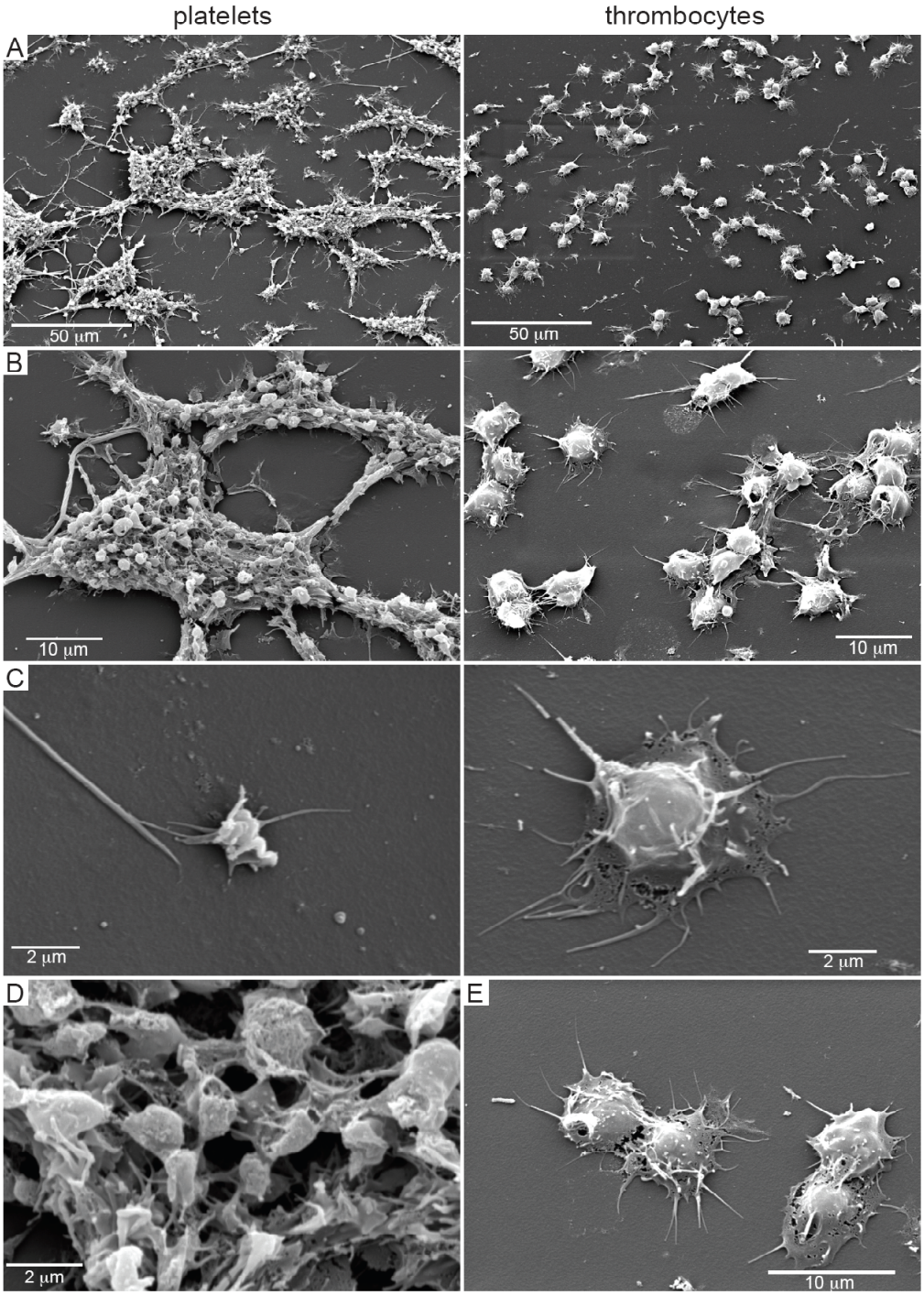

Figure 3-7. Scanning electron microscopy of platelets and thrombocytes following adhesion to collagen under whole blood flow. PPACK-anticoagulated human or chicken whole blood was perfused through a tapered-wall parallel plate flow chamber for 5 min over a chicken collagen-coated slide. Images were obtained by scanning electron microscopy at regions corresponding to a shear rate of approximately 1300 s^{-1}. Platelets and thrombocytes were imaged at magnifications of 650 X (A), 2000X (B), and 8000 X (C). D. The inside of a platelet aggregate imaged at 10,000 X. E. Adherent thrombocytes forming membrane contacts at 3500 X.

Figure 3-8. Thrombocyte adhesion to collagen under flow is sensitive to Src-family kinase inhibition.

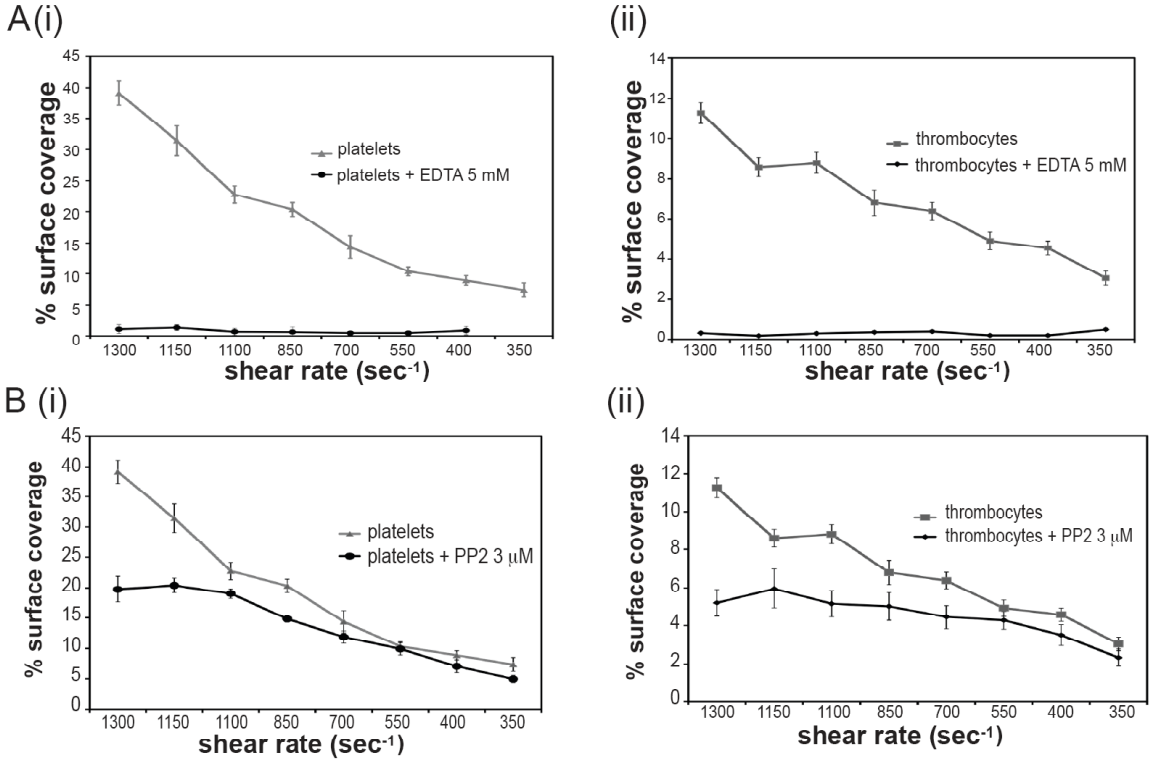

Figure 3-8. Thrombocyte adhesion to collagen under flow is sensitive to Src-family kinase inhibition. A. Percent collagen surface area coverage of platelets (i) or thrombocytes (ii) following perfusion of 5 mM EDTA-treated whole blood for 5 min was determined by analysis of fluorescent images. B. Percent collagen surface area coverage of human platelets (*i*) or chicken thrombocytes (*ii*) following perfusion of 10 μM PP2-treated whole blood for 5 min. Shown are the mean ± SEM; $n = 4$ experiments for each condition.

Figure 3-9. Thrombocytes express fewer $\alpha_{2b}\beta_3$ integrin receptors than do platelets and are not affected by $\alpha_{2b}\beta_3$ inhibition during adhesion to collagen under flow.

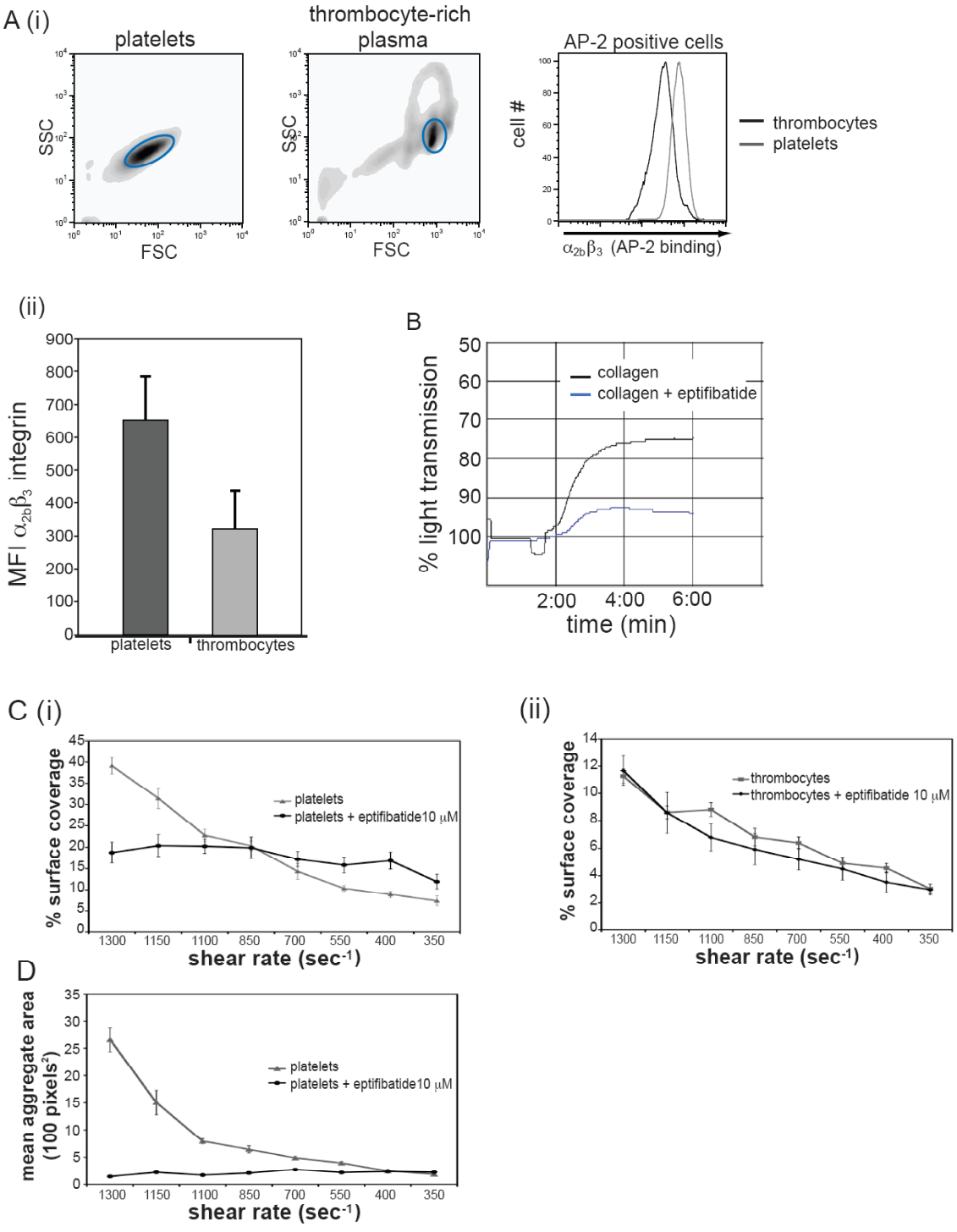

Figure 3-9. Thrombocytes express fewer $\alpha_{2b}\beta_3$ integrin receptors than do platelets and are not affected by $\alpha_{2b}\beta_3$ inhibition during adhesion to collagen under flow.

A. Levels of $\alpha_{2b}\beta_3$ integrin expression on washed human platelets and washed chicken thrombocyte-rich plasma were determined by staining with AP-2 mAb and analyzed by flow cytometry. *i*. Representative staining of human platelets and chicken thrombocytes for the $\alpha_{2b}\beta_3$ integrin, as determined by AP-2 mAb binding. Gates denote regions analyzed, and only AP-2 positive cells were analyzed for mean fluorescence intensity (MFI). *ii*. The histogram depicts MFI of AP-2 binding ± SD.

B. Eptifibatide inhibits chicken thrombocytes aggregation. Thrombocytes were stimulated with 1 μg/mL collagen in the presence or absence of 10 μM eptifibatide, and aggregation was measured by percent light transmittance in a luri-aggregometer.

C. Percent collagen surface area coverage of human platelets (*i*) or chicken thrombocytes (*ii*) following perfusion of 10 μM eptifibatide-treated whole blood for 5 min was determined by analysis of fluorescent images. D. Mean platelet aggregate area following perfusion of 10 μM eptifibatide-treated whole blood for 5 min. For panels C and D, shown are the mean ± SEM; $n = 4$ experiments for each condition.

Figure 3-10. The effect of P_2Y_{12} inhibition on platelet and thrombocyte adhesion to collagen under flow.

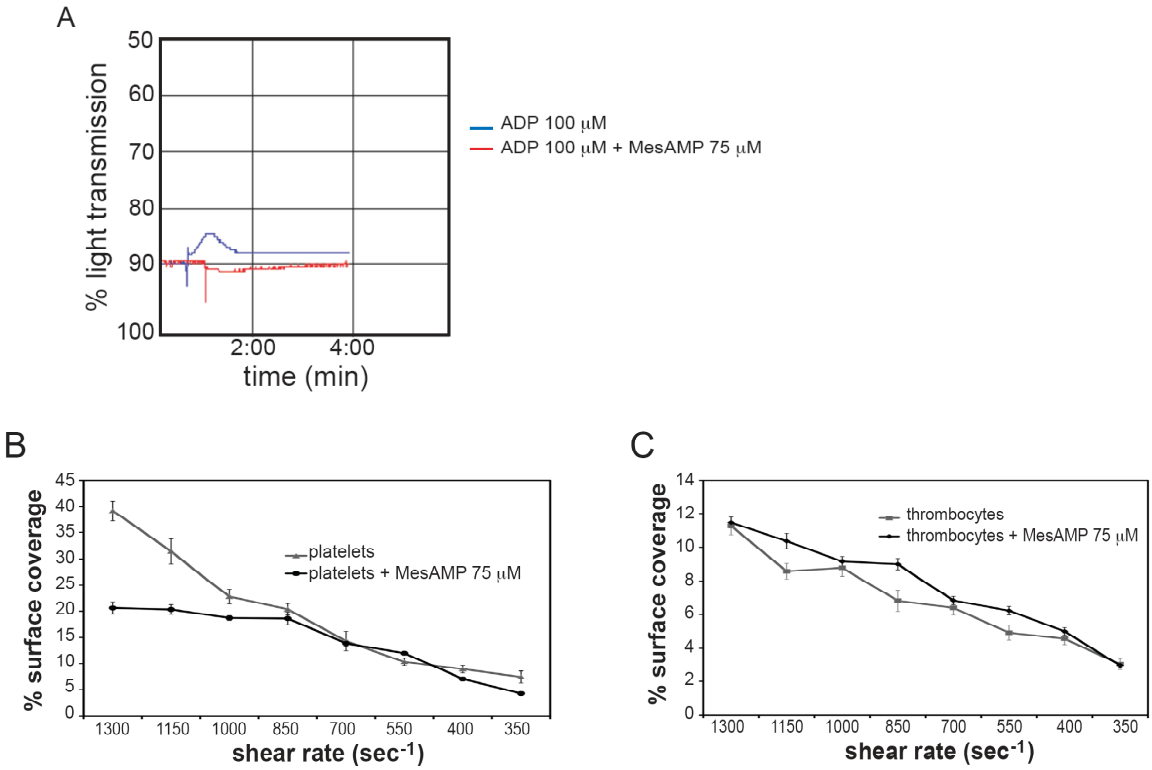

Figure 3-10. The effect of P_2Y_{12} inhibition on platelet and thrombocyte adhesion to collagen under flow. A. MesAMP inhibits thrombocyte aggregation. Thrombocytes were stimulated with 100 μM in the presence or absence of 75 μM MesAMP, and aggregation was measured by percent light transmittance in a luri-aggregometer. Percent collagen surface area coverage of human platelets (B) or chicken thrombocytes (C) following perfusion of 75 μM MesAMP-treated whole blood for 5 min was determined by analysis of fluorescent images. Shown are the mean ± SEM; n = 4 experiments for each condition.

Supplemental movie legends

For all movies, PPACK-anticoagulated human or chicken whole blood was labeled with AP-2 mAb and perfused through a tapered-wall parallel plate flow chamber for 5 min over a chicken collagen-coated glass slide. Each movie depicts cell adhesion at a shear rate of 1200 s^{-1}.

Supplemental movie 3-1. Adhesion of human platelets following perfusion of whole blood over chicken collagen.

Supplemental movie 3-2. Adhesion of chicken thrombocytes following perfusion of whole blood over chicken collagen.

Supplemental movie 3-3. Adhesion of human platelets following treatment with 30 μM PP2 and perfusion of whole blood over chicken collagen.

Supplemental movie 3-4. Adhesion of chicken thrombocytes following treatment with 30 μM PP2 and perfusion of whole blood over chicken collagen.

Supplemental movie 3-5. Adhesion of human platelets following treatment with 75 μM eptifibatide and perfusion of whole blood over chicken collagen.

Supplemental movie 3-6. Adhesion of chicken thrombocytes following treatment with 75 μM eptifibatide and perfusion of whole blood over chicken collagen.

Chapter 4—Conclusions and future directions

Summary

Collagen-induced activation of platelets is believed to be a primary step in platelet function during physiologic hemostasis and pathologic thrombosis. The immune-type receptor GPVI is a platelet-specific receptor required for collagen-induced activation. In Chapter 2, we demonstrate that the GPVI receptor contains a proline-rich domain, unique to GPVI compared to other homologous receptors, that constitutively binds and directly activates the Src-family kinase Lyn. The interaction of GPVI and Lyn via the proline-rich domain accelerates GPVI signaling kinetics and is required for efficient platelet adhesion to collagen under flow. In Chapter 3, we characterize the collagen response of the chicken thrombocyte, which expresses platelet-specific receptor orthologs but does not contain GPVI. Thrombocytes are capable of activating in response to collagen, using a signaling pathway analogous to that of GPVI, and they adhere to collagen under high shear. However, thrombocytes express a significantly lower level of $\alpha_{2b}\beta_3$ integrin than do platelets, and they do not form 3-dimensional aggregates under flow conditions. Our studies demonstrate fundamental conservation of responses to collagen by hemostatic cells but suggest that platelets have adapted additional mechanisms to promote aggregation under high shear conditions. Moreover, our findings raise new questions about GPVI signaling and thrombocyte function in hemostasis.

Use of immune-type receptor signaling to activate hemostatic cells in response to collagen

GPVI is well characterized as a platelet-activating receptor that uses an immune tyrosine kinase pathway to activate platelets. Most other activating receptors on platelets are G protein-coupled and use a fundamentally different signaling pathway. A potential, albeit simplified, explanation for why an immune signaling response to collagen may be advantageous compared to a G protein-coupled response is the fact that signaling via receptor clustering (immune-type receptors, driven by avidity) rather than conformational change (G protein-coupled receptors, driven by receptor-ligand affinity) allows for a graded and sustained signaling response. As the major component of the subendothelial matrix, collagen, exposed following vessel injury, may be the first ligand encountered by the platelet. Use of an immune receptor signaling pathway allows platelet activation to be modulated depending on the degree of collagen exposure. The response of platelets to collagen may be excessive in pathological situations where the balance shifts from hemostatic platelet activation to pathological thrombosis. Nevertheless, our findings in Chapter 2 show that the classical mechanism of immune receptor signaling employed by B-cells and T-cells has been modified by platelet GPVI to suit the unique context of collagen-induced activation under hemodynamic flow.

The fact that GPVI contains a proline-rich domain that constitutively binds and directly activates Lyn means that the receptor is primed for rapid activation following ligand binding. This molecular priming allows GPVI to function more effectively under arterial shear, where the platelet only has seconds to activate and firmly adhere. While

this adaption of GPVI increases platelet responses to collagen under flow, it is not absolutely essential for this response. Proline-rich domain-deleted GPVI platelets still adhere to collagen more effectively that GPVI-deficient platelets. It is unknown whether the collagen receptor(s) on thrombocytes employ a proline-rich domain to accelerate signal transduction. It could be difficult and misleading to calculate a relative adhesive efficiency for platelets compared to thrombocytes, but thrombocytes do not seem to be defective in transitioning from the rolling phase to the firmly adherent phase. Thrombocytes, like platelets, are clearly engineered for shear resistant adhesion to collagen under flow, and this behavior is equally sensitive to Src-family kinase inhibition in both cell types. Therefore, the initial response to collagen, in both signal transduction and adhesion under flow, appears conserved between platelets and thrombocytes. The fundamental difference between platelets and thrombocytes seems to lie outside of their relative responses to collagen and relates more significantly to their basic mechanisms promoting aggregate formation under high shear.

Future directions for GPVI and thrombocyte research

Our observations provide insight into the molecular function of GPVI in platelet biology and characterize the response of a more primitive hemostatic cell—the thrombocyte—during adhesion to collagen under whole blood flow. Our results uncover new questions that require future investigation.

Is GPVI / FcRγ embedded in the cell membrane to prevent constitutive signaling from bound and activated Lyn kinase?

Our findings in Chapter 2 suggest that GPVI keeps Lyn constitutively bound and held in an active state. We propose that, in order to prevent the undesirable effects of constitutive signaling through the GPVI / FcRγ complex, the GPVI cytoplasmic tail and/or the FcRγ chain is embedded in the platelet membrane, keeping the GPVI-bound Lyn and the FcRγ ITAM at a suitable distance from one another to prevent activation prior to receptor ligation. Xu et al. have demonstrated that the membrane-proximal basic residues on the CD3ε chain of the T-cell receptor mediate binding to the cell membrane and keep the CD3ε ITAM embedded in the lipid bilayer[112]. Both GPVI and FcRγ have an enrichment of positively charged amino acids on the proximal end of their cytoplasmic tails. We believe GPVI / FcRγ is an excellent model to test the functional requirements of these membrane-proximal basic residues in preventing constitutive GPVI signaling. GPVI is an extreme example of an immune-type receptor that exists in a tightly coupled off-on state due to its identity as a hemostatic receptor primed to mediate rapid cellular activation following receptor ligation.

Future studies aimed at determining whether the GPVI cytoplasmic tail and/or the FcRγ chain are embedded in the membrane should be performed using a fluorescence resonance energy transfer (FRET) approach in lipid micelles, similar to that employed by Xu et al. Membrane proximal basic residues in GPVI and FcRγ can be mutated to determine if they are required to prevent constitutive signaling through GPVI in the absence of receptor ligation. Use of retroviral complementation to express membrane

proximal mutants in GPVI-deficient bone marrow will be a useful strategy to determine the importance of these residues in GPVI surface expression and signaling in the platelet.

What are the selective roles of Lyn and Fyn kinase in the initial events of GPVI signaling?

Our findings in Chapter 2 are consistent with a model in which Lyn kinase is constitutively bound to GPVI and held in an activated state, primed to mediate immediate signaling following receptor ligation. However, Fyn co-immunoprecipitates with the GPVI / FcRγ signaling complex following receptor stimulation, and absence of Fyn confers a decrease in GPVI-induced platelet activation (see Chapter 2)[47]. Our studies support a model in which Lyn drives initial GPVI signaling, whereas Fyn is responsible for sustained GPVI signaling required for potentiating GPVI-induced platelet activation. What are the mechanisms that underlie this division of labor for the Src-kinases Fyn and Lyn in GPVI signaling? Our studies using a phage display suggest that Fyn does not have a high affinity for the GPVI proline-rich domain. However, our biochemical studies and those of others have demonstrated that both Lyn and Fyn can associate with the GPVI proline-rich domain or perhaps with other members of the GPVI signaling complex (see Chapter 2)[95].

Specific investigation should focus on the relative affinities of Lyn and Fyn for GPVI and determining whether Fyn and Lyn associate with other members of the GPVI signaling complex, such as Syk, Slp-76, LAT, or PLCγ2. We predict that association of Fyn with GPVI or other signaling effectors may be facilitated through ligand-induced

GPVI clustering, and this mechanism should be investigated more thoroughly. At an organism level, genetic experiments in collagen-dependent injury models using Fyn- and Lyn-deficient animals can determine if Lyn is selectively required for initial thrombus formation and Fyn is required for thrombus stability. Such studies would refine our knowledge of downstream signaling events following GPVI stimulation by determining distinct roles for Fyn and Lyn in collagen-induced thrombus formation.

What is the receptor responsible for activating thrombocytes in response to collagen? The fact that GPVI is a low-affinity receptor for collagen requires that alternative ligands other than native collagen had to be used to molecularly identify this platelet collagen receptor. The identification of GPVI was aided by the fact that patient autoantibodies against GPVI and the snake venom toxin convulxin could serve as high-affinity ligands for use in biochemical assays[157,158]. Identification of the thrombocyte collagen receptor is of interest because its lack of binding convulxin and CRP suggests it is structurally different from GPVI and may interact with collagen differently. Our findings in Chapter 3 suggest that the chicken thrombocyte collagen receptor uses an immunotyrosine kinase pathway dependent on Syk and Src-family kinases analogous to that of GPVI. Methods to isolate the thrombocyte collagen receptor could employ a Syk tandem SH2 domain GST fusion protein to pull down the receptor-ITAM adaptor complex for protein analysis. Identification of this receptor would provide further insight into the adaptation of immune receptors for collagen binding and signal transduction in hemostatic cells.

How is GPVI function conserved among mammalian species?

The observation that chicken thrombocytes are activated by fibrillar collagen implies that collagen-induced activation of hemostatic cells has been conserved throughout evolution. It is intriguing that collagen signaling in both thrombocytes and platelets is sensitive to inhibition of Src-family kinases and Syk. This finding suggests that the use of immune receptor signaling pathways to activate hemostatic cells in response to collagen has also been conserved—perhaps because the nature of immune receptor signaling allows for a graded response that is desirable for collagen-induced hemostatic activation. It is impossible to know if mammalian GPVI evolved from collagen-sensing immune receptors found in more primitive species. However, the fact that GPVI is not detectable in the platypus genome suggests that GPVI evolved *after* true non-nucleated platelets came be to utilized as dedicated hemostatic cells. If this is correct, then a lack of response to GPVI-agonists should be observed in platelets from monotreme species but not in platelets from marsupials, the species most evolutionarily distant from placental mammals that have a GPVI ortholog.

To test whether monotreme or marsupial platelets respond to GPVI agonists, we obtained platelet samples from an echidna (spiny anteater), a monotreme, and a striped opossum (a marsupial). While we would expect collagen-induced activation to be conserved in all these species, as they are conserved in more primitive thrombocytes, the ability to respond to GPVI-specific agonists like CRP is of interest because the echidna represents a "missing link"—a species that has platelets but does not express GPVI.

We have performed one set of preliminary experiments, and the results are somewhat consistent with gene ontology data suggesting that monotremes lack GPVI, while marsupials possess GPVI. Platelets from the echidna did not activate in response to convulxin, as demonstrated by a lack of spreading on a convulxin-coated surface and a lack of fibrinogen binding in response to convulxin (Fig. 4-1). In comparison, platelets from the opossum, a marsupial, spread on convulxin and bound fibrinogen in response to convulxin stimulation (Fig. 4-1). These data support results from genetic database searches that indicate the presence of a GPVI ortholog in marsupial, but not monotreme, species. Importantly, echidna, opossum, and mouse platelets all bind fibrinogen in response to ADP stimulation, suggesting that robust ADP-induced platelet activation is conserved and distinguishes platelet responses from those of thrombocytes. To date, it is unknown if thrombocytes are direct ancestors of mammalian platelets or if platelets evolved separately. Echidna platelets did not readily adhere to CRP, but those that did demonstrated spreading (Fig. 4-1A). The significance of this finding is unknown, but it is possible that there are subset populations among echidna platelets that may express receptors capable of interacting with CRP (Fig. 4-1B).

Interestingly, opossum platelets were not strongly activated by CRP, evidenced by only weak fibrinogen binding and a lack of robust spreading response (Fig. 4-1). This finding is difficult to reconcile with the identity of a true GPVI ortholog in the opossum, but it should be mentioned that the GPVI ectodomain region responsible for collagen interaction is only partially conserved from opossum to mouse to human (Fig 4-2). Key residues that have been implied in collagen and/or CRP binding are not present in

opossum GPVI, and the 11 amino acid deletion between GPVI and FcαRI that creates a collagen-binding apical groove in GPVI is only a 5 amino-acid deletion in opossum GPVI (Fig 4-2). Additionally, opossum GPVI contains an extracellular stalk that is 31 residues longer than that of human or mouse GPVI and is poorly conserved. It is difficult to speculate on the significance of these differences, but it is possible that the fundamental nature of the GPVI-collagen interaction has not been highly conserved in mammalian species and has undergone continued evolution. This lack of conservation is in contrast with the highly conserved cytoplasmic proline-rich domain studied in Chapter 2 and supports the characterization of GPVI as a collagen *sensor* selected through evolution for its signal transduction rather than its collagen binding properties. However, it is known that human GPVI has a higher affinity for CRP than does mouse GPVI[159]. The fact that opossum GPVI has little or no ability to be activated by CRP suggests that improving affinity for the GPO repeats constituting a fraction of the native collagen peptide may have increased the sensitivity of GPVI as a hemostatic collagen receptor.

If thrombocytes do not form aggregates on collagen under arterial flow conditions, how does cellular hemostasis function in avian species?

The use of flow chambers to model platelet adhesion to collagen under arterial shear conditions reproduces a fundamental aspect of platelet biology—the formation of a platelet-driven thrombus in both *in vivo* injury models in the mouse arterial system and in human coronary thrombosis following atherosclerotic plaque rupture. The fact that chicken thrombocytes do not form aggregates in the flow chamber system, whereas

platelets do, raises the question of how thrombocytes respond *in vivo* following arterial injury. Do injuries to bird arteries equivalent to those used in mouse injury models result in an occlusive thrombus? Are thrombocytes capable of forming aggregates in high-pressure vessels following exposure of ECM components? Alternatively, are there additional factors present *in vivo* that are not reproduced in flow chamber models that allow for shear-resistant aggregate formation? We hypothesize that cellular thrombus formation under arterial shear *in vivo* is a platelet-specific, and therefore mammalian-specific, phenomenon.

In order to answer these questions, an arterial injury model needs to be developed for avian species. We are working on establishing a model where we can isolate a bird carotid artery that is equivalent in size to that of a mouse carotid and use $FeCl_3$ to injure endothelial cells and expose subendothelial collagen[69]. This injury model reproducibly generates a platelet-driven occlusive thrombus in wild-type mice. A doppler flow probe will be used to determine the presence of, and time to, occlusion following $FeCl_3$ injury. We will also take vessel specimens for histology following injury to determine the thrombocyte response following application of $FeCl_3$. Identical experiments on wild-type mouse carotids will be performed as controls. We predict three possible results, all of which would be informative: (1) the avian carotid artery does not occlude following injury, consistent with the ability of thrombocytes to form a monolayer on collagen under arterial flow but not form 3-dimensional aggregates; (2) the avian carotid does occlude, but utilizes a more robust coagulation response to form a thrombocyte-poor thrombus; (3) the avian carotid occludes via a thrombocyte-rich thrombus, suggesting that mechanisms

not represented in the flow chamber, such as the contribution of thrombin or other agonists, are required for thrombocyte-mediated thrombosis.

These studies will determine if the ability of hemostatic cells to form occlusive thrombi *in vivo* is unique to mammals. The results of this work can provide insight into the evolutionary adaptations of the response to traumatic injury. These studies will also address whether, by acquiring the ability for shear-resistant aggregation, the presence of platelets, rather than thrombocytes, fundamentally predisposes humans to cardiovascular morbidity and mortality.

Concluding remarks: The evolution of platelet responses to collagen under conditions of hemodynamic flow

Fibrillar collagen is the major component of the subendothelial ECM and serves as both an adhesive surface and activating stimulus for platelets in the circulation. In multiple ways, platelets are uniquely engineered to arrest their flow, activate, and aggregate under the high shear conditions of the arterial system. Essential elements that mediate the function of platelets in hemostasis and pathological thrombosis include: the small size of the platelet; high platelet numbers in blood; robust signaling in response to several endogenous agonists; dynamic cell spreading behavior; and a high density of $\alpha_{2b}\beta_3$ to allow aggregation.

Our studies began with a focus on the collagen receptor GPVI, where we discovered a novel mechanism of direct Src-family kinase activation by the GPVI proline-rich domain that accelerates GPVI signaling to allow for more efficient platelet

activation in response to collagen under whole blood flow. The fact that this proline-rich region is highly conserved among all known GPVI receptors implies an importance for this domain in mediating collagen signaling in platelet biology. This finding prompted us to investigate the response to collagen of thrombocytes, which do not contain a GPVI ortholog. Our results, however, demonstrated that, even in the absence of GPVI, thrombocytes contain a receptor capable of robust collagen-induced activation and adhesion under flow. Our focus shifted away from the collagen-GPVI axis and concentrated instead on the remarkable finding that chicken thrombocytes do not form aggregates under shear conditions. Compared to any differences in the collagen receptor, the fact that thrombocytes contain a 10- to 20-fold lower density of $\alpha_{2b}\beta_3$ on the cell surface could account for their profound difference in behavior under hemodynamic flow conditions. To augment their aggregation response, platelets utilize positive feedback through an array of secondary agonists (ADP, thromboxane, and 5-HT), to which thrombocytes also lack a robust response. Whether increased $\alpha_{2b}\beta_3$ density, and therefore shear-resistant aggregation, preceded or co-evolved with the ability of platelets to maintain activation through secondary agonists is unknown.

The use of thrombocyte studies in zebrafish models has grown in popularity, based on the ease of genetic manipulation and relatively high-throughput whole organism hemostasis and thrombosis assays[144,160]. Based on our findings, we would caution against the assumption that thrombocyte function in primitive vertebrates is completely analogous to platelet function in mammals. The evolution of platelet responses to collagen under hemodynamic flow is most profoundly characterized by the response of

platelets *after* collagen-induced activation—aggregation and potentiation through secondary agonists. GPVI, which appears in evolution after the emergence of true platelets in primitive mammals, may represent the evolutionary fine-tuning of the robust collagen signaling that is inherent in all hemostatic cells. This fine-tuning may have been advantageous or even essential for mammalian survival following acute trauma, yet predisposes humans with atherosclerotic lesions to coronary and cerebrovascular occlusion.

Materials and methods

Isolation of platelets from echidna and opossum

Juvenile echidna and striped opossum studies were performed under supervision from the veterinarian staff at the Philadelphia Zoo. A juvenile echidna and striped opossum were anesthetized using isofluorine inhalation. Blood samples were collected from intra-nasal capillary beds into a syringe containing 15 U/mL heparin. Platelet-rich plasma was obtained by centrifugation of whole blood following dilution into 1:2 blood:Tyrode's buffer, as indicated in Chapter 2. All platelet function studies were performed as described in Chapter 2.

Figure 4-1. The response of echidna and opossum platelets to GPVI ligands.

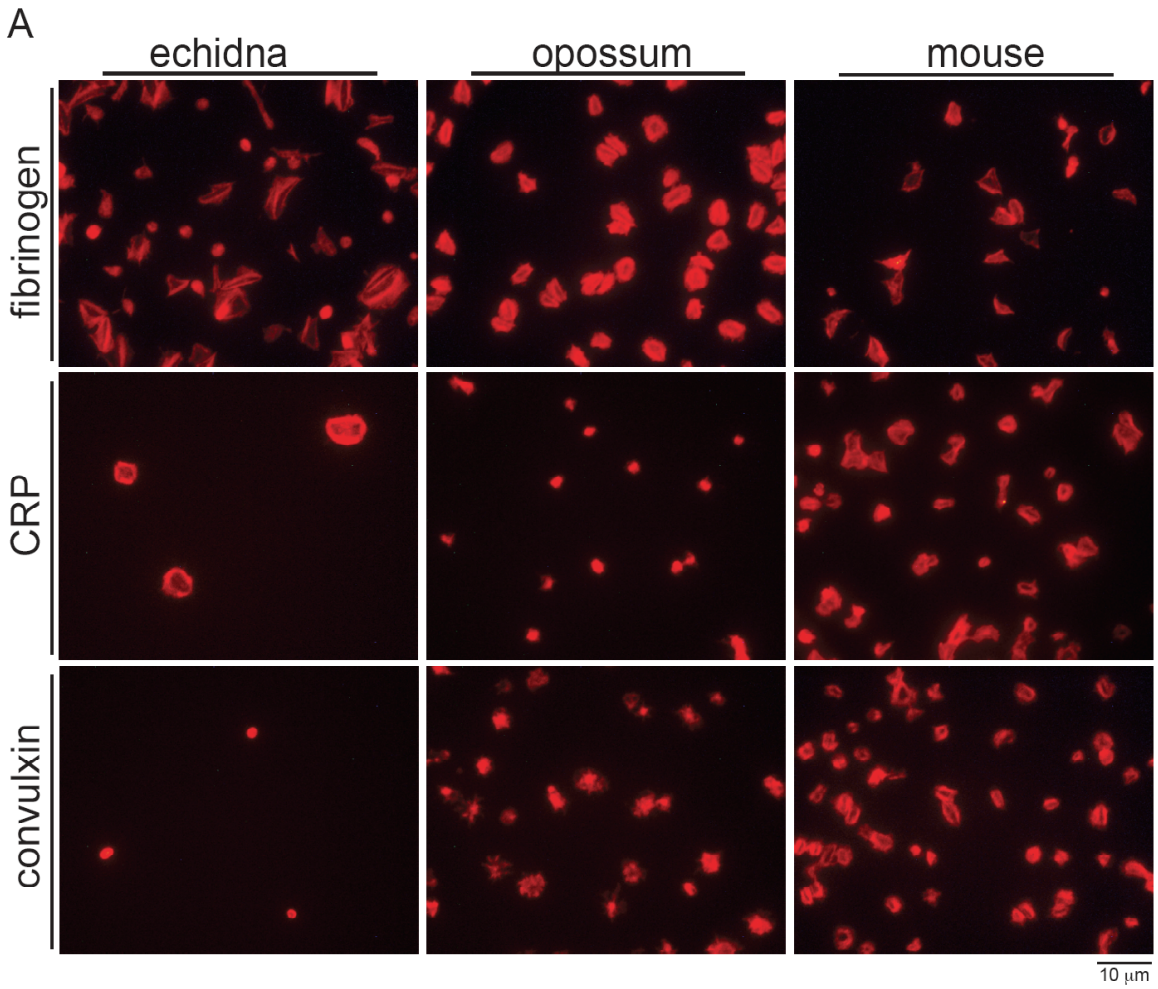

Figure 4-1 (cont'd). The response of echidna and opossum platelets to GPVI ligands.

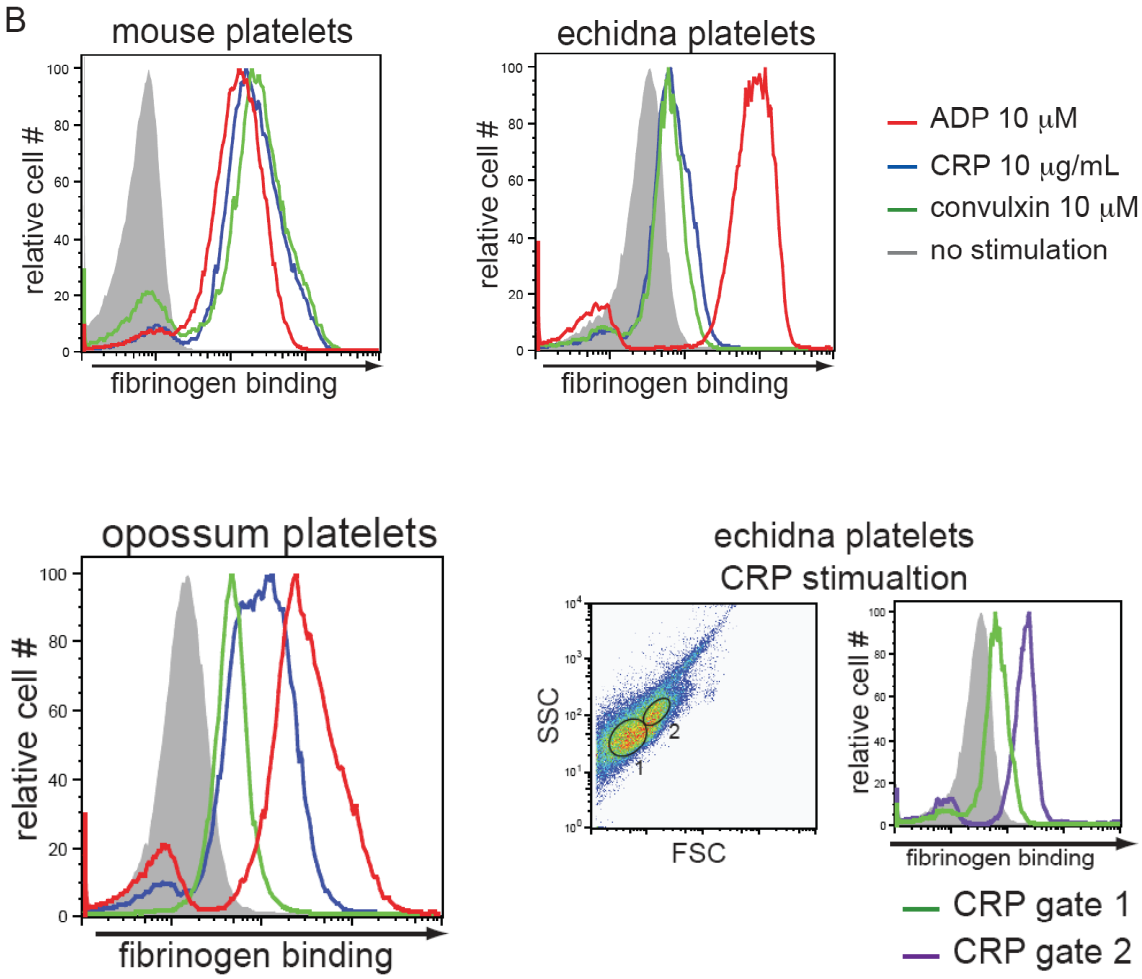

Figure 4-1. The response of echidna and opossum platelets to GPVI ligands.

A. Platelets from echidna, opossum, or mouse blood were allowed to spread on glass slides coated with fibrinogen, CRP, or convulxin. Platelets were fixed, permeabilized, and stained with Alexa-Fluor 594-conjugated phalloidin to detect actin filaments.

B. Stimulation of echidna, opossum, or mouse platelets with GPVI agonists. Platelets were stimulated with ADP, CRP, or convulxin for 10 min, and platelet activation was measured by the degree of fibrinogen binding, detected by flow cytometry. For echidna platelets, a subset of platelets could be detected (gate 2) that bound fibrinogen in response to CRP stimulation.

Figure 4-2. Alignment of GPVI sequences from opossum, mouse, and human.

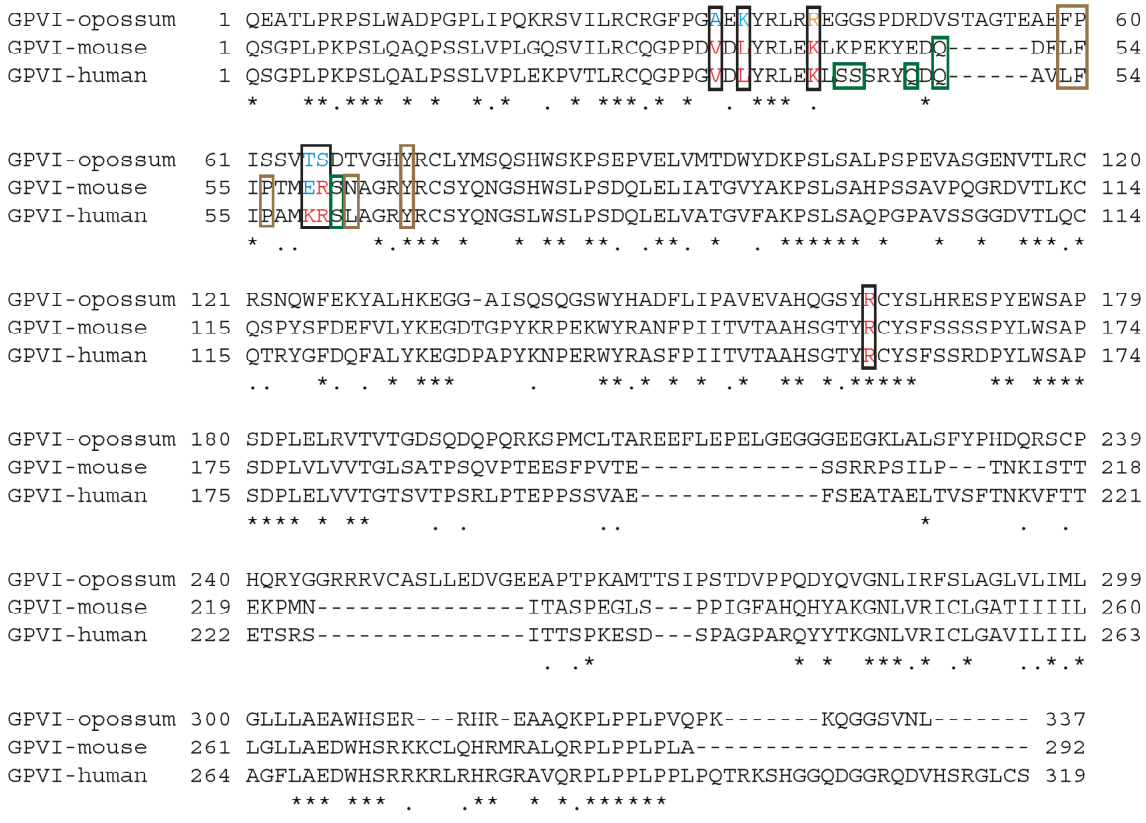

Figure 4-2. Alignment of GPVI sequences from opossum, mouse, and human. Amino acid residues implied in collagen or CRP binding are outlined in black, and conserved residues are shown in red text. Residues of similar charge or non-conserved residues are shown in blue and orange text, respectively. Polar residues believed to lie at the edge of the collagen-binding groove of GPVI are outlined in green. Hydrophobic residues believed to form the floor of the GPVI collagen binding groove are outlined in brown. Note the absence of many residues involved in collagen binding or formation of the collagen-binding groove in opossum GPVI. Also, note the absence a 6-residue deletion in opossum GPVI compared to mouse or human GPVI that is believed to form the collagen-binding groove.

References

1. Furie B, Furie BC. Mechanisms of thrombus formation. N Engl J Med. 2008;359:938-949.
2. van der Meijden PE, Munnix IC, Auger JM, et al. Dual role of collagen in factor XII-dependent thrombus formation. Blood. 2009;114:881-890.
3. Hansson GK. Inflammation, atherosclerosis, and coronary artery disease. N Engl J Med. 2005;352:1685-1695.
4. Fuster V, Badimon L, Badimon JJ, Chesebro JH. The pathogenesis of coronary artery disease and the acute coronary syndromes (1). N Engl J Med. 1992;326:242-250.
5. Falk E, Shah PK, Fuster V. Coronary plaque disruption. Circulation. 1995;92:657-671.
6. Davi G, Patrono C. Platelet activation and atherothrombosis. N Engl J Med. 2007;357:2482-2494.
7. Michelson AD. Platelets (ed 2nd). Burlington, MA: Academic Press, Elsevier; 2007.
8. Patel SR, Hartwig JH, Italiano JE, Jr. The biogenesis of platelets from megakaryocyte proplatelets. J Clin Invest. 2005;115:3348-3354.
9. Goldsmith HL, Turitto VT. Rheological aspects of thrombosis and haemostasis: basic principles and applications. ICTH-Report--Subcommittee on Rheology of the International Committee on Thrombosis and Haemostasis. Thromb Haemost. 1986;55:415-435.
10. Savage B, Almus-Jacobs F, Ruggeri ZM. Specific synergy of multiple substrate-receptor interactions in platelet thrombus formation under flow. Cell. 1998;94:657-666.
11. Strony J, Beaudoin A, Brands D, Adelman B. Analysis of shear stress and hemodynamic factors in a model of coronary artery stenosis and thrombosis. Am J Physiol. 1993;265:H1787-1796.
12. van Breugel HF, de Groot PG, Heethaar RM, Sixma JJ. Role of plasma viscosity in platelet adhesion. Blood. 1992;80:953-959.
13. Aarts PA, Heethaar RM, Sixma JJ. Red blood cell deformability influences platelets--vessel wall interaction in flowing blood. Blood. 1984;64:1228-1233.
14. Farndale RW. Collagen-induced platelet activation. Blood Cells Mol Dis. 2006;36:162-165.
15. Clemetson KJ, Clemetson JM. Platelet collagen receptors. Thromb Haemost. 2001;86:189-197.
16. Nieswandt B, Watson SP. Platelet-collagen interaction: is GPVI the central receptor? Blood. 2003;102:449-461.
17. Moroi M, Jung SM, Okuma M, Shinmyozu K. A patient with platelets deficient in glycoprotein VI that lack both collagen-induced aggregation and adhesion. J Clin Invest. 1989;84:1440-1445.

18. Clemetson JM, Polgar J, Magnenat E, Wells TN, Clemetson KJ. The platelet collagen receptor glycoprotein VI is a member of the immunoglobulin superfamily closely related to FcalphaR and the natural killer receptors. J Biol Chem. 1999;274:29019-29024.
19. Martin AM, Kulski JK, Witt C, Pontarotti P, Christiansen FT. Leukocyte Ig-like receptor complex (LRC) in mice and men. Trends Immunol. 2002;23:81-88.
20. Jandrot-Perrus M, Busfield S, Lagrue AH, et al. Cloning, characterization, and functional studies of human and mouse glycoprotein VI: a platelet-specific collagen receptor from the immunoglobulin superfamily. Blood. 2000;96:1798-1807.
21. Zheng YM, Liu C, Chen H, Locke D, Ryan JC, Kahn ML. Expression of the platelet receptor GPVI confers signaling via the Fc receptor gamma -chain in response to the snake venom convulxin but not to collagen. J Biol Chem. 2001;276:12999-13006.
22. Monteiro RC, Van De Winkel JG. IgA Fc receptors. Annu Rev Immunol. 2003;21:177-204.
23. Horii K, Kahn ML, Herr AB. Structural basis for platelet collagen responses by the immune-type receptor glycoprotein VI. Blood. 2006;108:936-942.
24. Miura Y, Takahashi T, Jung SM, Moroi M. Analysis of the interaction of platelet collagen receptor glycoprotein VI (GPVI) with collagen. A dimeric form of GPVI, but not the monomeric form, shows affinity to fibrous collagen. J Biol Chem. 2002;277:46197-46204.
25. Smethurst PA, Onley DJ, Jarvis GE, et al. Structural basis for the platelet-collagen interaction: the smallest motif within collagen that recognizes and activates platelet Glycoprotein VI contains two glycine-proline-hydroxyproline triplets. J Biol Chem. 2007;282:1296-1304.
26. Inoue O, Suzuki-Inoue K, McCarty OJ, et al. Laminin stimulates spreading of platelets through integrin alpha6beta1-dependent activation of GPVI. Blood. 2006;107:1405-1412.
27. Inoue O, Suzuki-Inoue K, Ozaki Y. Redundant mechanism of platelet adhesion to laminin and collagen under flow: involvement of von Willebrand factor and glycoprotein Ib-IX-V. J Biol Chem. 2008;283:16279-16282.
28. Asselin J, Gibbins JM, Achison M, et al. A collagen-like peptide stimulates tyrosine phosphorylation of syk and phospholipase C gamma2 in platelets independent of the integrin alpha2beta1. Blood. 1997;89:1235-1242.
29. Morton LF, Hargreaves PG, Farndale RW, Young RD, Barnes MJ. Integrin alpha 2 beta 1-independent activation of platelets by simple collagen-like peptides: collagen tertiary (triple-helical) and quaternary (polymeric) structures are sufficient alone for alpha 2 beta 1-independent platelet reactivity. Biochem J. 1995;306 (Pt 2):337-344.
30. Lu Q, Navdaev A, Clemetson JM, Clemetson KJ. Snake venom C-type lectins interacting with platelet receptors. Structure-function relationships and effects on haemostasis. Toxicon. 2005;45:1089-1098.

31. Staatz WD, Rajpara SM, Wayner EA, Carter WG, Santoro SA. The membrane glycoprotein Ia-IIa (VLA-2) complex mediates the Mg++-dependent adhesion of platelets to collagen. J Cell Biol. 1989;108:1917-1924.
32. Emsley J, Knight CG, Farndale RW, Barnes MJ, Liddington RC. Structural basis of collagen recognition by integrin alpha2beta1. Cell. 2000;101:47-56.
33. Inoue O, Suzuki-Inoue K, Dean WL, Frampton J, Watson SP. Integrin alpha2beta1 mediates outside-in regulation of platelet spreading on collagen through activation of Src kinases and PLCgamma2. J Cell Biol. 2003;160:769-780.
34. Chen H, Kahn ML. Reciprocal signaling by integrin and nonintegrin receptors during collagen activation of platelets. Mol Cell Biol. 2003;23:4764-4777.
35. Mazzucato M, Cozzi MR, Battiston M, et al. Distinct spatio-temporal Ca2+ signaling elicited by integrin alpha2beta1 and glycoprotein VI under flow. Blood. 2009;114:2793-2801.
36. Nieswandt B, Brakebusch C, Bergmeier W, et al. Glycoprotein VI but not alpha2beta1 integrin is essential for platelet interaction with collagen. Embo J. 2001;20:2120-2130.
37. Jung SM, Moroi M. Platelets interact with soluble and insoluble collagens through characteristically different reactions. J Biol Chem. 1998;273:14827-14837.
38. Shattil SJ, Kashiwagi H, Pampori N. Integrin signaling: the platelet paradigm. Blood. 1998;91:2645-2657.
39. Neeves KB, Maloney SF, Fong KP, et al. Microfluidic focal thrombosis model for measuring murine platelet deposition and stability: PAR4 signaling enhances shear-resistance of platelet aggregates. J Thromb Haemost. 2008;6:2193-2201.
40. Sarratt KL, Chen H, Zutter MM, Santoro SA, Hammer DA, Kahn ML. GPVI and alpha2beta1 play independent critical roles during platelet adhesion and aggregate formation to collagen under flow. Blood. 2005;106:1268-1277.
41. Pugh N, Simpson AM, Smethurst PA, de Groot PG, Raynal N, Farndale RW. Synergism between platelet collagen receptors defined using receptor-specific collagen-mimetic peptide substrata in flowing blood. Blood.
42. Locke D, Chen H, Liu Y, Liu C, Kahn ML. Lipid rafts orchestrate signaling by the platelet receptor glycoprotein VI. J Biol Chem. 2002;277:18801-18809.
43. Lingwood D, Simons K. Lipid rafts as a membrane-organizing principle. Science;327:46-50.
44. Abramson J, Pecht I. Regulation of the mast cell response to the type 1 Fc epsilon receptor. Immunol Rev. 2007;217:231-254.
45. Koretzky GA, Myung PS. Positive and negative regulation of T-cell activation by adaptor proteins. Nat Rev Immunol. 2001;1:95-107.
46. Watson SP, Auger JM, McCarty OJ, Pearce AC. GPVI and integrin alphaIIb beta3 signaling in platelets. J Thromb Haemost. 2005;3:1752-1762.
47. Quek LS, Pasquet JM, Hers I, et al. Fyn and Lyn phosphorylate the Fc receptor gamma chain downstream of glycoprotein VI in murine platelets, and Lyn regulates a novel feedback pathway. Blood. 2000;96:4246-4253.

48. Pasquet JM, Gross B, Quek L, et al. LAT is required for tyrosine phosphorylation of phospholipase cgamma2 and platelet activation by the collagen receptor GPVI. Mol Cell Biol. 1999;19:8326-8334.
49. Leo L, Di Paola J, Judd BA, Koretzky GA, Lentz SR. Role of the adapter protein SLP-76 in GPVI-dependent platelet procoagulant responses to collagen. Blood. 2002;100:2839-2844.
50. Poole A, Gibbins JM, Turner M, et al. The Fc receptor gamma-chain and the tyrosine kinase Syk are essential for activation of mouse platelets by collagen. Embo J. 1997;16:2333-2341.
51. Gross BS, Lee JR, Clements JL, et al. Tyrosine phosphorylation of SLP-76 is downstream of Syk following stimulation of the collagen receptor in platelets. J Biol Chem. 1999;274:5963-5971.
52. Gibbins JM, Okuma M, Farndale R, Barnes M, Watson SP. Glycoprotein VI is the collagen receptor in platelets which underlies tyrosine phosphorylation of the Fc receptor gamma-chain. FEBS Lett. 1997;413:255-259.
53. Judd BA, Myung PS, Leng L, et al. Hematopoietic reconstitution of SLP-76 corrects hemostasis and platelet signaling through alpha IIb beta 3 and collagen receptors. Proc Natl Acad Sci U S A. 2000;97:12056-12061.
54. Kato K, Kanaji T, Russell S, et al. The contribution of glycoprotein VI to stable platelet adhesion and thrombus formation illustrated by targeted gene deletion. Blood. 2003;102:1701-1707.
55. Lockyer S, Okuyama K, Begum S, et al. GPVI-deficient mice lack collagen responses and are protected against experimentally induced pulmonary thromboembolism. Thromb Res. 2006;118:371-380.
56. Clements JL, Lee JR, Gross B, et al. Fetal hemorrhage and platelet dysfunction in SLP-76-deficient mice. J Clin Invest. 1999;103:19-25.
57. Judd BA, Myung PS, Obergfell A, et al. Differential requirement for LAT and SLP-76 in GPVI versus T cell receptor signaling. J Exp Med. 2002;195:705-717.
58. Chen H, Locke D, Liu Y, Liu C, Kahn ML. The platelet receptor GPVI mediates both adhesion and signaling responses to collagen in a receptor density-dependent fashion. J Biol Chem. 2002;277:3011-3019.
59. Bori-Sanz T, Inoue KS, Berndt MC, Watson SP, Tulasne D. Delineation of the region in the glycoprotein VI tail required for association with the Fc receptor gamma-chain. J Biol Chem. 2003;278:35914-35922.
60. Goto S, Tamura N, Handa S, Arai M, Kodama K, Takayama H. Involvement of glycoprotein VI in platelet thrombus formation on both collagen and von Willebrand factor surfaces under flow conditions. Circulation. 2002;106:266-272.
61. Auger JM, Kuijpers MJ, Senis YA, Watson SP, Heemskerk JW. Adhesion of human and mouse platelets to collagen under shear: a unifying model. FASEB J. 2005;19:825-827.
62. Kuijpers MJ, Schulte V, Bergmeier W, et al. Complementary roles of glycoprotein VI and alpha2beta1 integrin in collagen-induced thrombus formation in flowing whole blood ex vivo. FASEB J. 2003;17:685-687.

63. van Zanten GH, de Graaf S, Slootweg PJ, et al. Increased platelet deposition on atherosclerotic coronary arteries. J Clin Invest. 1994;93:615-632.
64. Penz S, Reininger AJ, Brandl R, et al. Human atheromatous plaques stimulate thrombus formation by activating platelet glycoprotein VI. FASEB J. 2005;19:898-909.
65. Reininger AJ, Bernlochner I, Penz SM, et al. A 2-step mechanism of arterial thrombus formation induced by human atherosclerotic plaques. J Am Coll Cardiol;55:1147-1158.
66. Dubois C, Panicot-Dubois L, Gainor JF, Furie BC, Furie B. Thrombin-initiated platelet activation in vivo is vWF independent during thrombus formation in a laser injury model. J Clin Invest. 2007;117:953-960.
67. Dubois C, Panicot-Dubois L, Merrill-Skoloff G, Furie B, Furie BC. Glycoprotein VI-dependent and -independent pathways of thrombus formation in vivo. Blood. 2006;107:3902-3906.
68. Vandendries ER, Hamilton JR, Coughlin SR, Furie B, Furie BC. Par4 is required for platelet thrombus propagation but not fibrin generation in a mouse model of thrombosis. Proc Natl Acad Sci U S A. 2007;104:288-292.
69. Woollard KJ, Sturgeon S, Chin-Dusting JP, Salem HH, Jackson SP. Erythrocyte hemolysis and hemoglobin oxidation promote ferric chloride-induced vascular injury. J Biol Chem. 2009;284:13110-13118.
70. Massberg S, Gawaz M, Gruner S, et al. A crucial role of glycoprotein VI for platelet recruitment to the injured arterial wall in vivo. J Exp Med. 2003;197:41-49.
71. Hechler B, Nonne C, Eckly A, et al. Arterial thrombosis: relevance of a model with two levels of severity assessed by histologic, ultrastructural and functional characterization. J Thromb Haemost;8:173-184.
72. Bultmann A, Herdeg C, Li Z, et al. Local delivery of soluble platelet collagen receptor glycoprotein VI inhibits thrombus formation in vivo. Thromb Haemost. 2006;95:763-766.
73. Cheli Y, Jensen D, Marchese P, et al. The Modifier of hemostasis (Mh) locus on chromosome 4 controls in vivo hemostasis of Gp6-/- mice. Blood. 2008;111:1266-1273.
74. Mangin P, Yap CL, Nonne C, et al. Thrombin overcomes the thrombosis defect associated with platelet GPVI/FcRgamma deficiency. Blood. 2006;107:4346-4353.
75. Croft SA, Samani NJ, Teare MD, et al. Novel platelet membrane glycoprotein VI dimorphism is a risk factor for myocardial infarction. Circulation. 2001;104:1459-1463.
76. Bigalke B, Lindemann S, Ehlers R, et al. Expression of platelet collagen receptor glycoprotein VI is associated with acute coronary syndrome. Eur Heart J. 2006;27:2165-2169.
77. Bigalke B, Stellos K, Geisler T, et al. Expression of platelet glycoprotein VI is associated with transient ischemic attack and stroke. Eur J Neurol;17:111-117.

78. Santoso S, Kunicki TJ, Kroll H, Haberbosch W, Gardemann A. Association of the platelet glycoprotein Ia C807T gene polymorphism with nonfatal myocardial infarction in younger patients. Blood. 1999;93:2449-2453.
79. Bigalke B, Stellos K, Geisler T, Lindemann S, May AE, Gawaz M. Glycoprotein VI as a prognostic biomarker for cardiovascular death in patients with symptomatic coronary artery disease. Clin Res Cardiol;99:227-233.
80. Bigalke B, Haap M, Stellos K, et al. Platelet glycoprotein VI (GPVI) for early identification of acute coronary syndrome in patients with chest pain. Thromb Res;125:e184-189.
81. Arthur JF, Dunkley S, Andrews RK. Platelet glycoprotein VI-related clinical defects. Br J Haematol. 2007;139:363-372.
82. Hermans C, Wittevrongel C, Thys C, Smethurst PA, Van Geet C, Freson K. A compound heterozygous mutation in glycoprotein VI in a patient with a bleeding disorder. J Thromb Haemost. 2009;7:1356-1363.
83. Dumont B, Lasne D, Rothschild C, et al. Absence of collagen-induced platelet activation caused by compound heterozygous GPVI mutations. Blood. 2009;114:1900-1903.
84. Stoll G, Kleinschnitz C, Nieswandt B. Molecular mechanisms of thrombus formation in ischemic stroke: novel insights and targets for treatment. Blood. 2008.
85. Varga-Szabo D, Pleines I, Nieswandt B. Cell adhesion mechanisms in platelets. Arterioscler Thromb Vasc Biol. 2008;28:403-412.
86. Savage B, Saldivar E, Ruggeri ZM. Initiation of platelet adhesion by arrest onto fibrinogen or translocation on von Willebrand factor. Cell. 1996;84:289-297.
87. Gardiner EE, Arthur JF, Shen Y, et al. GPIbalpha-selective activation of platelets induces platelet signaling events comparable to GPVI activation events. Platelets;21:244-252.
88. Nesbitt WS, Westein E, Tovar-Lopez FJ, et al. A shear gradient-dependent platelet aggregation mechanism drives thrombus formation. Nat Med. 2009;15:665-673.
89. Goldsmith MA, Weiss A. Early signal transduction by the antigen receptor without commitment to T cell activation. Science. 1988;240:1029-1031.
90. Bakema JE, de Haij S, den Hartog-Jager CF, et al. Signaling through mutants of the IgA receptor CD89 and consequences for Fc receptor gamma-chain interaction. J Immunol. 2006;176:3603-3610.
91. Ono M, Yuasa T, Ra C, Takai T. Stimulatory function of paired immunoglobulin-like receptor-A in mast cell line by associating with subunits common to Fc receptors. J Biol Chem. 1999;274:30288-30296.
92. Locke D, Liu C, Peng X, Chen H, Kahn ML. Fc Rgamma -independent signaling by the platelet collagen receptor glycoprotein VI. J Biol Chem. 2003;278:15441-15448.
93. Call ME, Wucherpfennig KW. Common themes in the assembly and architecture of activating immune receptors. Nat Rev Immunol. 2007;7:841-850.

94. Rickles RJ, Botfield MC, Weng Z, et al. Identification of Src, Fyn, Lyn, PI3K and Abl SH3 domain ligands using phage display libraries. Embo J. 1994;13:5598-5604.
95. Suzuki-Inoue K, Tulasne D, Shen Y, et al. Association of Fyn and Lyn with the proline-rich domain of glycoprotein VI regulates intracellular signaling. J Biol Chem. 2002;277:21561-21566.
96. Ezumi Y, Shindoh K, Tsuji M, Takayama H. Physical and functional association of the Src family kinases Fyn and Lyn with the collagen receptor glycoprotein VI-Fc receptor gamma chain complex on human platelets. J Exp Med. 1998;188:267-276.
97. Alexandropoulos K, Cheng G, Baltimore D. Proline-rich sequences that bind to Src homology 3 domains with individual specificities. Proc Natl Acad Sci U S A. 1995;92:3110-3114.
98. Li SS. Specificity and versatility of SH3 and other proline-recognition domains: structural basis and implications for cellular signal transduction. Biochem J. 2005;390:641-653.
99. Zou Z, Chen H, Schmaier AA, Hynes RO, Kahn ML. Structure-function analysis reveals discrete beta3 integrin inside-out and outside-in signaling pathways in platelets. Blood. 2007;109:3284-3290.
100. Berlanga O, Tulasne D, Bori T, et al. The Fc receptor gamma-chain is necessary and sufficient to initiate signalling through glycoprotein VI in transfected cells by the snake C-type lectin, convulxin. Eur J Biochem. 2002;269:2951-2960.
101. Karkkainen S, Hiipakka M, Wang JH, et al. Identification of preferred protein interactions by phage-display of the human Src homology-3 proteome. EMBO Rep. 2006;7:186-191.
102. Moarefi I, LaFevre-Bernt M, Sicheri F, et al. Activation of the Src-family tyrosine kinase Hck by SH3 domain displacement. Nature. 1997;385:650-653.
103. Trible RP, Emert-Sedlak L, Smithgall TE. HIV-1 Nef selectively activates Src family kinases Hck, Lyn, and c-Src through direct SH3 domain interaction. J Biol Chem. 2006;281:27029-27038.
104. Mori J, Pearce AC, Spalton JC, et al. G6b-B inhibits constitutive and agonist-induced signaling by glycoprotein VI and CLEC-2. J Biol Chem. 2008;283:35419-35427.
105. Tomlinson MG, Calaminus SD, Berlanga O, et al. Collagen promotes sustained glycoprotein VI signaling in platelets and cell lines. J Thromb Haemost. 2007;5:2274-2283.
106. Hanna Z, Weng X, Kay DG, Poudrier J, Lowell C, Jolicoeur P. The pathogenicity of human immunodeficiency virus (HIV) type 1 Nef in CD4C/HIV transgenic mice is abolished by mutation of its SH3-binding domain, and disease development is delayed in the absence of Hck. J Virol. 2001;75:9378-9392.
107. Vincent P, Priceputu E, Kay D, Saksela K, Jolicoeur P, Hanna Z. Activation of p21-activated kinase 2 and its association with Nef are conserved in murine cells but are not sufficient to induce an AIDS-like disease in CD4C/HIV transgenic mice. J Biol Chem. 2006;281:6940-6954.

108. Young MA, Gonfloni S, Superti-Furga G, Roux B, Kuriyan J. Dynamic coupling between the SH2 and SH3 domains of c-Src and Hck underlies their inactivation by C-terminal tyrosine phosphorylation. Cell. 2001;105:115-126.
109. Engen JR, Wales TE, Hochrein JM, et al. Structure and dynamic regulation of Src-family kinases. Cell Mol Life Sci. 2008;65:3058-3073.
110. Lerner EC, Smithgall TE. SH3-dependent stimulation of Src-family kinase autophosphorylation without tail release from the SH2 domain in vivo. Nat Struct Biol. 2002;9:365-369.
111. Quek LS, Bolen J, Watson SP. A role for Bruton's tyrosine kinase (Btk) in platelet activation by collagen. Curr Biol. 1998;8:1137-1140.
112. Xu C, Gagnon E, Call ME, et al. Regulation of T cell receptor activation by dynamic membrane binding of the CD3epsilon cytoplasmic tyrosine-based motif. Cell. 2008;135:702-713.
113. Litman GW, Cannon JP, Dishaw LJ. Reconstructing immune phylogeny: new perspectives. Nat Rev Immunol. 2005;5:866-879.
114. Laun K, Coggill P, Palmer S, et al. The leukocyte receptor complex in chicken is characterized by massive expansion and diversification of immunoglobulin-like Loci. PLoS Genet. 2006;2:e73.
115. Warren WC, Hillier LW, Marshall Graves JA, et al. Genome analysis of the platypus reveals unique signatures of evolution. Nature. 2008;453:175-183.
116. Chan VW, Meng F, Soriano P, DeFranco AL, Lowell CA. Characterization of the B lymphocyte populations in Lyn-deficient mice and the role of Lyn in signal initiation and down-regulation. Immunity. 1997;7:69-81.
117. Sebzda E, Hibbard C, Sweeney S, et al. Syk and Slp-76 mutant mice reveal a cell-autonomous hematopoietic cell contribution to vascular development. Dev Cell. 2006;11:349-361.
118. Pear WS, Miller JP, Xu L, et al. Efficient and rapid induction of a chronic myelogenous leukemia-like myeloproliferative disease in mice receiving P210 bcr/abl-transduced bone marrow. Blood. 1998;92:3780-3792.
119. Ohmori T, Kashiwakura Y, Ishiwata A, Madoiwa S, Mimuro J, Sakata Y. Silencing of a targeted protein in in vivo platelets using a lentiviral vector delivering short hairpin RNA sequence. Arterioscler Thromb Vasc Biol. 2007;27:2266-2272.
120. Nieswandt B, Aktas B, Moers A, Sachs UJ. Platelets in atherothrombosis: lessons from mouse models. J Thromb Haemost. 2005;3:1725-1736.
121. Hanumanthaiah R, Day K, Jagadeeswaran P. Comprehensive analysis of blood coagulation pathways in teleostei: evolution of coagulation factor genes and identification of zebrafish factor VIIi. Blood Cells Mol Dis. 2002;29:57-68.
122. Smith FM. Blood Pressure Regulation by Aortic Baroreceptors in Birds. Physiological Zoology. 1994;67:1402-1425.
123. Kunicki TJ, Newman PJ. Synthesis of analogs of human platelet membrane glycoprotein IIb-IIIa complex by chicken peripheral blood thrombocytes. Proc Natl Acad Sci U S A. 1985;82:7319-7323.

124. Wigley P, Hulme SD, Barrow PA. Phagocytic and oxidative burst activity of chicken thrombocytes to Salmonella, Escherichia coli and other bacteria. Avian Pathology. 1999;28:567-572.
125. Belamarich FA, Fusari MH, Sherpo D, Kien M. In vitro studies of aggregation of non-mammalian thrombocytes. Nature. 1966;212:1579-1580.
126. O'Toole ET, Hantgan RR, Lewis JC. Localization of fibrinogen during aggregation of avian thrombocytes. Exp Mol Pathol. 1994;61:175-190.
127. Belamarich FA, Simoneit LW. Aggregation of duck thrombocytes by 5-hydroxytryptamine. Microvasc Res. 1973;6:229-234.
128. Grant RA, Zucker MB. Avian thrombocyte aggregation and shape change in vitro. Am J Physiol. 1973;225:340-343.
129. Lacoste-Eleaume AS, Bleux C, Quere P, Coudert F, Corbel C, Kanellopoulos-Langevin C. Biochemical and functional characterization of an avian homolog of the integrin GPIIb-IIIa present on chicken thrombocytes. Exp Cell Res. 1994;213:198-209.
130. Stiller RA, Belamarich FA, Shepro D. Aggregation and release in thrombocytes of the duck. Am J Physiol. 1975;229:206-210.
131. Daimon T, Uchida K. Electron microscopic and cytochemical observations on the membrane systems of the chicken thrombocyte. J Anat. 1978;125:11-21.
132. Lam KM. Activation, adhesion, migration and death of chicken thrombocytes. Comparative Haematology International. 1997;7:81-87.
133. Charo IF, Feinman RD, Detwiler TC. Interrelations of platelet aggregation and secretion. J Clin Invest. 1977;60:866-873.
134. Pidard D, Montgomery RR, Bennett JS, Kunicki TJ. Interaction of AP-2, a monoclonal antibody specific for the human platelet glycoprotein IIb-IIIa complex, with intact platelets. J Biol Chem. 1983;258:12582-12586.
135. Wagner CL, Mascelli MA, Neblock DS, Weisman HF, Coller BS, Jordan RE. Analysis of GPIIb/IIIa receptor number by quantification of 7E3 binding to human platelets. Blood. 1996;88:907-914.
136. Gartner TK, Bennett JS. The tetrapeptide analogue of the cell attachment site of fibronectin inhibits platelet aggregation and fibrinogen binding to activated platelets. J Biol Chem. 1985;260:11891-11894.
137. Cosemans JM, Munnix IC, Wetzker R, Heller R, Jackson SP, Heemskerk JW. Continuous signaling via PI3K isoforms beta and gamma is required for platelet ADP receptor function in dynamic thrombus stabilization. Blood. 2006;108:3045-3052.
138. Nergiz-Unal R, Cosemans JM, Feijge MA, et al. Stabilizing role of platelet P2Y(12) receptors in shear-dependent thrombus formation on ruptured plaques. PLoS One;5:e10130.
139. Phillips DR, Charo IF, Parise LV, Fitzgerald LA. The platelet membrane glycoprotein IIb-IIIa complex. Blood. 1988;71:831-843.
140. DaMatta RA, Manhaes L, Lassounskaia E, de Souza W. Chicken thrombocytes in culture: lymphocyte-conditioned medium delays apoptosis. Tissue Cell. 1999;31:255-263.

141. Gregory M, Jagadeeswaran P. Selective labeling of zebrafish thrombocytes: quantitation of thrombocyte function and detection during development. Blood Cells Mol Dis. 2002;28:418-427.
142. Jagadeeswaran P, Sheehan JP, Craig FE, Troyer D. Identification and characterization of zebrafish thrombocytes. Br J Haematol. 1999;107:731-738.
143. Thattaliyath B, Cykowski M, Jagadeeswaran P. Young thrombocytes initiate the formation of arterial thrombi in zebrafish. Blood. 2005;106:118-124.
144. O'Connor MN, Salles, II, Cvejic A, et al. Functional genomics in zebrafish permits rapid characterization of novel platelet membrane proteins. Blood. 2009;113:4754-4762.
145. Jarvis GE, Raynal N, Langford JP, et al. Identification of a major GpVI-binding locus in human type III collagen. Blood. 2008;111:4986-4996.
146. O'Connor MN, Smethurst PA, Farndale RW, Ouwehand WH. Gain- and loss-of-function mutants confirm the importance of apical residues to the primary interaction of human glycoprotein VI with collagen. J Thromb Haemost. 2006;4:869-873.
147. Viertlboeck BC, Schmitt R, Hanczaruk MA, Crooijmans RP, Groenen MA, Gobel TW. A novel activating chicken IgY FcR is related to leukocyte receptor complex (LRC) genes but is located on a chromosomal region distinct from the LRC and FcR gene clusters. J Immunol. 2009;182:1533-1540.
148. Belov K, Sanderson CE, Deakin JE, et al. Characterization of the opossum immune genome provides insights into the evolution of the mammalian immune system. Genome Res. 2007;17:982-991.
149. Nikolaidis N, Makalowska I, Chalkia D, Makalowski W, Klein J, Nei M. Origin and evolution of the chicken leukocyte receptor complex. Proc Natl Acad Sci U S A. 2005;102:4057-4062.
150. Viertlboeck BC, Habermann FA, Schmitt R, Groenen MA, Du Pasquier L, Gobel TW. The chicken leukocyte receptor complex: a highly diverse multigene family encoding at least six structurally distinct receptor types. J Immunol. 2005;175:385-393.
151. Dennis G, Jr., Kubagawa H, Cooper MD. Paired Ig-like receptor homologs in birds and mammals share a common ancestor with mammalian Fc receptors. Proc Natl Acad Sci U S A. 2000;97:13245-13250.
152. Chung KS, Lillehoj HS, Jenkins MC. Avian leucocyte common antigens: molecular weight determination and flow cytometric analysis using new monoclonal antibodies. Vet Immunol Immunopathol. 1991;28:259-273.
153. Schmaier AA, Zou Z, Kazlauskas A, et al. Molecular priming of Lyn by GPVI enables an immune receptor to adopt a hemostatic role. Proc Natl Acad Sci U S A. 2009;106:21167-21172.
154. Cliche S, Amiot J, Avezard C, Gariepy C. Extraction and characterization of collagen with or without telopeptides from chicken skin. Poult Sci. 2003;82:503-509.

155. San Antonio JD, Lander AD, Karnovsky MJ, Slayter HS. Mapping the heparin-binding sites on type I collagen monomers and fibrils. J Cell Biol. 1994;125:1179-1188.
156. Sarratt KL, Chen H, Kahn ML, Hammer DA. Platelet receptor glycoprotein VI-mediated adhesion to type I collagen under hydrodynamic flow. Ann Biomed Eng. 2004;32:970-976.
157. Polgar J, Clemetson JM, Kehrel BE, et al. Platelet activation and signal transduction by convulxin, a C-type lectin from Crotalus durissus terrificus (tropical rattlesnake) venom via the p62/GPVI collagen receptor. J Biol Chem. 1997;272:13576-13583.
158. Sugiyama T, Okuma M, Ushikubi F, Sensaki S, Kanaji K, Uchino H. A novel platelet aggregating factor found in a patient with defective collagen-induced platelet aggregation and autoimmune thrombocytopenia. Blood. 1987;69:1712-1720.
159. Smethurst PA, Joutsi-Korhonen L, O'Connor MN, et al. Identification of the primary collagen-binding surface on human glycoprotein VI by site-directed mutagenesis and by a blocking phage antibody. Blood. 2004;103:903-911.
160. Lang MR, Gihr G, Gawaz MP, Muller, II. Haemostasis in Danio rerio - Is the zebrafish a useful model for platelet research? J Thromb Haemost. 2010 Feb 17. [Epub ahead of print]